University of Alberta

Palmitoylation targets calnexin to the MAM and regulates its functions

by

Emily Marian Lynes

A thesis submitted to the Faculty of Graduate Studies and Research
in partial fulfillment of the requirements for the degree of

Doctor of Philosophy

Cell Biology

Spring 2013
Edmonton, Alberta

Abstract

The mitochondria associated membranes (MAMs) of the endoplasmic reticulum (ER) are the points of contact between the ER, which is the organelle responsible for lipid and secreted protein synthesis and calcium storage, and the mitochondria, which are organelles responsible for cellular energy production. The MAM has many roles including the transfer of lipids and metabolites between these two organelles, as well as the mediation of calcium signaling between the ER and mitochondria. Calcium transfer at MAMs is of vital importance as it regulates mitochondrial metabolism and apoptosis, or programmed cell death. Although the MAM has been well-characterized in recent years, very little is currently known about how proteins target there and how these contact sites are maintained. In this thesis, I have identified a novel MAM targeting mechanism, palmitoylation, using a chimeric mutagenesis strategy. I have also identified two proteins, TMX and calnexin, which use this signal to target to MAM. Furthermore, I have characterized the role of calnexin at MAM by overexpressing wildtype and non-palmitoylatable calnexin in calnexin knockout cells. This led to the discovery that calnexin plays a role in ER-mitochondria calcium transfer and may affect structural changes at MAM during cellular stress. These findings have implications for the study of diseases where mitochondrial metabolism and deregulated cell death are factors, for example cancer and neurodegenerative disease.

Acknowledgements

I particularly wish to thank my supervisor Thomas Simmen for providing me with a safe and happy work environment, and excellent mentorship. I benefitted immensely from his dedication to this project and his guidance, and especially from his enthusiasm for this work in the face of challenges that seemed insurmountable to me at the time. I also thank my colleagues in the Simmen Lab, as well as colleagues and friends in the departments of Cell Biology and Biochemistry and beyond, for their help and support. They have truly shared in the ups and downs of graduate school life and research with me. A heartfelt thank you to Mom, Dad, Meredith and Alison, the Zimmermann family, and to my partner Aaron and his family, for their encouragement.

Table of Contents

List of Tables

List of Figures

List of Abbreviations

List of Tables

List of Figures

List of Abbreviations

Aβ	Amyloid beta protein
ACAT	Acyl-CoA: cholesterol acyltransferase
AD	Alzheimer Disease
APP	Amyloid precursor protein
APT	Acyl Protein Thioesterase
ATP	Adenosine Triphosphate
BiP	Binding immunoglobulin protein
BSA	Bovine serum albumin
Ca2+	Calcium
CDP	Cytidine diphosphate
CNX	Calnexin
COPI/II	Coat Protein complexes I and II
DGAT	Diglyceride acyltransferase
DHHC	Aspartic acid-Histidine-Histidine-Cysteine
DMEM	Dulbecco's Modified Eagle Medium
DMSO	Dimethyl Sulphoxide
DNA	Deoxy ribonucleic acid
DRM	Detergent Resistant Membrane
DTT	Dithiothreitol
EDEM	ER degradation enhancing mannosidase-like protein
eIF2	Eukaryotic translastion initiation factor 2A

EM	Electron microscopy
ER	Endoplasmic reticulum
ERAD	ER associated degradation
ERES	ER exit sites
ERGIC	ER Golgi intermediate compartment
ERMES	ER mitochondria encounter structure
Ero1	ER oxidoreductase
FAD	Flavin Adenine dinucleotide
FBS	Fetal Bovine Serum
Grp	Glucose regulated protein
HO-1	Hemeoxygenase-1
HRP	Horseradish Peroxidase
INCL	Infant Neuronal Ceroid Lipofuscinosis
IP_3	Inositol triphosphate
IF	Immunofluorescence microscopy
kDa	Kilo Dalton
LDL-R	Low density lipoprotein receptor
LRP6	Low density lipoprotein receptor-related protein 6
MAM	Mitochondria associated membrane
MEF	Mouse embryonic fibroblast
MFN	Mitofusin
mRNA	Messenger ribonucleic acid

PACS-2	Phosphofurin acidic cluster sorting protein 2
PAT	Protein acyl transferase
PBS	Phosphate Buffered Saline
PCR	Polymerase Chain Reaction
PDI	Protein Disulphide Isomerase
PPT	Protein palmitoyl thioesterase
PtdCho	Phosphatidyl choline
PtdEtn	Phosphatidyl ethanolamine
PtdIns	Phosphatidyl inositol
PtdSer	Phosphatidyl serine
SERCA	Sarco/Endoplasmic reticulum Ca^{2+} ATPase
shRNA	Short hairpin ribonucleic acid
siRNA	Small interfering ribonucleic acid
SDS-PAGE	Sodium Dodecyl Suphate Polyacrylamide Gel Electrophoresis
SOCE	Store Operated Calcium Entry
SRP	Signal recognition particle
TAE	Tris base, Acetic acid, EDTA
TEMED	Tetramethylethylenediamine
TBS(-T)	Tris buffered saline (Tween 20)
TG	Thapsigargin
Tm	Tunicamycin
TMX	Transmembrane thioredoxin

UPR	Unfolded protein response
VDAC	Voltage dependent anion channel

Chapter 1: Introduction

Portions of this chapter have been published:

Lynes, E.M. and T. Simmen. (2011) Urban planning of the endoplasmic reticulum (ER): How diverse mechanisms segregate the many functions of the ER. *Biochim Biophys Acta.* **1813:** 1893-905.

Simmen, T., Lynes, E.M., Gesson, K., and G. Thomas. (2010) Oxidative protein folding in the endoplasmic reticulum: Tight links to the mitochondria-associated membrane (MAM). *Biochim Biophys Acta*. **1798:** 1465-73.

Chapter 1: Introduction

1.1 The Endoplasmic Reticulum (ER)

The endoplamic reticulum (ER) is a cellular organelle with one continuous membrane, but very diverse functions. Initial observations of the ER by electron microscopy and biochemical methods led identification of two types of ER (Dallner et al., 1963; Palade and Siekevitz, 1956). The rough ER is covered in ribosomes, which translate mRNA into protein, suggesting that the ER is important for protein synthesis. Indeed, the ER is very abundant in cell types that produce a lot of protein, termed professional secretory cells. These include pancreatic β cells, which secrete insulin (Marchetti et al., 2007), and the plasma cells of the immune system, which produce and secrete immunoglobulins (Tagliavacca et al., 2003). As ribosomes begin translation, a signal sequence in the nascent polypeptide destined for the secretory system is recognized by the signal recognition particle (SRP). The SRP is in turn recognized by SRP receptors on the rough ER membrane, and this interaction mediates the binding of the ribosome to the translocon, a complex of ER transmembrane proteins that facilitate the translocation of nascent polypeptides into the ER lumen or into the ER membrane (Egea et al., 2005). Unlike proteins that are translated in the cytosol, proteins targeted to the ER are destined to become integral membrane proteins, or be secreted from the cell (Palade, 1975). Inside the ER lumen, the signal peptidase complex, which associates with translocons, cleaves the hydrophobic signal sequence (Kalies et al., 1998).

Once safely in the ER lumen or membrane, the oxidizing environment within the ER, along with various chaperone proteins, help the polypeptide to fold and reach its native state. The oxidizing environment in the ER lumen is maintained by the tripeptide glutathione, which is the major redox buffer in the cell, and the ratio of reduced glutathione (GSH) to oxidized glutathione (GSSG) has been measured at 1:1-1:3 in the ER lumen, as compared to 30:1-100:1 in the cytosol, although it is unclear how this discrepancy is maintained across the ER membrane (Bass et al.,

2004; Hwang et al., 1992). The chaperone protein Protein Disulphide Isomerase (PDI) takes advantage of the oxidizing environment within the ER to mediate the formation and isomerisation of disulphide bonds between cysteines (Tu and Weissman, 2004). Another example of a chaperone is Grp78, or BiP, which localizes to the translocon (Hamman et al., 1998), where it can immediately interact with nascent proteins. At the expense of ATP, BiP associates with hydrophobic regions of unfolded proteins, which should normally be buried within the protein structure, preventing unfolded proteins from forming aggregates (Kleizen and Braakman, 2004; Knarr et al., 1995).

The N-linked glycosylation of proteins at asparagine residues also begins in the ER, a process which is continued when mature, folded proteins progress through the secretory system to the Golgi and eventually the plasma membrane, or into the extracellular space. Folding of glycosylated proteins in the ER is assisted by the transmembrane lectin chaperone calnexin and its luminal homologue calreticulin (Lederkremer, 2009). Calnexin and calreticulin bind to the sugar moiety of unfolded glycoproteins, retaining them in the ER in proximity with other chaperones, such as the PDI-like protein ERp57 (Elliott et al., 1997). In addition to the production of secretory and membrane proteins, chaperone proteins in the ER are responsible for quality control, or ensuring that misfolded proteins do not aggregate in the ER or progress through the secretory system (Sitia and Braakman, 2003). This includes of the binding and sequestration of misfolded protein aggregates, for example by BiP or the calnexin/calreticulin system, and the export or retrotranslocation of misfolded proteins to the cytosol for degradation by the proteasome, a process termed ER-associated degradation (ERAD) (Lederkremer, 2009). The degradation of misfolded proteins is thought to take place at the ER quality control compartment (ERQC), a juxtanuclear ER subdomain which forms when cells are subjected to ER stress (Kamhi-Nesher et al., 2001). Targeting of misfolded glycoproteins for ERAD is mediated by the mannosidase EDEM1, which trims the sugar moiety of N-glycosylated proteins, freeing them from the calnexin cycle (Ruddock and Molinari, 2006).

A large proportion of the ER, as observed by electron microscopy, is not covered in ribosomes, however, and is termed the smooth ER. Aside from the absence of ribosomes, there are several other morphological differences between rough and smooth ER. While rough ER tends to form sheets mediated by the presence of Climp63 (Shibata et al., 2010), smooth ER is often more tubular, with a high degree of membrane curvature maintained by a group of proteins called reticulons (Voeltz et al., 2006). The smooth ER is also highly branched, with 3-way junctions between tubules maintained by the atlastin family of GTPases. When these proteins are deleted or their GTPase activity is abrogated, these junctions fail to form (Hu et al., 2009; Orso et al., 2009). Smooth ER has been identified as the site of phospholipid biosynthesis (Higgins, 1974). Consequently, smooth ER is particularly abundant in cells that are active in lipid metabolism; for example, testicular and ovarian cells that produce steroid hormones from cholesterol, and hepatocytes, which break down lipid-soluble toxins into soluble compounds that can be eliminated in urine. Indeed, the smooth ER is also enriched in proteins that mediate drug detoxification such as epoxide hydroxylase (Galteau et al., 1985) and cytochrome P4502E1, which is induced by ethanol consumption (Takahashi et al., 1993). Phospholipids are synthesized on the cytosolic leaflet of the ER membrane, and are assembled from soluble cytosolic precursors. Flippase enzymes then catalyze the translocation of newly made phospholipids across the bilayer (Sharom, 2011). The smooth ER is also the site of cholesterol synthesis. Proteins involved in cholesterol synthesis reside in the ER membrane and are regulated by a negative feedback loop triggered by cholesterol levels in the ER membrane (Radhakrishnan et al., 2008).

The ER is also the biggest intracellular store of calcium (Hales et al., 1974; McGraw et al., 1980). Measurements of the concentration of calcium within the ER have been variable and range from 100 to 700 μM, or about 1000 times higher than that of the cytosol (Meldolesi and Pozzan, 1998; Miyawaki et al., 1997). This difference in calcium concentration across the ER membrane is maintained

by sarco- endoplasmic reticulum calcium ATPase pumps (SERCA) that pump calcium into the ER lumen from the cytosol in exchange for ATP (Gunteski-Hamblin et al., 1988). Calcium enters the cytosol via channels on the plasma membrane, for example the arachidonic acid-regulated Ca(2+)-selective channels (ARC channels) (Shuttleworth et al., 2007). Influx of calcium from the extracellular space directly into ER, termed store-operated calcium entry (SOCE), can also occur at sites of contact between the ER and the plasma membrane (Marchant, 2005). Many of the ER chaperones that mediate protein folding are also calcium binding and buffering proteins (Michalak et al., 2002), and calcium is an important signalling molecule that can trigger many diverse signalling pathways when released from the ER. Calcium release occurs after inositol triphosphate receptors (IP_3R), which act as gated calcium channels on the ER surface, are activated via the phospholipase C (PLC) pathway. This pathway is triggered when $G_{q\alpha}$-protein coupled receptors, which include the serotonin (Albert and Tiberi, 2001) and histamine (Kuhn et al., 1996) receptors, on the plasma membrane are stimulated, activating PLC. PLC then cleaves phosphatidlyinositol 4,5-bisphosphate in the plasma membrane into diacylglycerol and inositol 1,4,5-triphosphate (IP_3), which diffuses into the cytosol and binds to IP_3 receptors (Berridge, 2009). Calcium release from the ER can trigger an extraordinary range of downstream signalling pathways governing diverse cell processes such as neural plasticity and exocytosis, depending on the cell type and stimulus (Berridge, 2009). For this reason, calcium homeostasis within the ER must be under tight spatial and temporal control. In order to visualize calcium stores in the ER, cells were fixed for electron microscopy using compounds that precipitatated calcium. These precipitates were found specifically in the smooth ER of adipocytes and neurons, demonstrating that the smooth ER is especially important for calcium storage and signalling (Hales et al., 1974; McGraw et al., 1980). Calcium was unevenly distributed within the smooth ER, with greater concentrations found at sites of contact of the smooth ER with lipid droplets (Hales et al., 1974). Calcium handling proteins such as IP_3 receptors, calcium ATPases and the calcium binding protein calsequestrin, are unevenly distributed

within the ER as well, and their localizations do not completely overlap by immunofluorescence microscopy (Takei et al., 1992). This heterogeneity in this distribution of calcium and calcium binding and handling proteins may provide a mechanism for directing the varied downstream effects of calcium signalling.

1.2 Contact sites of ER with other organelles

Although the basic subdivisions of the rough ER and smooth ER have long been identified, it is only recently that it has come to light that the ER is further subdivided (Sitia and Meldolesi, 1992). Aside from protein and lipid synthesis and calcium storage, the ER has several lesser-known functions which are related to and facilitated by contact sites with other organelles (Levine and Rabouille, 2005). These contact sites are summarized in Figure 1.1. The most obvious and best-recognized of these is the formation of the nuclear envelope, which delineates the nucleus of the cell and is contiguous with the rough ER membrane (Anderson and Hetzer, 2007). Likewise, the perinuclear space is contiguous with the ER lumen. Like the rough ER, the outside of the nuclear envelope is covered in ribosomes, but it is distinguished from the remainder of the ER by the presence of nesprins (Zhang et al., 2001). Nesprins rely on an interaction with the inner nuclear envelope proteins to localize to the outer nuclear envelope. There, they act as a bridge between the cytoskeleton and the nucleus, mediating nuclear anchoring and migration (Mellad et al., 2011).

The remainder of ER interorganellar contact sites involve the smooth ER. The transitional ER (tER) is the site of apposition of the ER and Golgi apparatus (Bannykh et al., 1996). This is where ER exit sites (ERES) form and where properly folded and glycosylated proteins leave the ER to progress through the Golgi apparatus and the remainder of the secretory system. Budding and vesiculation of the ER membrane occurs due to the recruitment of coat proteins from the COPII family, which polymerize at ERES and drive membrane deformation (Duden, 2003). The initial formation of ERES is dependent on the localization of Sec16 to the cytosolic side of the ER membrane (Watson et al.,

2006) via a positively-charged central domain of the protein, which may interact with a certain subset of polar phospholipids or a receptor protein at ERES (Hughes et al., 2009; Ivan et al., 2008). Knockdown of Sec16 leads to the dissolution of ERES (Bhattacharyya and Glick, 2007). Several studies now point to the lipid composition of the ER membrane as being important in mediating ERES formation, vesicle budding and ER-Golgi trafficking. COPII component Sar1, a GTPase, has been shown to activate phopholipase D at ERES, causing phosphatidic acid to accumulate at ERES, which is required for vesiculation (Pathre et al., 2003). Furthermore, phosphatidyl inositol 4-phosphate also preferentially accumulates at ERES, and knockdown of the enzyme that catalyzes the formation of this phospholipid, PtdIns (4) KII-alpha, reduces ERES formation (Blumental-Perry et al., 2006).

Sec16 recruits the other components of the COPII coat to the ER membrane. These include the GTPase Sar1, which recruits the Sec23-24 heterodimer. Sec23-24 has several functions; it has a concave surface that could induce membrane curvature, Sec23 is a GTPase activating protein that activates Sar1, and Sec24 binds cargo either directly or through adaptor proteins. A heterotetramer, Sec13-31, binds to Sec 23-24 and forms the outer COPII coat. The mechanisms whereby cargo that is destined for the ERGIC and Golgi is targeted to ERES for packaging into COPII vesicles are not yet fully defined. Receptor proteins such as ERGIC53 and Bap31 that interact with the COPII coat may be responsible for recruiting specific proteins to the vesicles (Lambert et al., 2001; Moussalli et al., 1999). In addition, palmitoylation of certain membrane proteins has been shown to target them to ERES (Abrami et al., 2008; Lam et al., 2006). The COPI coat mediates the retrieval of ER resident proteins and membranes from the ERGIC back to the ER. COPI interacts with the cytosolic adaptor protein PACS-2, which is involved in the formation of another contact site between the ER and mitochondria, which will be discussed in section 1.3.7 (Simmen et al., 2005).

The ER is also the point of origin for peroxisomes, which are organelles that play a role in lipid metabolism, mediating the degradation of fatty acids (Wanders et al., 2010). Peroxisomes can originate at the pre-peroxisomal compartment of the ER and some proteins destined for peroxisomes traffic first through the ER (Mast et al., 2010; Tam et al., 2005). Specifically, Pex19p and Pex3p are required for the import of peroxisomal matrix and membrane proteins. If fluorescently-tagged Pex3p is re-expressed in cells that do not make peroxisomes due to mutations in Pex3p or Pex19p and followed by live-cell microscopy, it traffics first through the ER, and then buds off into newly-made peroxisomes, in a Pex19p-dependent manner (Hoepfner et al., 2005). Without Pex19p, Pex3p becomes trapped in the ER (Hoepfner et al., 2005). Although the mechanisms of vesicular budding at the pre-peroxisomal compartment are not fully elucidated, one component of the COPII coat has been found to localize there (Marelli et al., 2004).

Another lipid metabolism-related organelle originating at the ER is the lipid droplet, where excess triacylglycerol (TG) is stored (Kalantari et al., 2010). Electron micrographs of lipid droplets reveal that they are often in contact with both ER membranes and mitochondria (Walther and Farese, 2009). Lipid droplets originate at sites where DGAT2, an ER protein which catalyzes the final step in TG synthesis, is active (McFie et al., 2011). Several ER proteins, for example the oxidoreductases ERp29 and peroxiredoxin 4, as well as BiP and Calnexin, are found on lipid droplet surfaces, which suggests that lipid droplets might originate from ER (Hodges and Wu, 2010). The integral membrane protein methyltranserase-like 7B (AAM-B) is first targeted to the ER, then to lipid droplets via an N-terminal hydrophobic sequence (Zehmer et al., 2009). Members of the PAT family, the most well-characterized of which is perilipin, also target to the surface of lipid droplets in a COPI and COPII-dependent manner, implying that there is a vesicular trafficking mechanism linking the ER and lipid droplets (Bickel et al., 2009; Soni et al., 2009). However, unlike most other organelles, lipid droplets are surrounded only by a single leaflet of phospholipids, posing

some problems for understanding how they arise (Farese and Walther, 2009), and most models proposed are very speculative.

The ER is also associated with plasma membrane, and this contact site is termed the Plasma Membrane associated membrane, or PAM. This interaction is the site of non-vesicular traffic of sterols and phospholipids from the ER to the plasma membrane. Sleight and Pagano demonstrated that the transport of newly synthesized phosphatidylethanolamine to the plasma membrane was unaffected by drugs that halted vesicular traffic in the cells (Sleight and Pagano, 1983), which led to the hypothesis that lipid trafficking was happening either spontaneously between closely apposed membranes, or via lipid trafficking proteins such as those from the steroidogenic acute regulatory protein related lipid transfer (START) family (Wirtz, 2006). Sterol trafficking also occurs at sites of ER-plasma membrane contacts, and is mediated by lipid transfer proteins from the oxysterol binding protein homologue (OSH) family (Raychaudhuri et al., 2006; Schulz and Prinz, 2007). The PAM is also important in the influx of calcium to the ER from the extracellular space via store-operated calcium entry (SOCE). SOCE is mediated by calcium-release activated calcium (CRAC) channels, which are formed by the oligomerization of Orai1 (Prakriya et al., 2006). The ER protein STIM1 is sensitive to the calcium concentration in the ER lumen, and regulates CRAC channels accordingly. Upon depletion of ER calcium stores, STIM1 translocates to the PAM, oligomerizes and interacts with Orai1, causing CRAC channel assembly and activation (Roos et al., 2005; Zhang et al., 2005). As with Orai1, STIM1 can also interact with transient receptor potential cation (TRPC) channel subunits, causing them to assemble into SOCE channels as well (Yuan et al., 2007).

1.3 The mitochondria associated membrane (MAM) is the site of apposition of ER with mitochondria

The subject of this thesis is the interaction between the ER and the mitochondria, called the mitochondria associated membrane (MAM). It has long been observed

by electron microscopists that the ER and the mitochondria are in close contact with each other, but not fused (Copeland and Dalton, 1959). More recently, the subdomain of the Endoplasmic Reticulum (ER) that makes close contacts with the mitochondria has been termed the Mitochondria Associated Membrane or MAM. Protein tethers have been shown by electron tomography to maintain the distance between the two organelles at the MAM between 10 and 25 nm (Csordas et al., 2006). The MAM is a dynamic structure; live cell microscopy wherein the interplay between the ER and mitochondrial networks is observed has shown that the sites of contact between the two organelles are constantly in flux. The following sections will discuss the functions of the MAM, tools for studying the MAM, mechanisms of MAM formation and protein targeting to the MAM.

1.3.1 Lipid trafficking at the MAM

The first function of the MAM to be elucidated was its role in facilitating lipid transfer from the ER to mitochondria (Rusinol et al., 1994; Vance, 1990). MAM is enriched in proteins involved in lipid biosynthesis and trafficking, such as phosphatidyl serine synthase 1 and 2 (Stone and Vance, 2000), acyl-coA synthase 4 (FACL4) (Lewin et al., 2001), acyl-coA cholesterol acyl transferase (ACAT), and acyl-coA:diacylglycerol acyltransferase (DGAT) (Rusinol et al., 1994). The MAM has been found to play an important role in aminoglycerophospholipid synthesis. Phosphatidylethanolamine (PtdEtn) and phosphatidylcholine (PtdCho) can be synthesized via two pathways: the Phosphatidlyserine (PtdSer) decarboxylase pathway, wherein PtdSer is converted to PtdEtn by decarboxylation, and the Kennedy pathway, wherein ethanolamine or choline are directly incorporated into phopholipids using CDP ethanolamine or CDP choline as an intermediate. In the PtdSer decarboxylase pathway, PtdSer is synthesized on the cytosolic surface of the ER, but requires transport to the mitochondria and inner mitochondrial membrane enzyme PtdSer decarboxylase 1 to complete the synthesis of PtdEtn (Voelker, 2003). PtdCho can be synthesized by the methylation of PtdEtn by PtdEtn N-methyltransferase, which is found on the ER membrane. Therefore, transfer of PtdEtn back to the ER after synthesis in the

mitochondria is necessary for this pathway to occur (Vance, 1991). It has been observed that newly synthesized phospholipids, in contrast to pre-existing phospholipids in the ER and mitochondrial membranes, are more readily translocated between ER and mitochondria and involved in these pathways (Vance, 1991). The importance of the de novo pathway is illustrated by observations that when PtdSer decarboxylase 1 is inhibited, PtdSer accumulates in the MAM fraction, as well as the fact that the majority of PtdEtn is synthesized through this pathway in some cell types (Shiao et al., 1995).

The mechanisms whereby lipids are transported between the ER and the mitochondria are the subject of active research. Many studies support the collision model of lipid transfer, where transfer occurs due to the juxtaposition of the ER and mitochondrial membranes, as transfer occurred in the absence of cytosolic proteins (Vance, 1991). ATP enhances lipid transfer between isolated microsomes and mitochondria in mammalian cells (Voelker, 1989) but not in yeast (Achleitner et al., 1999). Although lipid transfer occurs in vitro in the absence of cytosolic proteins (Voelker, 1989) S100B, a calcium-binding protein with an EF hand domain, enhances lipid transport at MAM (Kuge et al., 2001). Voelker et al have also demonstrated that in yeast, a ubiquitin-ligase, Met30p, regulates transport of PtdSer from MAM to mitochondria (Schumacher et al., 2002). The transfer of lipids between the ER and the mitochondria requires an intact MAM. After the treatment of crude mitochondrial fractions containing MAM with proteases, there was a marked reduction in lipid transfer (Achleitner et al., 1999). Voss et al found that ER shaping proteins, which maintain the tubular structure of the smooth ER, facilitated lipid transfer between ER and mitochondria (Voss et al., 2012), suggesting that MAM contacts where lipid transfer is taking place consist of smooth ER.

1.3.2 Calcium trafficking and signalling at the MAM

As previously mentioned, calcium, which is stored at high concentration in the ER, is a very important second messenger within the cell (Hales et al., 1974;

McGraw et al., 1980). It has long been postulated that different pools of calcium in the cell might be in communication with one another (Schulz et al., 1989), and it has since been demonstrated that one of the important roles of the MAM is to facilitate calcium signalling and homeostasis (Filippin et al., 2003; Rizzuto et al., 1993). The close proximity between the ER and the mitochondria allows for even small changes in the cytosolic calcium level in proximity of the mitochondria, termed calcium puffs, to have a profound effect on signalling (Rizzuto et al., 1998). In fact, calcium signalling at the MAM has been described as having an almost synaptic quality (Csordas et al., 1999). Recent studies have shown that agonist-induced release of calcium caused a cessation of the movements of both the mitochondrial and ER networks (Brough et al., 2005). Moreover, Yi et al demonstrated that upon release of calcium, mitochondria move closer to the ER (Yi et al., 2004). Once released from the ER through the IP_3R, calcium crosses the outer mitochondrial membrane through the voltage-dependent anion channel, or VDAC (Bathori et al., 2006) and is subsequently taken up into the mitochondrial matrix through the inner mitochondrial membrane by the recently identified mitochondrial calcium uniporter (MCU) (De Stefani et al., 2011). There is some evidence calcium signalling between ER and mitochondria goes both ways, in that mitochondrial uptake of calcium can in itself regulate calcium release from IP_3 receptors in smooth muscle cells (Olson et al., 2010).

Transfer of calcium from the ER to the mitochondrial matrix is essential for maintaining the enzymatic reactions that occur in oxidative phosphorylation (Cardenas et al., 2010). In particular, calcium is an important factor for the activation of pyruvate dehydrogenase (PDH), isocitrate dehydrogenase, and α-ketoglutarate dehydrogenase, which catalyze the formation of NADH, driving the tricarboxylic acid (TCA) cycle and ATP production. In cells treated with xestospongin-B to abrogate IP_3R activity, or in cells treated with the MCU inhibitor Ru360, PDH became hyperphosphorylated and inactive, leading to the activation of autophagy, a cell survival response to a lack of nutrients (Cardenas et al., 2010). In addition, mTOR has recently been shown to positively regulate

IP_3R (Fregeau et al., 2011; Regimbald-Dumas et al., 2011), which further ties the cell's nutritional status to calcium signaling.

1.3.3 Apoptotic calcium signalling at the MAM

In addition to its important role in mitochondrial metabolism, ER-mitochondrial calcium transfer at the MAM is also essential for apoptotic calcium signalling (Pinton et al., 2008; Szabadkai and Rizzuto, 2004). Recent studies have shown that interrupting MAM leads to less efficient induction of cell death after apoptotic insult to the cell (de Brito and Scorrano, 2008; Simmen et al., 2005). Moreover, it has also been observed that ER-mitochondrial linkages become tighter and more numerous during stress conditions such as drug induced ER stress or nutrient deprivation (Csordas et al., 2006). Mitochondrial uptake of calcium during apoptosis is dependent on the VDAC1 isoform, which forms a complex with IP_3 receptors on the ER that is strengthened during apoptosis induction (De Stefani et al., 2012). A massive mitochondrial uptake of calcium causes changes in mitochondrial morphology and permeability transition pore opening, leading to the loss of mitochondrial membrane potential and ATP-producing capability (Bernardi and Rasola, 2007). When cytochrome C is released from the mitochondria, it has two apoptotic effects; it both participates in the formation of the apoptosome as well as binding to IP_3 receptors on the ER, causing the release of even greater amounts of calcium from the ER, which amplifies the apoptotic signal (Boehning et al., 2003). The ER and mitochondria are therefore mutually dependent on one another during the activation of cell death pathways.

Cell death can initiate at the ER when ER homeostasis has been disrupted, either by the accumulation of unfolded proteins or the depletion of calcium from the ER lumen. In mice, a member of the caspase family called caspase-12 is associated with the cytosolic face of the ER and is activated specifically by ER stressors, but not by extrinsic or mitochondrial cell death triggers (Nakagawa et al., 2000). A caspase-12 homologue has not been found in humans. However, caspase-8,

which has very limited substrate specificity, has been associated with the apoptotic cleavage of ER-localized proteins (Breckenridge et al., 2002). The formation of apoptotic complexes has also been reported at the MAM. The ER protein Bap31 is cleaved by caspase-8 upon activation of cell death receptors at the cell surface to create a pro-apoptotic fragment called p20, which releases calcium from the ER (Breckenridge et al., 2003a; Breckenridge et al., 2002). This leads to mitochondrial fission and release of cytochrome c to the cytosol (Breckenridge et al., 2003b). Calnexin has been proposed to act as a scaffold for this complex formation (Guerin et al., 2008), and in its absence, Bap31 cleavage is impaired (Groenendyk et al., 2006). Bap31 is also involved in the formation of another complex during apoptosis onset. Fis1, a mitochondrial fission protein, and Bap31 associate (Iwasawa et al., 2011), bridging the MAM and recruiting caspase-8. Furthermore, the pro-apoptotic translocation of Bid to mitochondria and cleavage of Bid to t-Bid is also mediated by caspase-8 and requires the presence of PACS-2, a protein involved in MAM formation (Simmen et al., 2005).

1.3.4 The role of chaperone proteins at the MAM

The chaperone protein whose MAM localization is best characterized is the Sigma1 receptor (Hayashi and Su, 2007). Sigma1 receptors form a complex with IP_3R at the MAM, stabilizing them and protecting them from degradation, and prolonging calcium signalling from ER to mitochondria in the event of ER stress. Sigma1 receptors also form a complex with the ER chaperone BiP, which dissociates as the ER calcium concentration drops during ER stress. Furthermore, the Hayashi and Su also demonstrate that the Sigma1 receptor has an anti-aggregation and chaperone activity in a citrate synthase refolding assay. Recently, a novel splice variant of Sigma1 receptor has been characterized, giving more insight into the functions of the protein. Unlike full-length Sigma1 receptor, the truncated variant does not interact with IP_3 receptors at the MAM, although it does interact with its full-length version. Expression of the truncated form of

Sigma1 receptor has a detrimental effect on mitochondrial metabolism and increases the cell's susceptibility to apoptosis (Shioda et al., 2012).

There is evidence of several other chaperone proteins localizing to MAM or having MAM related functions. As part of the Sigma1 receptor study, other ER chaperones including BiP and calreticulin were found to localize to MAM (Hayashi and Su, 2007). Calnexin and calreticulin, which are lectin chaperones involved in quality control of glycoprotein synthesis in the ER, have both been demonstrated to play roles in modulating SERCA2b function and calcium signalling (Li and Camacho, 2004; Roderick et al., 2000). Furthermore, calreticulin also acts as a calcium buffer within the ER lumen and can inhibit IP_3 receptor mediated calcium signalling (Camacho and Lechleiter, 1995). A cytosolic chaperone protein, Grp75, is also known to associate with IP_3 receptors and VDAC at the MAM, mediating ER-mitochondria contacts. However, it is unclear whether Grp75 has any chaperone function in this complex (Szabadkai et al., 2006). Several chaperone proteins involved in oxidative protein folding also localize to MAM and play important roles there, and they will be discussed in the next section.

Importantly, many chaperone proteins such as BiP and calnexin depend on ATP for their folding functions (Braakman et al., 1992; Wada et al., 1994). Furthermore, many of the other functions that the ER performs are powered by ATP, including the import of calcium by SERCA2b (Gunteski-Hamblin et al., 1988), protein synthesis, translocation, folding, and retrotranslocation, and lipid transport (Voelker, 1989). Consistent with the dependence of many ER enzymes on ATP availability, low glucose conditions or inhibition of the mitochondrial electron transport chain cause ER stress and block the production of secretory proteins (Kozutsumi et al., 1988; Osibow et al., 2006). Overexpressing mitochondrial adenine nucleotide translocase, which mediates export of ATP from the mitochondrial matrix to the rest of the cell, has been shown to reduce ER to mitochondria calcium transfer (Wieckowski et al., 2006), which demonstrates

the mutual dependence of the various signalling and transport events occurring at the MAM.

1.3.5 The relationship between oxidative protein folding and calcium signaling at the MAM

Oxidative protein folding, or the formation of disulphide bonds between cysteines in a protein's sequence, is one of the many important functions of the ER. One of the defining characteristics of the ER is that the lumen is far more oxidizing than the cytoplasm. This allows a special group of chaperone proteins known as oxidoreductases mediate disulphide bond formation and isomerization between cysteines, allowing for the proper folding of the protein into its native conformation. Protein Disulphide Isomerase (PDI) is the most well-known of this group of chaperone proteins (Klappa et al., 1997), using its CXXC motif to form mixed disulphides with substrates that have reduced free cysteines or incorrect disulphide bonds (Horibe et al., 2004; Walker and Gilbert, 1995). A key component of this system is Ero1α, the oxidoreductase that mediates the reoxidation of PDI after its enzymatic reaction (Cabibbo et al., 2000; Pagani et al., 2000). Ero1α accomplishes this using its CXXCXXC active site and subsequently transferring electrons from cysteines to molecular oxygen using its flavin adenine dinucleotide (FAD) prosthetic group.

We have recently demonstrated that Ero1α is a MAM-enriched protein (Gilady et al., 2010). Retention of Ero1α at the MAM requires normoxic and oxidizing conditions, although the exact mechanism of Ero1α's MAM targeting is unknown. During hypoxia, or when the cell is treated with reducing agents, Ero1α was released from MAMs and secreted from the cell (Gilady et al., 2010). Ero1α has also recently been shown to regulate calcium signaling at the MAM (Anelli et al., 2003), which is consistent with studies demonstrating that it can stimulate the function of IP_3 receptors during apoptosis (Li et al., 2009), and also has a calcium binding domain. Furthermore, Ero1 proteins require FAD for their function and depend on the availability of free FAD in the ER lumen (Tu and Weissman,

2002). FAD is synthesized from riboflavin by FAD synthase in the mitochondrial matrix, where it is a key cofactor in the tricarboxylic acid cycle and oxidative decarboxylation (Barile et al., 2000). The importance of the relationship between FAD production in the mitochondria and Ero1 function in the ER is illustrated by the finding that riboflavin deficiency impairs oxidative protein folding and protein secretion (Depeint et al., 2006; Manthey et al., 2005). Although the carrier protein required for transfer of FAD from the mitochondria into the ER in mammalian cells is unknown, these proteins have been identified in yeast (Protchenko et al., 2006). However, it is not known whether FAD carriers localize to MAM.

Two members of the PDI family are involved in the regulation of calcium signalling at the ER by virtue of their interactions with SERCA2b and the IP_3 receptor. ERp57 is well known for its interaction with calnexin, which allows it to mediate disulphide bond formation in a specific subset of glycoproteins (Jessop et al., 2007). However, it also interacts with SERCA2b's ER luminal cysteines under oxidizing conditions in the ER lumen, thus inhibiting SERCA2b's calcium pumping function (Li and Camacho, 2004). Conversely, ERp44 interacts with the luminal cysteines of IP_3 receptor type I when conditions in the ER lumen are reducing or luminal calcium concentration is low, inhibiting calcium signalling (Higo et al., 2005). This redox dependent control of ER calcium homeostasis serves to keep input and output of calcium under tight control, and illustrates the interdependence of the ER redox state and ER calcium concentration. In addition to its role in modulating SERCA2b function, ERp57 also modulates store operated calcium influx via its interaction with STIM1 at ER-plasma membrane contact sites (Prins et al., 2011).

1.3.6 Tools for studying the MAM

A variety of imaging methods, biochemical fractionation methods and functional assays have been used to study the MAM, each having their own particular strengths and drawbacks. As previously mentioned, the earliest observations of

the MAM were made by electron microscopy (Copeland and Dalton, 1959). The resolution of electron microscopy is sufficient to distinguish the ultrastructure of the cell, and measure the distance between the ER and mitochondrial membranes. Electron microscopy can be enhanced by immunostaining techniques, called immuno EM, using antibodies conjugated to gold particles of varying sizes, and can therefore be used to study protein localization to the MAM. Disadvantages of electron microscopy include the impossibility of visualizing live cells, the incompatibility of certain antibodies with fixation techniques, and the propensity of fixation techniques to distort cellular membranes. Even more information about intracellular structures can be obtained by electron tomography, which images by sections of a sample that can then be reconstituted into a 3D image. Using this technique, Csordas et al were able to demonstrate the proteinaceous tethers that hold the MAM in place (Csordas et al., 2006).

Fluorescence microscopy and live-cell fluorescence microscopy have been widely used to study ER-mitochondrial contact sites. Fluorescent dyes and targeted fluorescent proteins such as aequorins (Rizzuto et al., 1998) can be used in order to study the interplay between the two organelles, and learn how contact sites are affected by overexpressing or knocking down a specific protein, drug treatments, or other parameters. Immunostaining techniques using fluorescently tagged antibodies can also be used to visualize the colocalization of specific ER proteins with mitochondria. Colocalization of ER and mitochondria or of ER proteins with mitochondria can be measured by establishing a Mander's coefficient describing overlap between two fluorescent signals (Manders et al., 1996) As the resolution limit of fluorescence microscopy is greater that the span of the MAM, these experiments must be very cautiously interpreted and are not sufficient to establish the MAM localization of a protein. However, dimerization-dependent fluorescent proteins can be used to visualize contact sites between organelles. In this technology, two non-fluorescent monomers are targeted to mitochondria and MAM, respectively, by creating chimeras of the fluorescent monomers with a mitochondria and MAM-localized protein. Contact sites between the two

organelles lead to dimerization and fluorescence of the monomers (Alford et al., 2012). One of the big advantages of fluorescence microscopy is that it can be used to study MAM in live cells, which is important because ER-mitochondria contact sites are dynamic. Confocal fluorescence microscopy can be an especially valuable technique when used in conjunction with electron tomography as in an elegant study of ER-mitochondria contacts and mitochondrial fission (Friedman et al., 2011).

Biochemical fractionation methods have also been used to study the MAM and its lipid and protein composition. MAM was first biochemically isolated from rat liver cells in 1990 (Vance, 1990). In this method, tissue is first homogenized and differential centrifugation fractionation is used to obtain a crude mitochondrial fraction, which includes mitochondria and some ER membranes. The ER component of the crude mitochondrial fraction is then separated from mitochondria by Percoll density fractionation. This ER fraction has been found to have a different lipid and protein composition than the rest of the ER (Vance, 1990). This technique has since been adapted for use with mammalian cells (Wieckowski et al., 2009). A great deal of care must also be taken in selecting the appropriate homogenization method, Percoll percentage and centrifugation parameters for the cell line or tissue used, lest the MAM fraction become contaminated with rough ER. Careful use of marker proteins is also required in order to establish the efficacy of the fractionation. Another difficulty with the Percoll fractionation technique is the large amount of starting material that must be used in order to visualize the MAM band after Percoll fractionation. In order to circumvent this difficulty, a number of studies have simply compared crude mitochondrial fractions to microsomal fractions, ignoring the mitochondrial component of the crude mitochondrial fraction (Delom et al., 2007). This can be useful when it has already been established that the protein being studied is not present in mitochondria.

In addition to microscopical methods to study ER-mitochondrial contacts and biochemical methods to isolate the MAM, several assays to analyze the primary functions of the MAM have been developed. Firstly, calcium-sensitive fluorescent dyes or proteins can be used to measure calcium levels (Bononi et al., 2012; Rizzuto et al., 1998). By targeting these dyes or proteins to the ER or cytosol, the release of calcium from the ER upon stimulation of IP3 receptors or disabling SERCA2b pumps can be measured. In order to measure the uptake of calcium by the mitochondria after it has been released from the ER, a mitochondrially-targeted protein or fluorescent dye can be used, such as GEM-GECO1 (Zhao et al., 2011), aequorin (de Brito and Scorrano, 2008) or Rhod2 (Fonteriz et al., 2010). Alternatively, cytosolic calcium levels can be measured with or without disabling the mitochondrial calcium uniporter with ru360. The difference between the two measurements can be used to assess the effect of mitochondrial calcium buffering (De Stefani et al., 2012). Using fluorescent dyes or targeted fluorescent proteins, the transfer of calcium from the ER to mitochondria can be visualized and even quantified by flow cytometry, fluorimetry, and live cell microscopy.

The translocation of PtdSer to the mitochondria, where PtdSer decarboxylase is located, during the synthesis of PtdEtn is dependent of ER-mitochondria apposition. Therefore, the biochemical analysis of lipid synthesis can also be used to measure MAM function. To measure the decarboxylation of newly synthesized PtdSer to PtdEtn or lysoPtdEtn by mitochondrial PtdSer decarboxylase, isolated MAM and mitochondria are co-incubated with tritiated serine, then lipids are isolated from the membranes and the incorporation of radioactivity into each lipid is measured (Shiao et al., 1998; Vance, 1991). The incorporation of radioactivity into the decarboxylation products PtdEtn and lysoPtdEtn is compared with the total radioactivity incorporated into PtdSer, PtdEtn and lysoPtdEtn combined, to give an indication of phospholipid translocation to mitochondria. MAM can also be pre-labelled with tritiated PtdSer, then incubated with mitochondria before calculating the percentage of

translocation-dependent decarboxylation that occurs (Shiao et al., 1998). Acyl-CoA: cholesterol acyltransferase 1 (ACAT1) is the enzyme that catalyzes the conversion of cholesterol to cholesterol ester, and is also enriched in MAM (Lee et al., 2000; Rusinol et al., 1994). For this reason, analysis of cholesterol levels has also been used to study MAM function (Area-Gomez et al., 2012).

1.3.7 Mechanisms of MAM formation

Several proteins have been found to play a role in maintaining the structural integrity of the MAM. These include tethering protein complexes that form a physical link between the ER and mitochondrial membranes. One example of a tethering complex is the ER-Mitochondria Encounter Structure (ERMES) complex that was identified in yeast by an elegant screening study (Kornmann et al., 2009; Kornmann and Walter, 2010). The screen identified yeast mutants with phenotypes that could be rescued by expressing an artificial protein tether between the ER and mitochondria. ERMES is composed of four proteins: two integral outer mitochondrial membrane proteins, Mdm10 and Mdm34, one ER transmembrane protein Mmm1, and a cytosolic protein, Mdm12. When the components of the ERMES complex are mutated, metabolic flow through the aminoglycerophospholipid biosynthesis pathway was slowed, but not completely abrogated, indicating that ERMES plays a role in lipid transfer at MAMs but is not entirely responsible (Kornmann et al., 2009). ERMES mutants also display a variety of mitochondrial phenotypes including enlarged, spherical mitochondria and compromised respiratory growth. The size and number of ERMES complexes in yeast can be regulated by the calcium-sensitive GTPase Gem1 (Kornmann et al., 2011). The human orthologue of Gem1, Miro-1, also localizes to sites of ER-mitochondria contact marked by ERMES (Kornmann et al., 2011). Interestingly, Miro-1 is an atypical Rho GTPase that is responsible for mitochondrial trafficking and the morphology of the mitochondrial network (Fransson et al., 2006).

Recently, Nguyen et al. found that Gem1 and ERMES are not in fact involved with lipid transfer and their role is confined to tethering ER to mitochondria and regulating mitochondrial morphology. They provide evidence that the lipid transfer defects discovered upon deletion of ERMES components are rather a secondary consequence of the loss of ER mitochondrial tethering (Nguyen et al., 2012). Indeed, current models of the role of ERMES complex at the MAM suggest that ERMES merely increases the efficiency of soluble lipid transporters such as oxysterol-binding proteins and ceramide transporters (D'Angelo et al., 2008). However, their studies do confirm the importance of the ERMES complex as a stable ER-mitochondrial tether, and reiterate the importance of this tethering to various MAM functions including lipid transfer and regulation of the ER and mitochondrial networks.

The identification of ER-mitochondria tethering complexes has not been limited to yeast. Homologues of ERMES complex members have been discovered in *Neurospora Crassa*, however, unlike in yeast, the main functions of the proteins were the assembly of β-barrel proteins in the outer mitochondrial membrane, and control of mitochondrial morphology (Wideman et al., 2010). Three members of the ERMES complex, Mdm12p, Mdm34p and Mmm1p, contain synaptotagmin-like, mitochondrial and lipid-binding protein (SMP) domains with extremely diverse functions (Lee and Hong, 2006). Interestingly, SMP domains have been implicated in targeting proteins to membrane contact sites in yeast (Toulmay and Prinz, 2012). Along with the ERMES complex at the MAM, SMP domains play a role in targeting proteins to the nucleus-vacuole junction (NVJ) and ER-plasma membrane contact sites, or PAM. Although human homologues of the ERMES complex members have not been identified and the search for functional orthologues containing SMP domains is ongoing, several unrelated tethering complexes have been identified in mammalian cells. The VDAC-GRP75-IP_3R complex has mitochondrial, cytosolic and ER components, respectively, and was discovered by subjecting the purified MAM fraction of rat liver cells to 2D blue native PAGE followed by SDS-PAGE. These results were then corroborated by

coimmunoprecipitation experiments (Szabadkai et al., 2006). The findings extend the function of this complex from merely a structural tether to playing a role in calcium transfer from ER to mitochondria. Furthermore, another tethering complex forms between Bap31 on the ER and mitochondrial fission protein Fis1, which bridges the MAM under resting conditions. During apoptosis, caspase-8 is recruited to the complex causing the formation of the pro-apoptotic Bap31 fragment, p20 (Grimm, 2012; Iwasawa et al., 2011).

Mitofusins (MFN) 1 and 2 are GTPases that are involved in mitochondria tethering and fusion. MFN2 is of particular interest because it has lower GTPase activity and is therefore thought to have a greater role in tethering than in fusion (Ishihara et al., 2004), and because MFN2 knockout mouse embryonic fibroblasts (MEFs) display altered ER morphology along with the expected fragmented mitochondrial network. Percoll MAM fractionation demonstrated that MFN2 was in fact found in MAM membranes as well as on mitochondria, whereas MFN1's distribution was confined to mitochondria. Depletion of MFN2 led to a reduction of the juxtaposition of the ER with mitochondria as well as a loss of ER-mitochondrial calcium signalling and defects in the morphology of the ER and mitochondrial networks (de Brito and Scorrano, 2008).

Other proteins have been shown to play less direct roles in the formation and maintenance of MAM. The Phosphofurin acidic cluster sorting protein (PACS)-2 has been shown to play a role in the formation of MAM (Simmen et al., 2005). Although the mechanism by which it happens is unknown, PACS-2 works in conjunction with the cytosolic protein coat COPI, which mediates retrieval of vesicles from the cis-Golgi to the ER (Beck et al., 2009), suggesting that the ER-Golgi trafficking may play a role in the distribution of proteins to the MAM. Depleting cells of PACS-2 using siRNA led to a decrease in the apposition of the ER with the mitochondria, as observed by immunofluorescence microscopy and electron microscopy. Furthermore, absence of PACS-2 altered calcium signals from the ER and interfered with the uptake of calcium by mitochondria, delaying

the induction of apoptosis. The GTPase Rab32 also regulates the composition of the MAM by an unknown mechanism, and active Rab32 has been shown to relocalize MAM proteins to the periphery of the cell and alter cellular calcium signalling (Bui et al., 2010). There is also some evidence that the mitochondrial fission protein Drp1 is involved in controlling the apoptotic response to calcium signalling by fragmenting the mitochondrial network and preventing the uptake of calcium by mitochondria (Szabadkai et al., 2004). The authors reason that as the number of ER-mitochondria contact sites remained constant even as the mitochondrial network fragmented, more mitochondria would be isolated from the ER.

Nogo B is a member of the reticulon family of proteins, which controls the formation of tubular smooth ER. Sutendra et al. (2011) have observed that Nogo B expression is increased in the pulmonary arteries of patients suffering from pulmonary arterial hypertension (PAH), a disease that features overproliferation of vascular cells, which narrows the arteries and increases arterial pressure. Abnormally high levels of Nogo B in response to hypoxia disrupted the formation of ER mitochondria contacts, which resulted in a decrease of mitochondrial calcium and subsequent downregulation of mitochondrial metabolism, as described in section 1.3.2. The authors postulate that as in the Warburg effect observed in tumour cells, this alteration in mitochondrial metabolism is responsible for the overproliferation of vascular cells observed in PAH (Dromparis et al., 2010). In mouse models of hypoxia-induced PAH, Nogo B is required for the disruption of MAMs, mitochondrial metabolism phenotype and subsequent development of the disease (Sutendra et al., 2011). These data strongly suggest that Nogo B plays a role in the regulation of MAM formation.

1.3.8 MAM-enriched proteins and their targeting mechanisms

The proteins related to the MAM functions described above as well as many others are known to be found in MAM, and furthermore, some are specifically enriched in this subcompartment. The physical characteristics of MAM and of

these proteins that lead to this specific enrichment are not yet well understood. As the MAM functions that have been described so far are important for cell functions and MAM-resident proteins are essential for these functions, a better grasp of MAM targeting mechanisms is crucial to understanding the cell biology of the MAM.

There is good evidence that specific targeting mechanisms exist for several MAM-localized proteins. Acyl-CoA:diacylglycerol acyltransferase (DGAT)2 is an enzyme that catalyzes the final step in triacylglycerol (TG) synthesis. This process is highly spatially regulated, and different aspects of TG synthesis and storage take place on different membranes, including those of the ER and mitochondria. When cells are stimulated with oleate to produce TG, DGAT2 localizes to the surface of lipid droplets, where mitochondria are also found. Efforts to determine the subcellular localization of DGAT2 by biochemical fractionation pointed to the MAM. A cryptic mitochondrial localization signal was found within the cytoplasmic tail of DGAT2: while full-length DGAT2 is a transmembrane ER localized protein, a 67-amino acid fragment of its cytosolic N-terminus targeted RFP to mitochondria. This fragment contained a sequence consisting of 3 positively –charged amino acids that were necessary to target RFP to mitochondria (Stone et al., 2009). The authors hypothesize that this sequence within the tail of DGAT2 retains the protein at the MAM by tethering it to mitochondria. If this is the case, DGAT2 may also play a role in the structural integrity of the MAM, by physically linking ER and mitochondria, although this was not tested.

It has long been known that MAM contains many lipid synthesis and transfer enzymes, such as phosphatidyl serine synthase and acetyl-CoA:cholesterol acyltransferase (ACAT1) and DGAT2, however, it was not known whether the actual lipid content of the MAM was different from that of the rest of the ER. The lipid composition of the MAM was compared to that of the rest of the ER following biochemical fractionation of MAM from microsomes (Hayashi and

Fujimoto, 2010). It was found that MAM contained higher amounts of cholesterol and ceramide than the microsomal fraction. It is not certain whether the presence of the lipid synthesis enzymes influences the lipid composition of the MAM, but it has been determined that lipid microdomains at the MAM determine the targeting of certain proteins, specifically the Sigma-1 receptor and IP_3 receptor (Hayashi and Fujimoto, 2010). There is also considerable evidence that the MAM consists of detergent-resistant microdomains (Area-Gomez et al., 2012; Hayashi and Fujimoto, 2010; Lynes et al., 2012; Sano et al., 2009). Hayashi and Fujimoto demonstrated that the localization of Sigma-1 receptor to MAMs depends on the cholesterol content of the membrane (2010). There is evidence that lipid microdomains at the ER-plasma membrane interface regulate store-operated calcium entry by clustering STIM1 at the PAM in proximity with store-operated calcium channels (Pani et al., 2008). It is therefore plausible that lipid rafts or microdomains with high cholesterol content are performing a similar function in calcium signalling at the MAM. However, Fugimoto et al. demonstrated that treatment of MAM and mitochondria with methyl-b-cyclodextrin, which depletes cholesterol from membranes, actually increased ER-mitochondria apposition and the MAM translocation-dependent production of PtdEtn from radiolabelled PtdSer (Fujimoto et al., 2012). Clearly more investigation is required to determine the role of lipid microdomains and cholesterol content in MAM targeting and function.

1.4 Protein palmitoylation, its regulation and its importance in transmembrane protein targeting and trafficking

The palmitoylation of transmembrane proteins has been implicated in protein targeting to lipid microdomains (Charollais and Van Der Goot, 2009), such as the ones found at the MAM. Palmitoylation is a post-translation lipid modification that involves the attachment of palmitate, a 16-carbon long chain fatty acid, to cysteine residues within a protein. Palmitoylation is a reversible process that is mediated by a growing family of putative palmitoyl acyltransferases (PAT), polytopic membrane proteins that are characterized by a DHHC motif (Asp-His-

His-Cys) within a cysteine-rich domain. Although there is no consensus sequence for palmitoylation, palmitoylated cysteines are often found next to other lipid modification sites, such as myristoylation sites, within a region of hydrophobic or basic amino acids, and adjacent to or within transmembrane domains (Salaun et al., 2010). Protein palmitoylation often has consequences for the trafficking of that protein; there are several examples of transmembrane proteins that require palmitoylation to be trafficked into ER exit sites, including Chs3 (Lam et al., 2006) and LRP6 (Abrami et al., 2008). Defects in protein palmitoylation have been implicated in human disease, particularly neurological and psychiatric disease (Young et al., 2012). Three proteins that mediate the removal of palmitate have also been identified: acylprotein thioesterases 1 and 2 (APT1 and -2) and protein palmitoyl thioesterase PPT1. APT1 and 2 have been shown to play a role in palmitoylation cycling for several proteins, notably H-Ras (Dekker et al., 2010), but have not found to be implicated in human disease. PPT1, on the other hand, is localized to lysosomes and deletions or mutation of the gene have been shown to be responsible for infantile neuronal ceroid lipofuscinosis (INCL) (Kim et al., 2006). Although PPT1 localizes to lysosomes, there is compelling evidence that its absence causes abnormal accumulation of palmitoylated proteins in the ER, ER stress and apoptosis, which may be the mechanism underlying the neurodegeneration seen in INCL. Interestingly, in another model of neuronal ceroid lipofuscinosis MAMs were defective, leading to a redistribution of certain mitochondrial proteins to the ER, and a decrease in expression and activity of certain MAM-specific phospholipid biosynthetic enzymes (Vance et al., 1997).

1.4.1 Detection of protein palmitoylation

There are two main methods whereby protein palmitoylation can be detected in the cell. The original method involves palmitate analogues radioactively labelled with either [^{3}H] or [^{125}I] (Berthiaume et al., 1995). The disadvantages of these methods are exposure of lab personnel to radiation and the length of time required to detect palmitoylated proteins by autoradiography, as long as 3 months. More recently, an alternative, safer, non-radioactive method has been developed, which

also accelerated the detection of palmitoylated proteins. In this method, a palmitic acid analog, ω-alkynyl palmitate, is incorporated in proteins. The palmitic acid analog can then be detected by click chemistry, as described by Yap et al. (Kostiuk et al., 2009; Yap et al., 2010) and in the Materials and Methods section (Chapter 2).

1.5 The MAM in human health and disease

1.5.1 Alzheimer Disease

As the MAM is the interface between the ER and mitochondria and mediates calcium signalling between the two organelles, it follows that MAM functions and MAM proteins are implicated in human disease, particularly those disease where apoptosis is implicated, such as cancer and neurodegenerative disease. Perhaps the best-studied example is Alzheimer Disease (AD) (Area-Gomez et al., 2009; Area-Gomez et al., 2012; Schon and Area-Gomez, 2012). The key feature of AD is the death of hippocampal and cortical neurons, which leads to the loss of cognitive and physical abilities, and inevitably, death (Goedert and Spillantini, 2006). Although the reasons for neuronal cell death are not yet completely understood, there are many changes at the cellular level that feature in AD. In normal cells, the amyloid precursor protein (APP), a type I transmembrane protein and is subject to cleavage by α- and β-secretases, at the plasma membrane or in endosomes, which generate non-pathogenic fragments. The normal role of APP in neurons is not well understood, although the most convincing evidence shows that it is involved in the formation and repair of synapses (Priller et al., 2006). In AD, there is an abnormal increase in APP processing by the γ-secretase enzyme complex, forming Amyloid-β (Aβ), which is secreted from cells causing extracellular plaques consisting primarily of Aβ to form. However, the localization of APP processing by γ-secretase has been the subject of some debate. Mutations in APP and the presenilin proteins that lead to altered processing of APP or the increased production of Aβ are thought to underlie the inherited or familial form of AD (Goedert and Spillantini, 2006).

Most interestingly in the context of MAM research, calcium homeostasis (Bezprozvanny and Mattson, 2008) and mitochondrial function is altered in neurons affected by AD (Wang et al., 2009; Wang et al., 2008), as well as lipid metabolism (Stefani and Liguri, 2009). Recently, it was reported that presenilins-1 and -2, which form part of the γ-secretase enzyme complex that cleaves amyloid precursor protein, localize to the MAM, along with APP (Area-Gomez et al., 2009). It was already known that γ-secretase activity is concentrated in lipid rafts and that amyloidogenic processing of APP occurs in lipid rafts (Ehehalt et al., 2003; Vetrivel et al., 2004), but until recently, it was thought that lipid rafts were mainly found in the plasma membrane. This created a spatial paradox in the model of AD progression, as APP and γ-secretase colocalize to the greatest extent in the ER and Golgi, and γ-secretase cleavage of APP is thought to occur in pre-Golgi compartments, perhaps in the ERGIC (Annaert et al., 1999; Cupers et al., 2001). However, more recently several groups have shown that MAM has lipid raft characteristics (Area-Gomez et al., 2012; Hayashi and Fujimoto, 2010; Sano et al., 2009), partially resolving this paradox. Area-Gomez et al. (2012) also demonstrated that presenilins may have an alternative role in AD pathology, in addition to their role in APP cleavage to Aβ. They reported that deletion of one or both presenilins increased ACAT1 activity and cellular cholesterols levels and increased the rate of phospholipid synthesis. In addition, the morphology of ER-mitochondrial contacts in presenilin knockout cells changed, becoming much larger, which could explain the increase in lipid transfer and synthesis observed. Interestingly, deletion of the presenilins also caused a proliferation of lipid droplets (Area-Gomez et al. 2012), which prompts a comparison with DGAT2, which is also a link between MAM and lipid droplets (Stone et al., 2009), and localizes to both. Zampese et al also reported that knockdown of presenilin-2, but not presenilin-1, or expression of PS2 mutants form in familial AD, increased ER mitochondrial contacts and calcium signalling at MAMs (Zampese et al., 2011).

The authors also demonstrated that mitofusin-2 (MFN2), a MAM-tethering and mitochondrial fusion protein (de Brito and Scorrano, 2008), and the presenilins

have opposing and related functions. This is not too surprising, as overproduction of Aβ has been shown to fragment the mitochondrial network and redistribute it to the perinuclear area (Wang et al., 2008). MFN2 deficient cells had reduced γ-secretase activity, although presenilin localization remained unchanged. Furthermore, while knocking down MFN-2 reduced the apposition of ER and mitochondria and disrupted calcium signaling at the MAM (de Brito and Scorrano, 2008), deletion of presenilins in this background restored MAMs, indicating that MFN-2 and presenilins may have opposing actions. Conversely, MFN2 knockdown in presenilin knockout cells corrected the increased MAM phenotype seen in presenilin knockout cells (Area-Gomez et al. 2012). Although many questions remain regarding the role of presenilins at the MAM, these findings open up an exciting new horizon in AD research and help to explain the calcium and lipid homeostasis defects seen in the disease.

1.5.2 Viral trafficking of MAM proteins

There have been several reports that mitochondrially-targeted viral proteins are synthesized in the ER and subsequently trafficked to the mitochondria through MAMs. One example of such a protein is the Human Cytomegalovirus (HCMV) UL37 exon 1 protein (pUL37x1) (Bozidis et al., 2008). HCMV impacts human health because fetuses whose mothers are infected or who suffer a reactivation of a prior infection during pregnancy are born congenitally infected, which can cause brain abnormalities, and hearing and vision loss. UL37x1 is an immediate early gene, meaning that it is among the first to be expressed following expression, and it is one of several UL37 isoforms. Many immediate early proteins have anti-apoptotic properties, and pUL37x1 is no exception; it is also known as vMIA, or viral mitochondria-localised inhibitor of apoptosis. Like its name suggests, pUL37x1/vMIA needs to traffic to the mitochondrial outer membrane in order to fulfill its anti-apoptotic function. There, it sequesters Bax and prevents Bax-mediated permeabilization of the mitochondrial membrane (Arnoult et al., 2004; Poncet et al., 2004). However, all UL37 isoforms first traffic to the ER, where they are inserted into the membrane by an N-terminal hydrophobic leader

sequence (Williamson and Colberg-Poley, 2009). From there, three isoforms, pUL37x1, pUL37NH2 and gpUL37COOH, traffic into MAM (Bozidis et al., 2008; Mavinakere et al., 2006). However, from the MAM only pUL37x1 and pUL37NH2 traffic to mitochondria, whereas pUL37COOH can migrate to the Golgi apparatus. Williamson and Colberg-Poley (2010) identified a signal sequence adjacent to the hydrophobic leader sequence that was required for mitochondrial import. Also of interest is the fact that pUL37x1/vMIA stimulate release of calcium stores from the ER, perhaps by interacting with calnexin or SERCA2b. Indeed, pUL37x1/vMIA colocalized with both these proteins, in immunofluorescence microscopy experiments, but not with the ER chaperone PDI, which is not MAM-localized (Sharon-Friling et al., 2006). Although it is not known whether this release of calcium occurred at MAMs, it is tempting to speculate that that might be the case.

Hepatitis C Virus (HCV) causes hepatitis, which in chronically infected individuals can lead to liver cirrhosis or hepatocellular carcinoma (Di Bisceglie, 1998). Translation of the HCV open reading frame results in a 3000 amino acid polyprotein that is subsequently cleaved into 10 different proteins by both cellular and viral proteases. The subcellular distribution of HCV core protein is fairly ubiquitous; it has been found mainly in the cytosol, but with populations in lipid droplets, in the nucleus, associated with the Golgi compartment, on the outer mitochondrial membrane, and most interestingly, on rER in proximity to mitochondria (Williamson and Colberg-Poley, 2009). Targeting to ER and mitochondria depends on amino acid sequences containing an amphipathic alpha-helix domain (Suzuki et al., 2005), but also on the expression level of the protein. HCV core protein has been implicated in altering several cellular functions that rely on MAM, such as lipid metabolism and apoptosis induction (Williamson and Colberg-Poley, 2009), however, it is unknown whether HCV core protein relies on transit through the MAM to achieve these effects.

A third example is HIV-1 Viral Protein R (Vpr) (Huang et al., 2012). Vpr has been implicated in the killing of CD4+ T lymphocytes that is a hallmark of HIV by mediating DNA damage response, cell cycle arrest and apoptosis. Like pUL37x1/vMIA, Vpr has been shown to traffic to mitochondria, but in contrast, there it permeabilizes the outer mitochondrial membrane and increases susceptibility of the cell to apoptosis. The mechanism of Vpr trafficking to mitochondria is unclear. Vpr is integrated into the ER membrane and the outer mitochondrial membrane (OMM) by its C-terminal transmembrane domain. Vpr overexpression led to a reduction in the amount of MAM-tethering protein MFN2 and a reduction in mitochondrial membrane potential, as well as morphological changes to the ER and mitochondria. The authors observed transport vesicles containing Vpr forming at the MAM and fusing with the mitochondrial membrane by time-lapse confocal fluorescence microscopy, and hypothesized that this could be one mechanism mediating the transit of viral proteins from the ER to the OMM.

Although the mechanisms whereby translocation of proteins from the ER membrane to the mitochondrial outer membrane occurs are not known, several intriguing possibilities have been suggested. Lipid microdomains at the MAM may be responsible for protein targeting to the MAM, and treatment with the cholesterol-depleting drug methyl β cyclodextrin reduced trafficking of UL37 exon 1 to the MAM (Williamson et al., 2011), like in the case of the sigma 1 receptor (Hayashi and Fujimoto, 2010). These microdomains could also be responsible for mediating trafficking between ER and mitochondrial membranes. It is also possible that viral proteins somehow take advantage of mechanisms such as transport proteins used to exchange lipids from the ER membrane to the mitochondria (Williamson and Colberg-Poley, 2009). Interestingly, some microscopical evidence of vesicular trafficking of Vpr between the MAM and mitochondria has come to light, and perhaps this mechanism applies to other protein traffic as well (Huang et al., 2012). Although the mechanism of this vesicular trafficking is unclear, it requires the mitochondrial proteins ATAD3A,

an ATPase, and the GTPases Drp1 and MFN2, which is also involved in MAM formation (Huang et al., 2012). As viral proteins are likely to take advantage of the trafficking mechanisms used by endogenous proteins to target to MAM and traffic through MAM to mitochondria, studying them could not only deepen our understanding of viral illnesses, but also our understanding of MAM biology.

1.5.3 The MAM in cancer

It has long been suspected that MAM could be implicated in cancer progression, given its involvement in regulating calcium signaling to the mitochondria and apoptosis (Grimm, 2012). However, until recently there was little concrete evidence that MAM proteins were playing a specific role in tumorigenesis, or that the MAM requirement for apoptotic signaling between ER and mitochondria translated into a role for MAM in cancer progression. However, upregulation of several stress-inducible ER chaperones and oxidoreductases, such as BiP (Li and Lee, 2006), has been found to play a role in protecting cancer cells from ER stress and apoptosis, as the ER in tumour cells is subjected to stress from hypoxia and increased demand for protein production (Grimm, 2012). For example, May et al. have demonstrated that Ero1α mRNA was upregulated in hypoxic tumours and that siRNA-mediated reduction of Ero1α expression reduced the secretion of vascular endothelial growth factor (VEGF), reduced proliferation or the cells and rendered them more susceptible to apoptosis (May et al., 2005).

The promyelocytic leukemia (PML) protein is encoded by a gene that is translocated and fused to the retinoic acid receptor α in acute promyelocytic leukemia (Ross et al., 2004). The two mutated proteins that results from the translocation block the differentiation of hematopoietic cells, creating a great deal of interest about the function of PML, and whether it is acting as a tumour suppressor in healthy cells (Pinton et al., 2011). Although PML is usually concentrated in nuclear bodies, a portion of its extranuclear population has recently been found at MAMs (Giorgi et al., 2010). In the absence of PML, the concentration of calcium in the ER is lower, and release of calcium from the ER

after agonist or apoptotic stimulation was smaller. This could be rescued by an exogenously expressed ER-targeted PML, but not a nuclear targeted version of the protein. PML -/- MEFs were also found to be resistant to apoptosis (Giorgi et al., 2010). These findings could explain the tumour suppression role of PML, and how the loss of PML through translocation could contribute to the pathogenesis of acute promyelocytic leukemia.

1.6 Goal of this thesis

Given the growing role attributed to the MAM in human health, it is important to understand how the MAM is formed, how proteins target there, and how it functions. Many ER chaperones have already been shown to localize to MAM and play a role in the modulation of ER calcium homeostasis and signalling. The aim of the work presented in this thesis is to identify MAM-enriched ER chaperones and redox proteins, elucidate their mechanisms of MAM enrichment, and determine their importance in cellular calcium handling. Given that the cytosolic sorting protein PACS-2 was found to be important for MAM formation, a study was undertaken to determine whether the PACS-2 interactor calnexin was found on MAM and whether it was dependent on PACS-2 for its localization. Subsequently, other possible PACS-2 interacting redox proteins, TMX and TMX4, were examined for MAM enrichment. In this study, our aim was to determine what further protein motifs or trafficking mechanisms, for example palmitoylation, might be responsible for targeting the proteins we identified as MAM-localized. Lastly, we sought to determine why the MAM-targeting of the multifunctional chaperone protein calnexin is important, and what the functional consequences of calnexin's intra-ER targeting are. Given the important functions of the MAM in cellular processes such as calcium and lipid trafficking, and in viral disease, neurodegenerative disease and cancer, it is of vital importance to understand how proteins traffic to MAM and how MAM localization affects protein function.

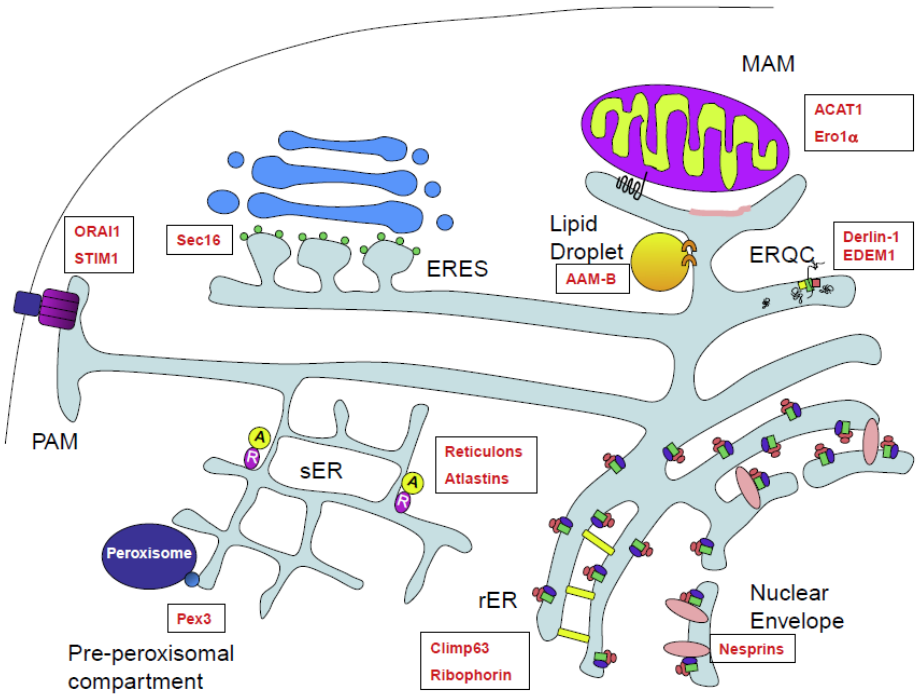

Figure 1.1: ER subdomains and selected marker proteins. Climp63 (yellow rectangle) maintains the sheet-like morphology of the Rough ER, and ribophorins (purple oval) mediate the interaction of ribosomes with the translocon; At the nuclear envelope, nesprins (pink ovals) form a bridge between the nuclear lamina and the cytoskeleton; the ER Quality Control Compartment (ERQC) forms during ER stress and Derlin1 and EDEM mediate export and degradation of misfolded proteins; reticulons and atlastins maintain the reticulated, tubular structure of the smooth ER, ER exit site (ERES) form at sites of Sec16 association with the cytosolic face of the ER membrane; AAM-B traffics first to the ER, then to lipid droplets; likewise, Pex3 traffics through ER to the pre-peroxisomal compartment and on to peroxisomes; Stim1 and Orai1 oligomerize at the plasma membrane associated membrane (PAM) to form a channel responsible for store-operated calcium entry; DGAT2 and Ero1a target Mitochondria associated membranes (MAM) via a cytosolic mitochondrial targeting sequence and ER redox conditions, respectively. Please see the text for further details.

Chapter 2: Materials and Methods

Chapter 2: Materials and Methods

2.1 Materials

2.1.1 Reagents

Table 2.1 Commercial sources of chemicals and reagents

Reagent	Source
2-Bromohexadecanoic Acid	Fluka
25x Complete Protease Inhibitors	Roche
6x DNA Gel Loading Buffer	New England BioLabs
Acetone	BDH Chemicals
Acrylamide	BioRad
Agarose	Invitrogen
Ammonium Persulfate	BioRad
Ampicillin	Sigma
β-Mercaptoethanol	BioShop
Bovine Serum Albumin	Sigma
Bovine Serum Albumin, fatty-acid free	Sigma
Bromophenol Blue	BioRad
CHAPS	Sigma-Aldrich
Dithiothreitol	Fisher Scientific
Dithiobis(Succinimidyl propionate) (DSP)	Thermo Scientific
Dulbecco's modified eagle medium	Gibco
Ethanol	Commercial Alcohols
EDTA	EMD
EZ-Link Sulfo-NHS-LC-Biotin	Thermo Scientific
Fetal Bovine Serum	Gibco
Fluo8	AAT Bioquest
Glycerol	BDH
HEPES	Sigma
Histamine dihydrochloride	Sigma
Hydrochloric Acid	Fisher Scientific
LB Agar, Miller	BD Biosciences
Luria Broth Base, Miller	BD Biosciences
Metafectene Pro	Biontex
Methanol	Fisher Chemical
Mitotracker Red CMX Ros	Invitrogen
Trans-blot nitrocellulose	BioRad
Oligofectamine	Invitrogen
OptiMEM	Gibco
Optiprep	Axis-Shield
Percoll	GE Healthcare

Phosphate Buffered Saline (PBS), 10x	Cellgro Mediatech, Inc
Phosphate Buffered Saline with calcium and magnesium, 10x	
ProLong Antifade resin	Invitrogen Molecular Probes
Protein A Sepharose Beads CL-4B	GE Healthcare Bio-Sciences
Rhod2	Invitrogen
Sodium azide	ICN Biomedical Inc.
Sodium dodecyl sulphate (SDS)	J.T. Baker
Streptavidin-agarose beads	Sigma Aldrich
Sucrose	EMD
Tetramethylethylenediamine (TEMED)	OmniPur/EMD
Thapsigargin	Alexis Biochemicals
TMRM	Sigma
Tris	Bio Basic Inc.
Triton X-100	Sigma
Triton X-114	Sigma
Trypsin 2.5%	Gibco
Tunicamycin	Alexis Biochemicals

Table 2.2 Enzymes

Enzyme	**Source**
T4 DNA ligase	Invitrogen
Restriction endonuleases	NEB
Restriction endonucleases	Fermentas

Table 2.3 Molecular size standards

Molecular size standard	**Source**
Precision Plus Protein Dual Colour Standards	BioRad
1 Kb Plus Marker	Fermentas

Table 2.4 Multicomponent systems

Kit	**Source**
QIAEX II gel extraction kit	QIAGEN
QIAGEN plasmid midi kit	QIAGEN
QiaQuick Gel extraction kit	QIAGEN
Phusion High Fidelity PCR Kit	Finnzymes

Table 2.5 Detection and analysis systems

Detection System	Source
Odyssey Infrared Imaging System	LiCor
Axioobserver Microscope, Axiocam digital camera, 100x Plan-Apochromat lens, Axiovision 4 acquisition software	Zeiss
ImageJ Software	Rasband, W.S., ImageJ, U. S. National Institutes of Health, http://imagej.nih.gov/ij/, 1997-2012.
Imaris 7.2 Software	Bitplane
Huygens Software	Scientific Volume Imaging
FluorChem Imaging System (Transilluminator, camera and computer software)	Alpha Innotech Corporation
FACS Scan Cytometer	BD Biosystems

2.1.2 Commonly used buffers

The composition of the buffers used throughout this work can be found below in Table 2.6.

Table 2.6 Common Buffers and Solutions

Solution	Composition
CHAPS lysis buffer	1% CHAPS, 10 mM Tris pH 7.4, 150 mM NaCl, 1 mM EDTA
Laemmli Buffer	60 mM Tris pH 6.8, 2% SDS, 10% glycerol, 5% βMercaptoethanol, 0.01% Bromophenol blue
IF Wash Solution	PBS++, 0.2% (w:v) BSA, 0.1% (v:v) Triton X-100
Mitochondrial Homogenization Buffer	10mM HEPES pH 7.4, 250 mM sucrose, 1mM EDTA, 1mM EGTA
mRIPA	1% NP40, 1% deoxycholine, 150 mM NaCl, 50 mM Tris, pH 8.0
Miniprep solution I	50 mM glucose, 10 mM EDTA, 25 mM Tris pH 8.0
Miniprep solution II	0.2 N NaOH, 1% SDS
Miniprep solution III	3M NaAc, pH 5
4x Separating Gel Buffer	1.5 M Tris pH 8.8, 0.4% SDS
4x Stacking Gel Buffer	0.5 M Tris pH 6.8, 0.4% SDS
Gel Running buffer (SDS-PAGE)	25 mM Tris, 200 mM Glycine, 0.1% SDS
TAE	40mM Tris, 20mM acetic acid, and 1mM EDTA
TBS-T	10 mM Tris pH 8.0, 0.15 M NaCl, 0.05% Triton X-100

TNE Buffer	10 mM Tris pH 7.4, 150 mM NaCl, 5 mM EDTA
Carbonate Transfer buffer	10 mM $NaHCO_3$, 3 mM Na_2CO_3, 20% Methanol
Western Blocking Solution	TBS-T +3% BSA

2.1.3 Plasmid Vectors and Oligonucleotides

The following is a summary of the plasmid vectors used in this study, followed by a table listing the oligonucleotides and strategies that were used to generate mutations and chimeric proteins from the original constructs.

Table 2.7 Plasmids

Plasmid	**Source**
pCEP4 FLAG CXN	Dr. Thomas Simmen
pCEP4 FLAG CXN SSAA	
pCEP4 FLAG CXN SSDD	
pcDNA3 myc TMX	
pcDNA3 myc TMX4	
pcDNA3 myc TMX M1	
pAR/G VSVG rAMP	Dr. T. Hobman
pAD tet7 Tac	Dr. Walter Hunziker

Table 2.8 Oligonucleotides and Construct Design

Simple PCR

Construct name	**Template**	**Forward Primer**	**Reverse Primer**	**Restriction site**
TMX-RQR	**Myc TMX**	**T7**_TAATACGACTCACTATAGGG	**TS368**_ATATCTCGAGCTAGGATTTATCTGTGGCCAATGATGGACCTAGGGATTTTTGTTTTATGGCATTCTGTGG	AvrII

Chimeric TMX/TMX4 Constructs

Constuct Name	Template	Forward primer	Reverse Primer	Restrict-ion Site
Myc 114	**myc TMX**	**T7**	**TS344_**GTGGCACATAGAAACATTCTGACACAAATATCATACAGAGTCC	**Acc65I, XhoI**
	mycTMX4	**TS343_**GGACTCTGTATGATATTTGTGTCAGAATGTTTCTATGTGCCAC	**Sp6_**ATTTAGGTGACACTATAGAA	
Myc 144	**myc TMX**	**T7**	**TS346_**CTATGACGAAAAACACATAAGATCCCCACACTGGCAATCCAAGG	
	Myc TMX4	**TS345_**CCTTGGATTGCCAGTGTGGGGATCTTATGTGTTTTTCGTCATAG	**Sp6**	
Myc 441	**Myc TMX4**	**T7**	**TS348_**TGAAGGACAAAGGCAATCTGCTATTACCACCAAGACCAGACC	
	Myc TMX	**TS349_**GGTCTGGTCTTGGTGGTAATAGCAGATTGCCTTTGTCCTTCA	**Sp6**	
Myc 411	**Myc TMX4**	**T7**	**TS350_**TAAAGCAAAAACAGTATATGAACACCAAGCAGGAATTCCAAG	
	Myc TMX	**TS351_**CTTGGAATTCCTGCTTGGTGTTCATATACTGTTTTTGCTTTA	**Sp6**	
Myc 414	**Myc 411**	**Same strategy as Myc 114**		
	Myc TMX4			
Myc 141	**Myc 144**	**Same strategy as Myc 441**		
	Myc TMX			

Addition of FLAG Tags

Construct Name	Template	Forward Primer	Reverse Primer	Restriction Site
FLAG-TMX	**Myc TMX**	**T7**	**TS363_**GTCATCGTCGTCCTTGTAGTCACCCCAAAGCAACGGCACCATGACTGCCAG	**Acc65I, XhoI**
		TS362_GACTACAAGGACGACGATGACAAGGGAGCTCCCTGGACGCACGGGCGGCGG	**Sp6**	
FLAG TMX4	**Myc TMX4**	**T7**	**TS365_**TCCCTTGTCATCGTCGTCCTTGTAGTCCGTCGCCGCCACAGCCGCGATCCAGGCGGCCAG	
		TS364_GACTACAAGGACGACGATGACAAGGGAGCAGGCCCCGAGGAGGCCGCGCTGCCGCCG	**Sp6**	
FLAG VSVG	**pAR/G VSVG rAMP**	**TS394_**ATTCATTGGGGTGAATTGCGACTACAAGGACGACGATGACAAGGGAAAGTTCACCATAGTTTTTCCACAC	**TS395_**ATATCTCGAGTTACTTTCCAAGTCGGTTCATCTC	**N/A**
	PCR product of previous reaction	**TS393_**ATATGAATTCACCATGAAGTGCCTTTTGTACTTAGCCTTTTTATTCATTGGGGTGAATTGCGACTACAAG		**EcoRI, XhoI**

Site Directed Mutagenesis

Construct Name	Template	Forward Primer	Reverse Primer	Restriction Site
FLAG TMX CCAA	**FLAG TMX**	**T7**	**TS370_**TCTGCGCCTTTTTTGAAGCAGCTAGCGCATCTGCCACAAATATCAT	**Acc65I, XhoI**
		TS369_ATGATATTTGTGGCAGATGCGCTAGCTGCTTCAAAAAGGCGCAGA	**Sp6**	
FLAG-CXN CCAA	**FLAG CXN**	**TS264_**ATATGGTACCACCATGGAAGGGAAATGGCTGCTGTGTATGTTACTGGTCCTTGGAACTAC	**TS384_**TGACTGTTTCTTTCCGCTAGCGGCGAAGAGGATAACAAGAAACAC	**EcoRI, XhoI**
		TS385_GTGTTTCTTGTTATCCTCTTCGCCGCTAGCGGAAAGAAACAGTCA	**TS261_**ATATCTCGAGTCACTCTCTTCGTGGCTTTCTG	

Construction of VSVG Chimeras

Construct Name	Template	Forward Primer	Reverse Primer	Restrict-ion Site
FLAG VSVG TMX	**FLAG VSVG**	**T7**	**TS396**_AAGCAAAAACAGTATATGAAGAGCTTTTCCAACTACTGAACCAAC	**Acc65I, XhoI**
	FLAG TMX	**TS397**_AGTAGTTGGAAAAGCTCTTCATATACTGTTTTTGCTTTAGCAAC	**Sp6**	
FLAG VSVG TMX4	**FLAG VSVG**	**T7**	**TS398_**CTATGACGAAAAACACATAAGAAGAGCTTTTCCAACTACTGAAC	
	FLAG TMX4	**TS399_**GTAGTTGGAAAAGCTCTTCTTATGTGTTTTTCGTCATAGCCACC	**Sp6**	
FLAG VSVG CXN	**FLAG VSVG**	**T7**	**TS400_**CTTGACTGTTTCTTTCCAGAGCAAGAGCTTTTCCAACTACTGAACC	**EcoRI, XhoI**
	FLAG CXN	**TS401_**GGTTCAGTAGTTGGAAAAGCTCTTGCTCTGGAAAGAAACAGTCAAG	**TS261**	

Construction of TAC Chimeras

Construct Name	Template	Forward Primer	Reverse Primer	Restrict-ion Site
TAC TMX	**pAD tet7 Tac**	**TS441_**ACACGGTACCGACACCATGGATTCATACCTGCTGATGTGGG	**TS442_**TAAAGCAAAAACAGTATATGACTGGTACTCTGTTGTAAATATGGA	**KpnI, XhoI**
	FLAG TMX	**TS443_**ACAACAGAGTACCAGTCATATACTGTTTTTGCTTTAGCAACTC	**TS240**_ATATCTCGAGATATCTAGGATTTATCTGTGGCCAATG	
TAC TMX4	**pAD tet7 Tac**	**TS441**	**TS444_**TATGACGAAAAACACATAAGACTGGTACTCTGTTGTAAATATGGA	
	FLAG TMX4	**TS445_**CAACAGAGTACCAGTCTTATGTGTTTTTCGTCATAGCCACCTTGG	**TS236**_ATATCTCGAGATATCTACAGTCCCTTGTCAGCATGC	
TAC CXN	**pAD tet7 Tac**	**TS441**	**TS446_**CGGTCAAAACGTAGACCACCTGGTACTCTGTTGTAAATATGGA	
	FLAG CXN	**TS447_**CGGTCAAAACGTAGACCACCTGGTACTCTGTTGTAAATATGGA	**TS261**_ATATCTCGAGTCACTCTCTTCGTGGCTTTCTG	
TAC TMX CCAA	**pAD tet7 Tac**	**Same strategy as for TAC TMX**		

	FLAG TMX CCAA	
TAC CXN CCAA	**pAD tet7 Tac**	**Same strategy as for TAC CXN**
	FLAG CXN CCAA	

Deletion

Construct Name	**Template**	**Forward Primer**	**Reverse Primer**	**Restriction Site**
TMX Δ Thio	**Myc TMX**	**T7**	**TS356_**CCATTCAGC AAAACTTTCCCAGT CTCCTTCCAGCAGT TCTCTCCA	**Acc65I, XhoI**
		TS355_GAAGGAGACT GGGAAAGTTTTGCTG AATGGGGAGAAGATC TTGAG	**Sp6**	

2.1.4 Antibodies used in this study

Table 2.9 Primary Antibodies

Specificity	**Host**	**Species reactivity**	**Dilution (Application)**	**Source**
ACAT1	rabbit	human, hamster, mouse	1:500 (WB)	Thermo Scientific
bCOP	mouse	human, hamster, rat, monkey	1:2000 (WB)	GeneTex
Biotin	mouse		1:5000 (WB)	Berthiaume Lab, University of Alberta
BiP	mouse	Human, dog, rat, mouse	1:5000 (WB)	BD Biosciences
Calnexin (cytosolic peptide)	rabbit	Human, mouse	1:1000 (WB) 1:100 (IP)	This study

Calnexin	rabbit	Human, monkey, mouse, rat, bovine, chicken, dog, guinea pig, hamster, unicorn, pig, quail, rabbit sheep, Drosophila, Xenopus	1:1000 (WB)	Stressgen
Calnexin	mouse	Dog, mouse, rat, human	1:1000 (WB)	BD Biosciences
Calnexin P534	rabbit		1:500 (WB)	This study
Calnexin P544	rabbit		1:500 (WB)	This study
Calnexin P563	rabbit	Human, mouse, rat	1:500 (WB)	Abcam
CD25/Tac	rabbit	human	1:1000 (WB)	AnaSpec
eIF2a	rabbit	Human, mouse, rat, monkey	1:1000 (WB)	Cell Signaling
ERGIC53	mouse	Human, pig, monkey	1:1000 (WB)	Alexis
ERp57	mouse	Human, mouse, bovine, canine, guinea pig, hamster, monkey, pig, rabbit, rat	1:1000 (WB)	StressMarq
FACL4	goat	human	1:2000 (WB)	Abcam
FLAG tag	mouse		1:1000 (WB)	Rockland, Gilbertsville, PA
FLAG tag	rabbit		1:100 (IP)	Rockland, Gilbertsville, PA
GRP75/HSPA9B	mouse	Human, monkey, canine, mouse	1:500 (WB)	Affinity BioReagents

Heme oxygenase-1	mouse	Human, rat, mouse, cow, dog, monkey	1:250	Abcam
IP3-Receptor Type 3	mouse	Human, dog, rat, mouse	1:1000 (WB)	BD BioSciences
Mitochondrial Complex II	mouse	Human, bovine, rat, mouse	1:1000 (WB)	MitoSciences, Eugene, OR
Myc tag	mouse		1:1000 (WB)	Millipore, Billerica, MA
Myc tag	rabbit		1:1000 (WB)	Millipore
PDI	mouse	Human, mouse, rat	1:5000 (WB) 1:100 (IF)	Affinity Bioreagents
QSOX1	rabbit	human	1:1000 (WB)	GeneTex
Ribophorin I	rabbit	Human, mouse, rat	1:1000 (WB)	ProteinTech
Ribophorin II	rabbit	human	1:1000 (WB)	Lifespan BioSciences
SERCA2b	Mouse	human	1:1000 (WB)	Millipore, Billerica, MA
TMX	Rabbit	human	1:1000 (WB) 1:100 (IF)	Sigma, Oakville, ON
TMX	Rabbit	human	1:1000 (WB)	This study
TMX2	Rabbit	Human, mouse, rat	1:1000(WB)	Lifespan Biosciences, Seattle, WA
TMX3	Rabbit	human	1:1000 (WB)	Ellgaard Lab, University of Copenhagen
TMX4	Rabbit	human	1:500 (WB)	This study
TMX4	Mouse	human	1:100 (IF)	ImmunoKontact/AMS Biotechnology, Abingdon, UK
VDAC1 (20B12)	Mouse	Human, mouse, rat	1:1000 (WB)	Abcam, Cambridge, UK
VDAC2	Rabbit	Human, cat, chimpanzee, cow, dog	1:1000 (WB)	Abcam, Cambridge, UK
VSVG	Rabbit		1:1000 (WB)	Hobman Lab, University of Alberta

Table 2.10 Secondary Antibodies

Antibody	Dilution	Application	Source
Goat anti mouse AlexaFluor 680	1:10 000	WB	Invitrogen
Goat anti rabbit Alexa Fluor 750			
Donkey anti goat AlexaFluor 680			
Goat anti mouse AlexaFluor 594	1:2000	IF	
Goat anti mouse AlexaFluor 488			
Goat anti mouse AlexaFluor 350			
Goat anti rabbit AlexaFluor 594			
Goat anti rabbit AlexaFluor 488			
Goat anti rabbit AlexaFluor 350			

2.1.5 Cell lines used in this study

Table 2.11 Cell lines

Mammalian Cell Line	Source
HeLa	ECACC
CXN -/- MEF	M. Michalak, University of Alberta
WT MEF	M. Michalak, University of Alberta
AKO MEF	M. Michalak, University of Alberta
A375P	Wellcome Trust Functional Genomics Cell Bank
Bacterial Cultures	
DH5a E. coli	G. Eitzen, University of Alberta

2.2 Methods

2.2.1 Mammalian cell culture techniques

2.2.1.1 Maintenance of cell lines

Cells were incubated at 37˚C in a humidified environment with 5% CO_2. All cell lines were maintained in Dulbecco's minimal essential medium (DMEM, Table 2.1) with 10% FBS (Table 2.1). Cells were passaged twice per week using Trypsin (Table 2.1) to a maximum passage number of 40.

2.2.1.2 Transient Transfection of cell lines

Exogenous DNA was introduced into cells using a lipid based transfection system. The evening prior to transfection, cells were trypsinized and seeded in DMEM+10% FBS (see Maintenance of cell lines, above) in 35 mm dishes (2mL volume) so as to become 90-100% confluent overnight. The following morning, the cells were transfected with 8 uL of Metafectene Pro reagent (Table 2.1) and 1.5 ug of plasmid DNA, according to the manufacturer's instructions. Transfection was allowed to proceed for 16-48 hours (see figure legends of individual experiments) before cells were harvested or processed for various experiments.

In order to verify the efficacy of the antibodies we generated for this study, siRNA knockdown of the target proteins was used. The evening prior to transfection, A375P or HeLa cells were seeded at 100 000 cells per 35 mm dish. Oligofectamine (Table 2.1) was used to transfect the cells according to the manufacturer's instructions. The siRNAs against TMX and TMX4 were from Sigma.

2.2.2 Molecular Biology techniques

2.2.2.1 Polymerase Chain Reaction (PCR)

Simple PCR was used to generate some of the mutants used in this study. PCR was performed according to the directions of the Phusion High Fidelity PCR Kit (Table 2.1.4) using an Eppendorf Mastercycler PCR machine. All primers were synthesized by Sigma-Genosys. The primers, template DNA and strategies used to generate mutant, chimeric, or deletion constructs are summarized in Table 2.8 and in the following section.

2.2.2.2 PCR-based splicing by overlap extension

PCR-based splicing by overlap extension was the prevalent technique used to create the mutations and chimeric proteins used in this study. Briefly, two or more sequential PCRs were performed to create gene segments that overlap each other, and were then used as templates in a subsequent PCR reaction to piece

together a whole gene (Heckman and Pease, 2007). In the case of site directed mutagenesis, internal primers carrying a mutation (and in some cases an engineered restriction site) were designed in such a way as to create overlapping complementary sequences. These internal primers were used in initial PCRs with primers that flanked the whole gene, in most cases the commercial primers T7 (5') and Sp6 (3'). For example, in the case of the introduction of the double Cysteine to Alanine mutation (CCAA) into the FLAG-TMX wt cDNA, internal primer TS 370 (reverse) which carried the mutation, was paired with T7 in one reaction using FLAG-TMX wt as template. Its complementary partner, TS369 (forward), which also carried the mutation, was paired with Sp6. These reactions generated overlapping products which were denatured and spliced together in a subsequent reaction driven by the external primers T7 and Sp6, which yielded a whole FLAG-TMX CCAA. Please see Table 2.8 for a list of all constructs generated in this way.

Jumping PCR was also used in this study to create chimeras of two different wildtype genes. In this case, internal primers without mutations were designed in such a way as to be complementary to each other and span the junction of the two different genes. An example of this is the creation of the Myc-114 chimera, which has the luminal and transmembrane domains of TMX1 fused to the cytosolic tail domain of TMX4. Reverse primer TS344, which was complementary to both the 3' end of the TMX segment and the 5' end of the TMX4 segment, was paired with the T7 primer and used to amplify the indicated section of WT Myc-TMX template. In a second reaction, forward primer TS343, which was also complementary to both the 3' end of the TMX segment and the 5' end of the TMX4 segment, was paired with Sp6 primer in a reaction to amplify the indicated section of the WT Myc-TMX4 template. These reactions generated overlapping products that were denatured and spliced together in a subsequent reaction driven by the external primers T7 and Sp6, which yielded a chimeric Myc-114 construct. Please see Figure 2.1 for an illustration of the generation of

the TMX chimeric constructs, and Table 2.8 for a list of all constructs generated in this way.

2.2.2.3 Restriction Digest

Restriction digest were generally performed in a volume of 50 μL (preparation of PCR products for ligation) or 10 μL (analysis of plasmid DNA isolated from bacterial clones). Reactions were prepared using 3-15 units of enzyme, and the buffer and Bovine Serum Albumin as indicated by the manufacturer's instructions, and allowed to proceed at 37˚C for 1.5 hours.

2.2.2.4 Separation of DNA fragments by agarose gel electrophoresis

Five volumes PCR products or restriction digest reactions were mixed with one volume of 6x DNA loading buffer (Table 2.1) and loaded into a 1.5% agarose gel prepared with 1x TAE (Table 2.6) containing 1x SYBRsafe (Table 2.1). Gels were subject to electrophoresis at 100 V in an apparatus containing 1x TAE. DNA fragments were visualized with an ultraviolet transilluminator apparatus and digital camera (Table 2.10).

2.2.2.5 Extraction of DNA from agarose gel

DNA fragments of interest were excised from gels using a razor, and purified from the agarose gel using either the QIAEX II gel extraction kit or QIAquick Gel Extraction Kit (Table 2.4), according to the supplied instruction. DNA was typically eluted in 30 μL of nuclease free water (Table 2.1).

2.2.2.6 DNA ligation

DNA inserts that were restriction digested and purified as described above were ligated into the multicloning site of pcDNA3 using 1.5 μL of T4 DNA ligase (Table 2.2) in the buffer supplied by the manufacturer. The reaction volume was 15 μL, and the ratio of plasmid to insert varied between 1:5 and 1:50. Ligation reactions were incubated overnight at room temperature.

2.2.2.7 DNA sequencing

DNA sequencing was performed by the Molecular Biology Facility, department of Biological Sciences, University of Alberta, using the BigDye Terminator v3.1 Cycle Sequencing kit to verify the sequences of the constructs used in this study.

2.2.2.8 Bacterial Culture

DH5α Escherichia coli were grown in Luria Broth (Table 2.1) with the appropriate antibiotic (generally 100 μg/mL Ampicillin) in culture tubes or flasks in a rotary shaker at 220 rpm, at 37 ˚C. Culture volumes were kept to approximately 20% of the flask volume. LB Agar plates (Table 2.1) with appropriate antibiotic were also used.

2.2.2.9 Preparation of competent cells for transformation

Competent E. coli were prepared for transformation using the Inoue method (Inoue et al., 1990). Briefly, a 250 ml culture of E. coli was grown to an OD_{600} of 0.55 in SOB medium (20 g/L Tryptone, 5 g/L yeast extract, 0.5 g/L NaCl, 2.5 mM KCl, pH 7.0, plus 10 mM $MgCl_2$ immediately before use) at 18-22˚C with moderate shaking. The flask was then transferred to an ice water bath for 10 minutes, and the cells were harvested by centrifugation at 2500g for 10 minutes at 4˚C. The cells were subsequently washed in 80 mls ice-cold Inoue transformation buffer (10 mM PIPES pH 6.7, 250 mM KCl, 15 mM $CaCl_2$, 55 mM $MnCl_2$) and re-centrifuged as above. Following this last centrifugation, the cells were resuspended in 20 mL ice-cold Inoue transformation buffer, and 1.5 mL DMSO was added. The mixture was incubated on ice for 10 minutes, then quickly aliquoted into pre-chilled sterile microfuge tubes, and frozen in a liquid nitrogen bath. Competent cells were stored at -80˚C.

2.2.2.10 Bacterial transformation

Competent DH5α *E. coli* bacteria, stored at -80˚C, were thawed on ice. One μL of DNA or 5 μL of ligation reaction were mixed with 100 μL of competent bacteria, and then incubated on ice for 20 minutes. This mixture was then heat-shocked in

a 42˚C water bath, then 1 mL of LB broth (Table 2.1) prepared according to the manufacturer's instructions, was added. In the case of a transformation of DNA, 50 μL of this mixture were then plated onto LB agar with the appropriate antibiotic and incubated overnight at 37˚C, or at room temperature for three days. In the case of the transformation of a ligation reaction, heat shocked bacteria were resuspended in 1 mL LB broth as above and left to recover for 1 hour on a 220 rpm shaker at 37˚C. Bacteria were then pelleted and the whole pellet resuspended in 100 μL LB. The entire suspension was then plated on LB agar with the appropriate antibiotic, and then incubated as above.

2.2.2.11 Isolation of plasmid DNA from bacteria (mini prep and midi prep)

Isolation of plasmid DNA from large bacterial cultures (25-50 mL) was performed using the Plasmid Midiprep Kit from QIAGEN (Table 2.4). Isolation of plasmid DNA from 2 mL cultures was performed as follows. All centrifugation steps were performed for 1 minute at 16 000g in a microcentrifuge at room temperature. Bacteria were pelleted by centrifugation and subsequently resuspended in 100 μL of cold Miniprep Solution 1 (Table 2.6). 200 μL of Miniprep Solution II (Table 2.6) were then added and mixed by inversion of the tubes. 150 μL of Miniprep Solution III were subsequently added to the tubes, and the mixture was vortexed for 10 seconds and centrifuged. Supernatants were transferred to fresh tubes and the centrifugation step repeated. The resulting supernatants were transferred to fresh tubes and DNA was precipitated with 1 ml 100% ethanol (Table 2.1). Precipitates were pelleted and then washed with 80% ethanol using the same procedure. DNA pellets were allowed to dry, and then resuspended in 50 μL of nuclease free water (Table 2.1).

2.2.3 Basic Biochemical Techniques

2.2.3.1 Preparation of whole cell lysates

Cells were lysed directly in 1x Laemmli buffer (Table 2.6). Lysates were then subjected to sonication and boiled for 5 minutes.

2.2.3.2 Protein Precipitation

Proteins were precipitated using a 1:5 volume ratio of sample to 100% Acetone (Table 2.1). In the case of samples obtained from the Optiprep fractionation protocol, 90% Acetone was used to prevent the co-precipitation of Optiprep itself from the samples. Samples were incubated overnight at -20˚C, after which precipitated proteins were pelleted at 16 000g for 20 minutes at 4˚C in a microcentrifuge. Pelleted proteins were then resuspended in 1x Laemmli Buffer (Table 2.6).

2.2.3.3 Sodium Dodecyl Sulphate Polyacrylamide Gel Electrophoresis (SDS-PAGE)

Protein samples were denatured by boiling for 5 minutes before separation by electrophoresis. Proteins and protein standards (Table 2.2) were separated using a 4% polyacrylamide stacking gel containing 125 mM Tris pH 6.8, 0.1% SDS 0.1% TEMED and 0.2% ammonium persulfate, and an 8% or 10% or 15% separating gel, depending on the size of the protein(s) of interest. Separating gel was made with 375 mM Tris pH 8.8, 0.1% SDS, 0.1% TEMED, and 0.1% ammonium persulfate (Tables 2.6 and 2.1). Gel electrophoresis was performed using the Mighty Small II gel running system (Amersham) under 150 Volts.

2.2.3.4 Western Blot

SDS-PAGE gels were transferred to nitrocellulose membranes (Table 2.1) in Carbonate Transfer Buffer (Table 2.6) at 400 mA at 4˚C for 2 hours, using a Mini Transblot Cell apparatus (BioRad). The membrane was then incubated in blocking solution (Table 2.6) for one hour to prevent the non-specific binding of antibodies. Blocked membranes were typically incubated with primary antibody (Table 2.9) in blocking solution or 2% milk in TBS-T for 1 hour at room temperature or overnight at 4˚C, according to the specifications of that particular antibody. Membranes were then washed three times for 5 minutes each on a rocker with TBS-T, and then incubated for one hour with the appropriate secondary antibody conjugated to an AlexaFluor fluorescent molecule (Table

2.10). Antigen-Antibody complexes were then visualized using an Odyssey Infrared Scanner (Table 2.5).

2.2.4 Cell Fractionation Techniques

2.2.4.1 Differential centrifugation fractionation

Approximately 10 000 000 HeLa cells were washed twice in PBS++ and collected in Mitochondria Homogenization buffer (Table 2.6). The cell suspension was passed 20 times through an 18 μm clearance ball bearing homogenizer (Isobiotech, Heidelberg, Germany). The cells were subsequently centrifuged for 10 minutes at 800xg at 4˚C, to pellet nuclei and unbroken cells. The supernatant was subsequently centrifuged for 10 minutes at 10 000g at 4˚C to pellet mitochondria. The mitochondrial pellet was resuspended in 1x Laemmli buffer (Table 2.6). The 10 000g supernatant was then centrifuged at 100 000g in a Beckman tabletop ultracentrifuge using a TLA 120.2 rotor to pellet the microsomal fraction. The microsomal pellet was resuspended in 1x Laemmli buffer. The 100 000g supernatant, representing the cytosolic fraction, was acetone precipitated and all fractions were analysed by SDS-PAGE and Western Blot.

2.2.4.2 Optiprep Gradient Fractionation

Ten to twenty million cells were washed twice in PBS++ and collected in mitochondria homogenization buffer (Table 2.6). The cell suspension was passed 15 times through an 18 μM clearance ball bearing homogenizer (Isobiotech, Heidelberg, Germany). The homogenate was subsequently centrifuged for 10 minutes at 800g at 4˚C, to pellet nuclei and unbroken cells. The resulting supernatant was layered over a 10%-30% discontinuous gradient of Optiprep density gradient medium (Axis-Shield, Norton, MA), and was centrifuged in an SW55 Ti rotor (Beckman Coulter, Mississauga, ON) for 3 hours at 32700 rpm. Six fractions were taken from the top of the gradient and analysed by SDS-PAGE and Western Blot.

2.2.4.3 Percoll MAM Fractionation

The Percoll MAM fractionation protocol was adapted from (Rusinol et al., 1994). Approximately 180 000 000 cells were used for each fractionation. Cells were seeded in 15 cm dishes and treated as indicated in figure legends. Cells were washed twice with cold PBS++ and harvested in 10 mL Mitochondrial Homogenization buffer (Table 2.6) with complete protease inhibitors (Table 2.1). Cells were homogenized by ten strokes in a dounce homogenizer. The homogenate was then centrifuged at 800g to pellet nuclei and unbroken cells, which were discarded. The supernatant was further centrifuged at 10 000g to obtain a crude mitochondrial pellet, which was resuspended in 1 mL fresh Mitochondrial Homogenization Buffer with Complete protease inhibitors. A 50 uL aliquot of crude mitochondria was retained, and the remaining suspension was carefully layered over 8.5 mL of 18% Percoll (Table 2.1) in polycarbonate tubes. Crude mitochondria were then centrifuged for 30 minutes at 30 500 rpm in a Beckman Ti-70 rotor. A heavy band of mitochondrial material was visible toward the bottom of the tube, with a lighter and thinner band of MAM floating above it. The two fractions were carefully aspirated with a Pasteur pipette, and transferred into separate tubes. In order to remove the Percoll, the MAM fraction was subsequently centrifuged at 60 000 rpm in a TLA 120.2 rotor. MAM membranes were pelleted on top of a Percoll pellet, and carefully removed and resuspended in 1x Laemmli buffer. The Percoll was then separated and removed from the mitochondrial fraction in a similar fashion, with a 10 000g centrifugation step.

The 10 000g supernatant that remained after the isolation of the crude mitochondrial pellet was further centrifuged at 60 000 rpm in a Beckman TLA120.2 rotor. The pellet, which represents the microsomal fraction, was resuspended in 1x Laemmli buffer. The supernatant, which represents the cytosolic fraction, was precipitated as indicated above. Equal proportions of each fraction were analyzed by SDS-PAGE and Western Blot.

2.2.4.4 Detergent-resistant membrane fractionation

The detergent-resistant membrane (DRM) fractionation protocol was adapted from (Hayashi and Fujimoto, 2010). Six million cells per condition were collected in Mitochondrial Homogenization Buffer and homogenized with 15 passes through an 18 micron clearance ball bearing homogenizer. A crude mitochondrial pellet, containing MAM, was obtained as in the above section 2.4.3. This pellet was carefully resuspended in TNE Buffer (Table 2.6) with Complete protease inhibitors (Table 2.1) and sonicated at 4˚C. All subsequent steps were performed in a cold room (4˚C) or on ice. A final concentration of 0.5% Triton X-114 (Table 2.1) was added to the suspension, which was incubated for 30 minutes, followed by centrifugation at 100 000g for 1 hour in a TLA 120.2 rotor. The pellet (DRM fraction) and supernatant (soluble fraction) were then analyzed by western blot.

2.2.5 Indirect Immunofluorescence Microscopy

2.2.5.1 Preparation of slides and data acquisition

One day prior to immunofluorescence microscopy experiments, cells were seeded onto glass coverslips immersed in 2 mLs DMEM+10%FBS in a 6-well plastic dish, and grown to approximately 50% confluency. Cells were then treated as required by each experiment. In the case that a transfection was required, transfected cells were re-seeded onto glass coverslips at the appropriate confluency the day following transfection. If mitochondrial staining was required, the cells were incubated at 37˚C with 0.2 uL of Mitotracker Red CMXRos (Table 2.1) which was added to each well 30 minutes prior to fixing. The coverslips were then washed twice in PBS++ and fixed for 30 minutes at room temperature in 4% paraformaldehyde in PBS++, then washed twice more with PBS++ and permeabilized for 1 minute with IF Wash Solution (Table 2.6), and washed twice more with PBS++. The coverslips were then incubated with the indicated primary antibodies (Table 2.9) for one hour at room temperature, then washed with PBS++ and incubated for a further hour at room temperature with secondary antibodies (Table 2.10). The coverslips were then washed twice with

PBS++ and once with water, then inverted onto slides with ProLong antifade resin (Table 2.1). Cells were imaged using an Axioobserver Microscope and Axiocam digital camera (Table 2.5).

2.2.5.2 Image quantification

Overlap between the ER proteins and the mitochondria, as represented by the Manders coefficient (Manders et al., 1996), was determined using Imaris 7.2 software (Bitplane, Zürich). Images were masked in three dimensions such that the outline of the region of interest (ROI) closely followed the outline of the cell. A PSF width of 0.218 was determined for the objective lens and used in all calculations. Images were thresholded automatically using the Imaris algorithm, and a Manders coefficient was determined for each image.

2.2.6 Biotin labelling and pulldown of surface proteins

Cells were washed twice with cold PBS ++ and then incubated with 0.3 mg/mL EZ Link Sulfo-NHS-LC-Biotin (Table 2.1) in cold PBS++ for 30 minutes on ice at 4˚C. The biotinylation reaction was then quenched for 5 minutes with 50 mM Glycine in PBS++, and rinsed twice with cold PBS. The cells were then lysed in mRIPA buffer (Table 2.6) with Complete Protease Inhibitors and collected in microcentrifuge tubes. Post-nuclear supernatants were obtained by centrifuging the lysates at 800g for 5 minutes at 4˚C. In parallel, lysates of non-biotinylated cells from each experimental condition were prepared as above and stored at -80˚C. The biotinylated samples were then incubated at 4˚C overnight on a rocker with 25 µL of 40% streptavidin-agarose beads (Table 2.1) prepared in PBS. The beads were washed once with PBS, and resuspended in Laemmli buffer, and heated at 100˚C for 5 minutes. The lysates of the non-biotinylated cells were denatured in a similar manner. All samples were then analyzed by SDS-PAGE and Western blot.

2.2.7 Immunoprecipitation experiments

2.2.7.1 Immunoprecipitation of Calnexin

Cells were washed twice with PBS++ and incubated for 30 minutes at room temperature with 2 mM Dithiobis (succinimidyl proprionate) (DSP, Table 2.1) in PBS++ to crosslink protein-protein interactions. The cells were then washed twice more and incubated in 10 mM NH4Cl in PBS++ for 10 minutes to quench the crosslinking reaction. The cells were then washed a final time in PBS++ and harvested in CHAPS lysis buffer (Table 2.6) containing complete protease inhibitors (Table 2.1). Post-nuclear supernatants were obtained by centrifuging the lysates for 5 minutes at 4˚C at 800g, and were subsequently incubated with rabbit α-calnexin antibody (Table 2.9) for one hour at 4˚C on a rocker. Protein A Sepharose beads (Table 2.1) were then added and the lysates incubated for a further hour. The beads were then washed 3 times in CHAPS buffer and resuspended in 1x Laemmli buffer (Table 2.6) and analyzed by SDS-PAGE and Western Blot for co-immunoprecipitating proteins

2.2.7.2 Immunoprecipitation of FLAG-tagged proteins

HeLa cells were transfected with plasmids carrying FLAG-tagged constructs. 24 hours post-transfection, cells were washed, crosslinked and harvested as above. Immunoprecipitation and analysis of co-immunoprecipitating proteins was carried out as above, instead using rabbit α-FLAG antibody (Table 2.9).

2.2.8 Labeling and Detection of Palmitoylated Proteins

HeLa cells were transfected with the indicated constructs and labelled with w-alkynyl palmitate, as in (Yap et al., 2010). Cells were starved of fatty acids by a one hour incubation in DMEM with 1% fatty acid free BSA (Table 2.1) The cells were subsequently labelled with ω-alkynyl palmitate as follows. The ω-alkynyl palmitate was first dissolved in DMSO at a concentration of 20 mM, then incubated at 65˚C for 15 minutes with 20% molar excess of KOH. This mixture was then added to pre-warmed culture medium containing 20% fatty acid free BSA, and incubated at 37˚C for a further 15 minutes, creating a 20x fatty acid-

BSA conjugate in serum-free medium. The cells were washed with PBS and incubated in fresh DMEM. The 20x ω-alkynyl palmitate-BSA conjugate mixture was then added to achieve a final concentration of 1% BSA and 100 μM ω-alkynyl palmitate. Cells were labeled for 3 hours, then FLAG-tagged proteins or endogenous calnexin were immunoprecipitated from lysates of the labeled cells. Control cells were treated instead with unlabelled fatty acids.

The incorporation of w-alkynyl palmitate into TMX and Calnexin was detected using click chemistry with an azido-biotin probe, which labels the acylated protein. SDS was added to immunoprecipitates to a concentration of 1%, as well as 100 uM tris-(benzyltriazolylmethyl)amine, 1 mM CuSO4, 1 mM tris-carboxyethylphosphine, and 100 uM azido-biotin. This mixture was incubated in darkness at 37C for 30 minutes, and the reaction was subsequently stopped by the addition of 10 volumes cold acetone. All reagents were obtained from the Berthiaume Lab, University of Alberta. Proteins were precipitated at -20C overnight, and were then pelleted at 16 000g for 15 minutes and resuspended in 1x Laemmli buffer containing 20 mM DTT (Table 2.1). Samples were boiled for 5 minutes, then separated by SDS-PAGE and transferred to PVDF membranes (Table 2.1). As a control, duplicate membranes were prepared and it was ensured that the biotin labelling was disrupted by an incubation of 1 hour with 0.2 M KOH, but not 0.2 M Tris-HCl, pH 7.0. PVDF membranes were probed with NeutrAvidin-HRP to detect the incorporated biotin.

2.2.9 Calcium Measurements by Flow Cytometry

AKO CXN -/- cells were transfected as indicated in figure legends. Cells were subsequently treated with tunicamycin (Table 2.1) as indicated in figure legends, or left untreated and subsequently loaded with either calcium-sensitive dyes 1 μM Fluo8 (cytosol), 1 μM Rhod2 (mitochondria), or 20 nM TMRM (mitochondria membrane potential) and incubated in DMEM for 30 minutes at 37˚C. Cells were then harvested in HEPES Buffered Saline (0.1% glucose, 0.1% BSA) and subjected to flow cytometry using a FACS Scan cytometer (BD Biosciences).

Samples were then stimulated to release calcium from the ER with thapsigargin (1.5 μM) or 50 μM histamine, and the signals from the fluorescent dyes were measured using flow cytometry as above.

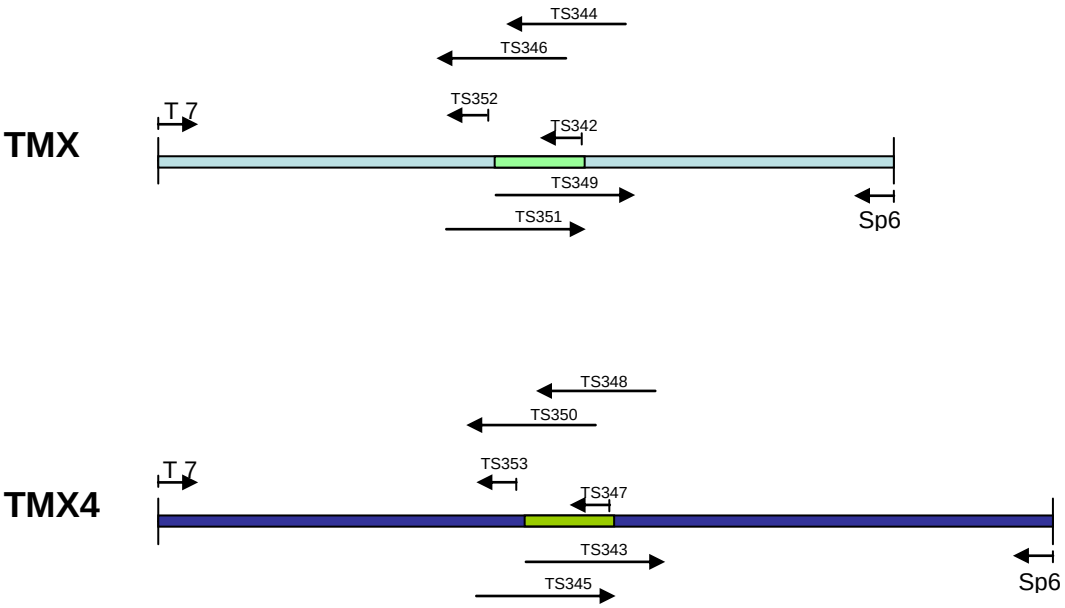

Figure 2.1: Strategy for the creation of TMX/TMX4 chimeric mutants. The Oligos used in the creation of the chimeric mutants bind the template DNA (pcDNA-myc-TMX and pcDNA myc-TMX4) at the indicated sites. The domains of TMX and TMX4 are depicted with the luminal thioredoxin domain on the left, transmembrane domain in green and cytosolic domain on the right. Oligo pairings and details of the PCR reactions are summarized in Table 2.8 and in Methods section 2.2.2.2.

Chapter 3: Calnexin's MAM localization is partially mediated by PACS-2

A version of this chapter has been published:
Myhill, N., Lynes, E.M., Nanji, J.A., Blagoveshchenskaya, A.D., Fei, H., Carmine Simmen, K., Cooper, T.J., Thomas, G. and T. Simmen. (2008) The subcellular distribution of calnexin is mediated by PACS-2. *Mol Biol Cell*. **19**: 2777-88.

Chapter 3: Calnexin's MAM localization is partially mediated by PACS-2

3.1: Introduction and Rationale

At the beginning of this project, very little was known about the proteins and other factors controlling formation of the MAM and targeting of proteins to the MAM. PACS-2, a multifunctional cytosolic sorting protein which interacts with the COP I coatomer, was identified as important for MAM formation, as knockdown of PACS-2 reduced the apposition of ER with mitochondria in the cell (Simmen et al., 2005). In this study, PACS-2 depletion also disrupted ER homeostasis, causing an upregulation of the ER chaperone protein BiP, and increasing the amount of calcium in the ER lumen that could be released upon histamine stimulation of the IP3 receptor. Interestingly, as PACS-2 is cytosolic, these findings suggested that there may be one or more transmembrane ER proteins that interact with PACS-2 and mediate some of its effects at the level of the ER.

A search was therefore performed for transmembrane ER proteins containing a PACS-2 consensus motif within their cytosolic domains, and three candidate proteins were identified (Figure 3.1) Calnexin is a transmembrane chaperone responsible for the folding and quality control of glycoproteins produced in the ER. TMX and TMX4 are two transmembrane members of the Protein Disulphide Isomerase (PDI) family of redox proteins, however very little is known about their functions. Each of these proteins has a PACS-2 consensus motif, or serines within an acidic cluster of residues, in its cytosolic domain. In this initial project, I focused on calnexin and its localization within the ER, its relationship with PACS-2, and how PACS-2 binding affected calnexin's localization. I hypothesized that a certain population of calnexin would localize to MAM, and that this would depend on an interaction with PACS-2.

3.2: Results

3.2.1 Calnexin is enriched on the MAM, and this enrichment is partially dependent on PACS-2

I first sought to determine whether calnexin was indeed found on MAMs. There are several methods by which MAMs can be identified and isolated, as discussed in the Introduction. Although using immunofluorescence microscopy to compare the colocalization of a suspected MAM protein with a mitochondrial marker to that of a non-MAM ER protein has been used, the resolution limitations of light microscopy mean that it alone cannot be used to confirm a protein's MAM localization. The resolution of a light microscope is approximately 200 nm and MAMs have been measured by electron tomography to be about 10-25 nm away from mitochondria (Csordas et al., 2006), therefore colocalization by immunofluorescence microscopy is not in itself sufficient to demonstrate the MAM localization of an ER protein. A biochemical fractionation method involving the isolation of a crude mitochondrial pellet through differential centrifugation fractionation and subsequently isolating MAMs from this pellet using Percoll density fractionation had been previously used with great success (Rusinol et al., 1994; Vance, 1990). However, although this method is optimal for separating MAM membranes from mitochondria, our research question required better separation between MAM and rough ER membranes. Furthermore, the Percoll fractionation was developed for use with rat liver tissue, and requires a great deal of starting material, so was unsuitable for use with transfected cells, for instance. I decided to experiment with Optiprep (Axis Shield, Dundee, Scotland) density gradient medium with the goal of separating MAM from other ER membranes. This fractionation method separates membranes on the basis of density, and is described in more detail in the Methods section 2.4.2.

Following labelling with biotin to mark cell surface proteins, HeLa cells were homogenized and the post-nuclear supernatants were loaded onto a 10-30% discontinuous gradient of Optiprep. Six fractions were obtained and markers for various membranes were analyzed by SDS-PAGE and western blot (Figure 3.2). Biotin-labelled proteins were observed in the first and second fractions of the gradient, indicating that this is where plasma membrane fractionates. Further down the gradient, we observed bCOP, which marks the vesicles and cisternae of the ER Golgi Iintermediate Compartment (ERGIC) and Golgi apparatus, in fraction 2, and ERGIC53, which marks the ERGIC, in fraction 3. Most importantly, Ribophorin 1, a rER marker, was found in fractions 3 and 4, whereas ACAT 1, a MAM marker, was found primarily in fractions 5 and 6, demonstrating that this protocol is able to distinguish rough ER from MAM. Mitochondria, marked by complex II, pellet at the very bottom of the gradient in fraction 6.

This protocol was next used to fractionate control HeLa cells and HeLa cells depleted of PACS-2 by siRNA, and observe calnexin's distribution on the gradient compared to marker proteins. In control cells, fraction six contained 36% of the calnexin signal detected by western blot, the largest amount of calnexin compared to any of the other fractions (Figure 3.1). However, a significant amount of calnexin did cofractionate as expected with rER marker ribophorin I in fractions 3 and 4. These data indicate that a significant population of Calnexin is on MAMs and confirm data obtained by immunofluorescence microscopy and simple fractionation in the same study (Myhill et al., 2008). PACS-2 depletion caused the redistribution of calnexin from fractions five and six to lighter fractions that correspond to ERGIC and Golgi membranes, confirming that PACS-2 is indeed involved in calnexin's MAM enrichment and retention of calnexin in the the ER. However, it was observed that a significant amount of calnexin remained in fraction six despite the depletion of PACS-2, indicating that there might be another mechanism retaining calnexin on MAM membranes.

3.2.2 Calnexin's MAM enrichment and its interaction with PACS-2 is dependent on phosphorylation

Calnexin's interaction with PACS-2 is regulated by phosphorylation of serines within a PACS-2 binding motif in its cytosolic tail, and phosphorylation of these serines is normally controlled by casein kinase II (CKII). PACS-2 binds to calnexin when the serines are dephosphorylated. Double mutants of the serines in calnexin's PACS-2 binding site were used to determine whether disrupting calnexin's interaction with PACS-2 in this way would alter calnexin's intra-ER localization. FLAG-CXN SSAA is a double S554A, S564A mutant which cannot be phosphorylated, and FLAG-CXN-SSDD is a double S554D S564D phosphomimetic mutant. It was confirmed that PACS-2 binds to the SSAA mutant but not the SSDD mutant through an in vitro binding experiment (Myhill et al., 2008).

These mutants, along with FLAG-tagged WT calnexin, were transfected into HeLa cells that were fractionated using the same Optiprep fractionation protocol as above. It was confirmed that the fractionation pattern of FLAG CXN WT is identical to that of endogenous calnexin (Figure 3.2). The distribution of FLAG-CXN SSAA is similar to that of WT but the SSDD mutant that cannot interact with PACS2 has a higher amount in lighter membranes (Figure 3.3) and on the cell surface (Myhill et al., 2008). This effect was subtle, confirming our suspicions that while PACS-2 clearly has a role in calnexin's subcellular distribution, other factors are certainly at play.

3.3 Discussion and Future Perspectives

While PACS-2 knockdown and alteration of the phosphorylation state of calnexin's PACS-2 binding site partially dislodge calnexin from the MAM, this disruption is not complete, leading us to wonder if calnexin's MAM localization is regulated by some other motif or interactor. We used differential centrifugation fractionation, immunofluorescence microscopy and Optiprep gradient fractionation to demonstrate calnexin's presence at the MAM, and our results

have concurrently and since been confirmed by other groups (Hayashi and Su, 2007; Wieckowski et al., 2009). However, since calnexin already has such a well established role as a chaperone and quality control protein, it led us to wonder if calnexin could have a novel role at the MAM, which is better known as a site of lipid and calcium transfer between the ER and mitochondria. In fact, it is not a novel thing for a chaperone protein to be found at the MAM, and several other chaperones have either been found to localize there, or been found to associate with and modulate ER calcium signalling molecules.

The most well known chaperone protein that localizes to the MAM is the Sigma1 receptor (Hayashi and Su, 2007). Sigma1 receptors form a complex with IP_3R at the MAM, stabilizing them and protecting them from degradation, and prolonging calcium signaling from ER to mitochondria in the event of ER stress. Sigma1 receptors also form a complex with the ER chaperone BiP, which dissociates as the ER calcium concentration drops during ER stress. The authors also demonstrated that Sigma1 receptor has an anti-aggregation and chaperone activity in a citrate synthase refolding assay. IP_3R and SERCA2b can also be regulated by PDI family chaperones ERp44 and ERp57 (Higo et al., 2005; Li and Camacho, 2004), respectively.

The two other proteins that were identified by screening for potential PACS-2 interactors, TMX and TMX4, are very similar to ERp57 and ERp44 (Ellgaard and Ruddock, 2005) and are part of the same PDI family of chaperones. TMX has been shown by one research group to interact with calnexin (Matsuo et al., 2009) and it is therefore not inconceivable that either TMX or TMX4 or both may also localize to MAM. These discussion points will be addressed in the two subsequent chapters.

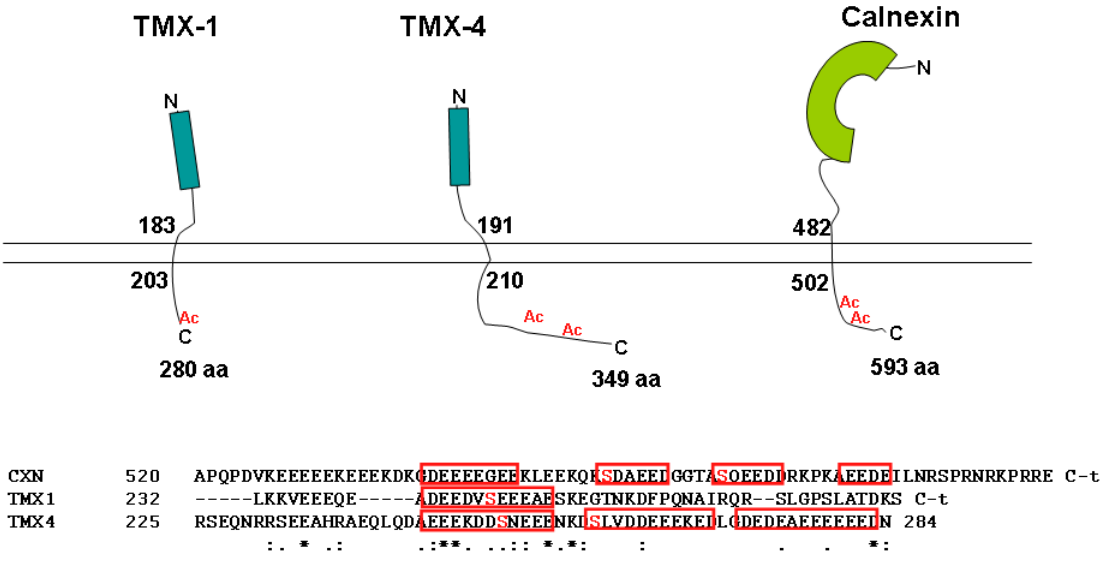

Figure 3.1: Identification of three possible ER transmembrane PACS-2 interactors. The C-terminal cytosolic tails of the three proteins are aligned, showing the CK2-phosphorylation sites (serines in red) embedded in clusters of acidic residues (red boxes). *Contributed by Thomas Simmen.*

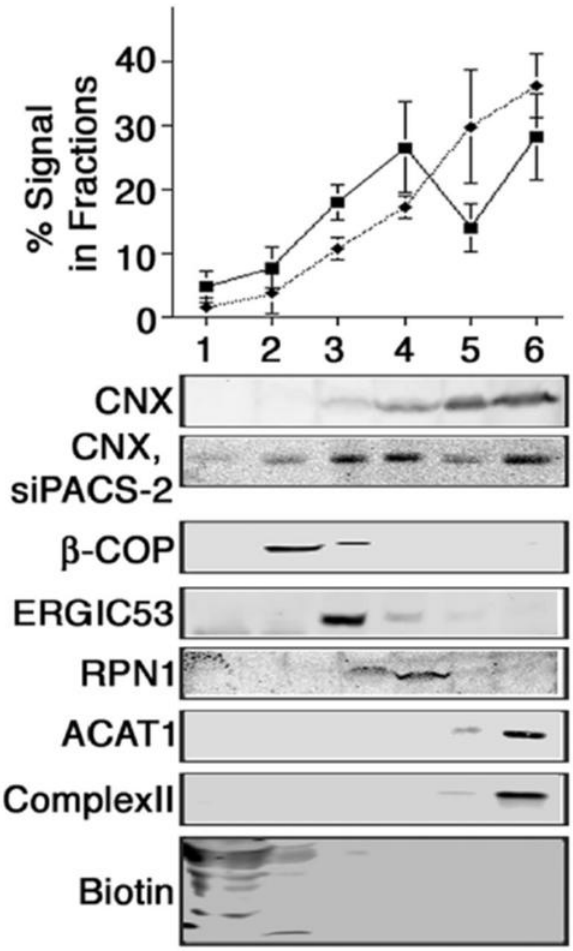

Figure 3.2. Optiprep gradient fractionation of control HeLa cells and Hela cells depleted by siRNA of PACS-2. Control HeLas were transfected with non-specific scrambled siRNA. Cell homogenates were fractionated on a 10-30% gradient of Optiprep. Marker proteins, which were not affected by PACS-2 knockdown, are biotinylated proteins (plasma membrane) Complex II (mitochondria), ACAT1 (MAM), Ribophorin I (rough ER), ERGIC 53 (ERGIC and ERES), and β-COP (Golgi). The distribution of calnexin was quantified over 4 independent experiments (chart-diamonds and dotted line=control data; squares and solid line=PACS-2 knockdown data). $p < 0.05$ for the difference in signal in fractions 5 and 6 between control and PACS-2 knockdown cells.

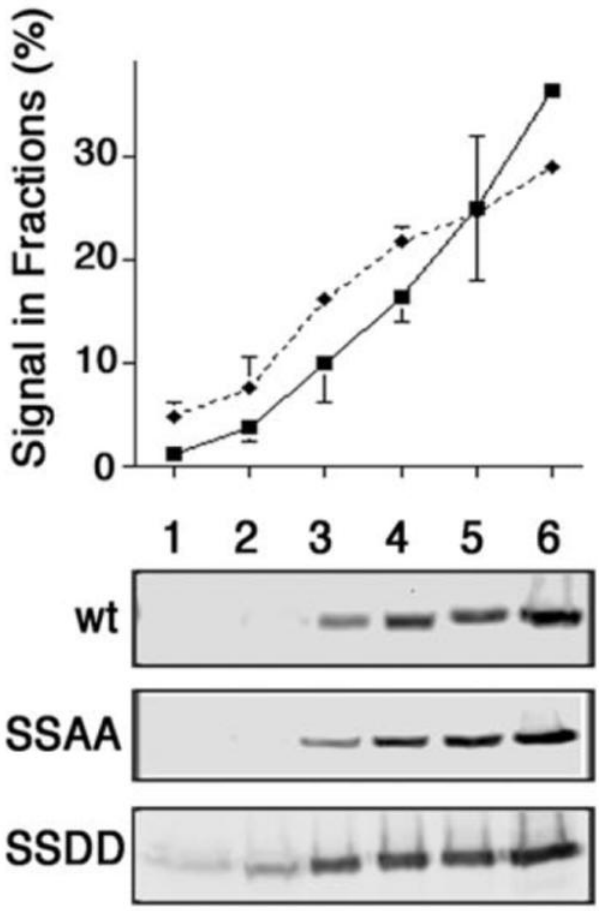

Figure 3.3: Optiprep gradient fractionation of HeLa cells overexpressing wildtype calnexin, calnexin SSAA and calnexin SSDD. Homogenates of these cells were fractionated on 10-30% Optiprep gradients. The signal from wildtype calnexin (squares, solid line) and calnexin SSDD (diamonds, dotted line) was quantified for each fraction and expressed as a percentage of the total signal. (n=3) $p < 0.01$ for the subtle difference in signal in fractions 6 between wildtype and SSDD calnexin.

Chapter 4: Calnexin and TMX share a juxtamembrane palmitoylation sequence that targets them to MAM

A version of this chapter has been published:
Lynes, E.M., Bui, M., Yap, M.C., Benson, M.D., Schneider, B., Ellgaard, L., Berthiaume, L.G. and T. Simmen. (2011) Palmitoylated TMX and calnexin target to the mitochondria associated membrane. *Embo J.* **31**: 457-70.

Chapter 4: Calnexin and TMX share a juxtamembrane palmitoylation site that targets them to the MAM

4.1 Introduction and Rationale

Because TMX and TMX4 share a PACS-2 interaction sequence with calnexin, we suspected that like calnexin, one or both of them might be found at MAMs. Several other factors also suggested that TMX or TMX4 might be MAM localized. TMX and TMX4 belong to the PDI family of redox chaperone proteins (Ellgaard and Ruddock, 2005), many of which function as disulphide bond isomerases in the ER. However, several PDI-related oxidoreductases also modulate calcium signalling, one of the main functions of the MAM. ERp57 binding to SERCA2b's luminal L4 loop suppresses SERCA2b's calcium pumping activity, whereas ERp44 binds to IP3 receptors and inhibits them (Higo et al., 2005; Li and Camacho, 2004). Both these studies showed that binding of ERp57 and ERp44 to their respective calcium signalling proteins was dependent on calcium levels in the ER lumen and the redox state of the ER lumen. Furthermore, Ero1α, the oxidoreductase that re-oxidizes PDI, is also present on the MAM (Gilady et al., 2010). Ero1α also has a role in modulating calcium signalling by IP3 receptors during apoptosis (Li et al., 2009), and its localization to MAM is dependent on oxidizing conditions within the ER and normoxic conditions (Gilady et al., 2010). Sigma-1 receptor, which also modulates IP3 receptor function by preventing its degradation, is also among the many ER chaperones that have been found on MAM (Hayashi et al., 2009). It is therefore not a novel concept that oxidoreductases and chaperone proteins have a role to play at MAM. Further suggesting that TMX may be a MAM protein is its known association with calnexin (Matsuo et al., 2009).

Given the paucity of information on how MAM is formed and how proteins target there, identifying more MAM targeted proteins could give insight into novel MAM targeting mechanisms or uncover common themes in MAM targeting mechanisms. In addition, characterizing the intra-ER localizations of TMX

family proteins might give some insight into the roles of the many family members. PDI proteins are primarily ER-localized, and some of them are known to act on specific substrates or groups of substrates; for example, ERp57's activity is specific to glycoproteins in the calnexin/calreticulin cycle (Jessop et al., 2007). To date, there are 20 members of the PDI family, including 5 transmembrane members (Kozlov et al., 2010). We decided to focus on transmembrane PDI family members as the majority of known MAM targeting mechanisms are cytosol-based, including PACS-2 interaction. Targeting to the MAM or exclusion from the MAM could be a way of assigning distinct roles or substrate specificities to transmembrane PDI-related proteins.

4.2 Results

4.2.1 TMX, but not TMX4, targets to MAM

Prior to attempting to determine the localization of TMX and TMX4, the antibodies that had been generated against TMX and TMX4 were tested for their ability to specifically detect TMX and TMX4, respectively, and for their function in required application. To knockdown the expression of TMX or TMX4, siRNA was used. Subsequently, a Western blot was performed to confirm that the signal from the band of molecular weight corresponding to that of the protein of interest decreased in intensity. This occurred in both cases (Figure 4.1) (Roth et al., 2009). A similar strategy was used in order to confirm which antibodies could be used for immunofluorescence microscopy (Figure 4.1). The antibodies used for each application are summarized in Materials and Methods, Table 2.9.

Various cell lines were tested by Western blot to ascertain the expression levels of TMX, TMX2, TMX3 and TMX4. A melanoma cell line was selected as redox signalling is known to be important in cancer, especially melanomas, which are resistant to redox stress (Wittgen and van Kempen, 2007). TMX4 was only highly expressed in A375P cells, but the other TMXs were highly expressed in HeLa, CaCo2 and A375P cells (Figure 4.2). HeLa and A375P cells were selected for gradient fractionation. A panel of TMX family proteins was examined using

the Optiprep density gradient in order to determine their intra-ER localization, using the protocol described in Methods and used in Chapter 3. Ribophorin II and ERp57 were used as rough ER markers, calnexin (Myhill et al., 2008) and ACAT1 (Lee et al., 2000; Rusinol et al., 1994) were used as MAM markers and complex II was used as a mitochondrial marker. TMX and TMX2 co-fractionated with calnexin and ACAT1 in both HeLa and A375P cells, whereas TMX3 did not have a consistent pattern in the two different cell lines. TMX4 was only highly expressed in A375P cells, and in that cell line was not enriched in MAM fractions, unlike TMX and TMX2 (Figure 4.3).

Before embarking on any further studies, a Percoll fractionation of HeLa cells was used to confirm TMX's presence on the MAM (Figure 4.4). TMX was found in the crude mitochondrial pellet, although unlike calnexin it was found exclusively in the crude mitochondrial pellet, with no population in the microsomes. The crude mitochondrial pellet was further fractionated into pure mitochondria and MAM, and like calnexin, TMX fractionated to MAM. Markers for the microsomes were eIF2α, which binds ribosomes, and Ribophorin II, and markers for the MAM were calnexin and Ero1α. Complex II was used as a mitochondrial marker.

Immunofluorescence microscopy and immunoelectron microscopy were also used to confirm the differences in localization between TMX and TMX4. HeLa cells were stained with an anti-TMX antibody and mitotracker was used to visualize the overlap between the TMX signal and mitochondria. A375P cells were stained with anti-TMX4 antibody and processed as above. Qualitatively, the TMX staining overlapped more with mitochondria than the TMX4 staining did, and a Manders coefficient was determined for each set of data, confirming this observation (Figure 4.5). Immunoelectron microscopy was also used with HeLa and A375P cells to visualize TMX and TMX4 staining in relation to the ultrastructure of the cell. Approximately 55% of TMX particles were detected in smooth ER tubules within 100nm of mitochondria in both cell lines, while only

17% percent of TMX4 staining met these criteria in A375P cells. Representative electron micrographs and a table summarizing the results are found in Figure 4.6. As TMX and TMX4 have 53% identity in their luminal thioredoxin domains, and have very similar domain organization (Figure 4.2 A), this difference in localization, observed by biochemical fractionation, immunofluorescence microscopy and immuno-electron microscopy, is very intriguing. A strategy was therefore devised to use the two proteins as a model to try to understand protein targeting to MAM.

4.2.2 TMX's transmembrane and cytosolic tail domains are necessary and sufficient for MAM targeting

In order to determine what part or parts of TMX determined its targeting to MAM, chimeric proteins of TMX and its non-MAM localized family member TMX4 were created (Figure 4.7 C). These luminally myc-tagged chimeric proteins were then expressed in HeLa cells, which were fractionated using the Optiprep protocol. First, it was confirmed that the localizations of the wildtype TMX and TMX4 constructs mirrored that of their endogenous counterparts (Figure 4.7 A and B). Then, the percentage of anti-myc signal found in fraction six was analyzed by western blot for the six chimeras of TMX and TMX4. We found that only in the case of the 411 chimera, which fused the luminal domain of TMX4 with the transmembrane and cytosolic domains of TMX, did the amount of signal in the MAM-containing fraction approach that of wildtype TMX (Figure 4.7 C and D).

Several motifs in TMX's sequence could be responsible for its MAM localization. Firstly, the CXXC thioredoxin motif in TMX's luminal domain could be responsible for binding to client proteins, to other oxidoreductases such as ERp44 (Anelli et al., 2003), or to MAM-localized calcium signalling molecules, thus altering its localization within the ER. Secondly, a C-terminal RQR motif could be responsible for retention of TMX in the ER, as it is for TMX4 (Roth et al., 2009). Thirdly, as mentioned in this and the previous chapter, TMX and TMX4

share a PACS-2 binding sequence that could be partially responsible for mediating localization changes. However, all of these motifs are shared with TMX4. Nonetheless, these motifs were abrogated and the resulting TMX mutants were analyzed by Optiprep gradient fractionation for any potential change in localization. None of the mutants showed significantly compromised MAM localization, however (Figure 4.7 E). Like the TMX4 RQR mutant that leaks out of the ER to the plasma membrane (Roth et al., 2009), the TMX RQR mutant could be found in lighter fractions corresponding to the later secretory pathway. However, a significant proportion of this mutant was retained in MAM. It was therefore concluded that a novel motif or motifs, found within a combination of the transmembrane and cytosolic domains of TMX, but not TMX4, must provide a signal for the MAM localization of TMX.

In order to confirm that the motif(s) found within TMX's transmembrane and cytosolic domains were sufficient for MAM targeting, further chimeric proteins were created, using the transmembrane and cytosolic tails of TMX and TMX4 grafted onto a viral protein, VSV-G. These chimeras were analyzed as the previous set was, with an Optiprep gradient fractionation. When FLAG-tagged VSVG alone was transfected into HeLa cells, it was found throughout the secretory system, but mostly in fraction 3, which corresponds to rER and ERGIC (Myhill et al., 2008). On the other hand, a large proportion of VSVG-TMX is targeted to fraction 6. This is not the case, however, with VSVG-TMX4 (Figure 4.7 F). These results confirmed that there must be a motif within TMX's TM and cytosolic domains that is necessary and sufficient for MAM enrichment.

4.2.3 A juxtamembrane palmitoylation site serves as TMX's MAM targeting signal

In order to discover the identity of the motif that targets TMX to MAM, the sequence of TMX was compared to that of calnexin. Since both proteins have been identified in several high throughput studies as palmitoylated proteins (Dowal et al., 2011; Forrester et al., 2011; Kang et al., 2008; Yount et al., 2010),

we hypothesized that palmitoylation could be the signal that targets both proteins to the MAM. Of particular interest was the fact that in both TMX and calnexin, the palmitoylation sequence identified by the CSS-PALM programme (Table 2.10) is localized right between the transmembrane and cytosolic domains, making the possibility that the motif has the same function in both proteins more likely.

This hypothesis was tested by the creation of a double cysteine to alanine mutation (CCAA) in TMX, abrogating the proposed palmitoylation site. TMX CCAA was then transfected into HeLa cells, and its intra-ER localization was examined by Optiprep gradient fractionation. Compared to wildtype TMX, the amount of TMX CCAA found in fraction six dropped from greater than 50% to less than 20% (Figure 4.8 A). Immunofluorescence microscopy was also used to analyze the colocalization of TMX CCAA with mitochondria as compared to that of wildtype TMX and TMX4. FLAG-tagged constructs were transfected into HeLa cells, and the overlap of the FLAG signal with mitochondria, marked by mitotracker, was quantified by calculating a Mander's coefficient. Compared to wildtype TMX, both TMX CCAA and TMX4 colocalized significantly less with mitochondria (Figure 4.8 B and C).

In order to verify the palmitoylation state of TMX and TMX4 and confirm that the CCAA mutation in TMX had actually abolished palmitoylation, the incorporation of ω-alkynyl palmitate into these proteins was measured using click chemistry (Kostiuk et al., 2009; Yap et al., 2010). Wildtype TMX but not the CCAA mutant was palmitoylated, and greatly reduced levels of palmitoylation were detected on TMX4 compared to TMX (Figure 4.8 D). The domain structures of the two TMX/TMX4 chimeric mutants 411 and 441 are depicted in Figure 4.7. These mutant were both were palmitoylated (Figure 4.8 E), although the 411 mutant had a higher palmitoylation signal that the 441 mutant. Interestingly, the extent of palmitoylation was correlated with the extent of MAM localization of the constructs (Figure 4.7 C). This led to the conclusion that the

TMX cytosolic domain alone provided the palmitoylation motif, regardless of which transmembrane domain was present. However, our findings raised the possibility that the transmembrane domain changes the susceptibility of the motif to palmitoylation. The TMX thioredoxin, RQR, and PACS-2 binding mutant constructs whose MAM localization was retained were also examined in this assay all had the same level of palmitoylation as the wildtype TMX (Figure 4.8 G).

In their 2010 paper, Hayashi and Fujimoto demonstrated that Sigma1 Receptor and other MAM proteins are associated with Triton X-114 detergent resistant membranes. We therefore decided to test whether TMX also localized to Triton X-114 resistant membrane, and if so, whether this localization was dependent on palmitoylation. First, HeLa cells were fractionated to yield a 10 000g heavy membrane pellet, which includes MAMs. These membranes were then resuspended and subject to incubation with the detergent Triton X-114. As expected, both TMX and the overexpressed FLAG-TMX wildtype construct were found primarily in the detergent-resistant pellet, whereas the FLAG-TMX CCAA mutant was found primarily in the supernatant (Figure 4.8 F). QSOX1, a transmembrane ER protein (Coppock and Thorpe, 2006), was used as a negative control in these experiments, and was found equally distributed between both fractions. From these data, we concluded that like Sigma1 receptor, TMX localizes to a region of the ER membrane that is resistant to Triton X-114, perhaps because of its lipid composition, and that palmitoylation is required for its localization to these membranes.

4.2.4 Palmitoylation also contributes to Calnexin's MAM localization

Calnexin has been identified as a MAM protein both in this study and by other groups (Hayashi and Su, 2007; Wieckowski et al., 2009). Calnexin's sequence contained a putative palmitoylation sequence (Figure 4.9 A) and calnexin had also been identified as a palmitoylated protein in high throughput scans. Furthermore, Ferrera et al confirmed that calnexin was phosphorylated in vivo, and suggested

that palmitoylation was important for targeting calnexin to lipid rafts on the plasma membrane of immature T cell precursors, in the context of T cell receptor signalling initiation (Ferrera et al., 2008). We decided to test whether, like TMX, calnexin was indeed palmitoylated in our cell lines and whether palmitoylation was required for its MAM localization. In the previous chapter, an interaction with the cytosolic sorting protein PACS-2 was identified as a factor contributing to calnexin's MAM localization, however, since the reduction in calnexin's MAM localization after PACS-2 knockdown was very modest, we hypothesized that palmitoylation may also be a contributing factor.

To test this hypothesis, a palmitoylation mutant of calnexin was created in a similar fashion to the FLAG-TMX CCAA mutant, where two juxtamembrane cysteines were mutated to non-palmitoylatable alanines using site directed mutagenesis by PCR-based splicing by overlap extension. This mutant was introduced into HeLa cells along with a FLAG-tagged wildtype calnexin construct. It was first verified that the wildtype calnexin replicated the fractionation pattern of endogenous calnexin. In comparing the fractionation pattern of the calnexin CCAA mutant to that of the wildtype, it was observed that, like with TMX, a significantly reduced proportion of calnexin CCAA was associated with fraction 6 (Figure 4.9 B). A palmitoylation labelling assay was also performed to ensure that the CCAA mutation effectively abrogated the palmitoylation signal from wildtype calnexin (Figure 4.9 C).

Furthermore, immunofluorescence microscopy was used to analyze the colocalization of calnexin CCAA with mitochondria as compared to that of wildtype calnexin. FLAG-tagged constructs were transfected into HeLa cells, and the overlap of the FLAG signal with mitochondria, which were marked by mitotracker, was quantified by calculating a Mander's coefficient. Compared to wildtype calnexin, calnexin CCAA colocalized significantly less with mitochondria (Figure 4.9 D and E). We decided to evaluate whether calnexin, like TMX, resided in the detergent resistant portion of the MAM fraction.

Interestingly, neither endogenous nor FLAG-tagged wildtype calnexin was particularly enriched in DRMs, with a slightly greater proportion of calnexin in soluble fractions (Figure 4.9 F). Mutating the palmitoylation site had no effect on the distribution of calnexin between the detergent resistant and soluble fractions. This would indicate that MAMs may be composed of both detergent resistant and non-resistant microdomains, and that detergent resistant microdomains may be a factor in MAM targeting for some MAM localized proteins, but not all. This lack of DRM targeting may explain why calnexin is comparatively less enriched in fraction 6 than TMX. Given the role of cholesterol in the targeting of Sigma1 receptor (Hayashi and Fujimoto, 2010) to MAM, HeLa cells were treated with methyl- β cyclodextran to deplete cholesterol from membranes, which were subsequently fractionated using an Optiprep gradient (Figure 4.9 H). The localizations of TMX and calnexin were not significantly different from controls on this gradient, indicating that membrane cholesterol levels may not play a role in the localization of TMX and calnexin to MAMs.

Finally, a VSVG chimeric construct was made, similar to the chimeric constructs made with TMX and TMX4. The cytosolic tail of calnexin was spliced to the viral protein VSVG, and the ability of calnexin's cytosolic tail to target VSVG to MAMs was analyzed using the Optiprep density gradient. The signal for VSVG alone was found throughout the secretory pathway, but primarily in fractions 3 and 4. Like the cytosolic tail of TMX, calnexin's cytosolic tail was able to redistribute the signal from VSVG to fraction 6 (Figure 4.9 G).

4.2.5 Tac reporter constructs confirm VSVG chimeric protein results

In order to confirm the results obtained with the VSVG chimera, chimeric constructs of calnexin's cytosolic tail with a Tac reporter protein were also created. Tac is the interleukin 2 receptor α chain, and has previously been used to evaluate the role of both furin and calnexin cytosolic tails in trafficking (Okazaki et al., 2000; Simmen et al., 1999). Chimeric constructs of Tac were made with the cytosolic tails of TMX, TMX CCAA, TMX4, Calnexin, and Calnexin CCAA.

These constructs were then transfected into HeLa cells, which were fractionated using a 10-30% discontinuous Optiprep gradient. Confirming the results obtained with the VSVG fusion constructs, the tails of TMX and calnexin were able to target the Tac reporter to fraction 6, corresponding to MAM membranes (Figure 4.10). Importantly, the CCAA mutant tails of both TMX and calnexin lost their ability to target Tac to fraction six, further confirming the importance of the palmitoylation site to MAM targeting.

4.2.6 2-Bromopalmitate, a palmitoylation inhibitor, displaces both TMX and calnexin from the MAM

An alternative approach was taken to confirm the role of palmitoylation in the MAM retention of TMX and calnexin. The palmitoylation inhibitor 2-bromopalmitate is a palmitate analogue that blocks the transfer of palmitate onto proteins by palmitoyl transferases (Resh, 2006). Immunofluorescence microscopy was used to measure the colocalization of TMX and calnexin signals with mitochondria in HeLa cells before and after 2-bromopalmitate treatment. In both the cases of TMX and calnexin, treatment with 2-bromopalmitate reduced the colocalization of the signal with mitotracker, as measured by a Mander's coefficient (Figure 4.11). The fact that these results were consistent with those obtained by abolishing the palmitoylation sequences of TMX and calnexin further confirmed the important role of palmitoylation in the MAM localization of these two proteins. In a second experiment, HeLa cells were treated with 2-bromopalmitate for 4 hours, then the effect of the drug on the subcellular localization of TMX, calnexin, and marker proteins was analyzed by Optiprep gradient fractionation. Although markers for mitochondria (complex II) and ER (PDI and IP3R) were unaffected by 2-bromopalmitate treatment, TMX and calnexin both lost their enrichment in fraction 6 and shifted towards lighter fractions corresponding to rER, while SERCA2b was slightly shifted towards heavier fractions (Figure 4.12).

4.2.7 Palmitoylation may be a targeting signal for other MAM localized proteins

Both TMX and calnexin are targeted to MAM by a similar juxtamembrane palmitoylation motif, which raised the question of other MAM proteins being targeted there by the same mechanism. We analyzed the four published studies of palmitoylation proteomes (Dowal et al., 2011; Forrester et al., 2011; Kang et al., 2008; Yount et al., 2010) for transmembrane ER or MAM proteins that might also use palmitoylation as a targeting mechanism. This analysis yielded four additional proteins; mouse heme oygenase-1, VDAC 1 and 2, and GRP75. Heme oxygenase 1 is a stress-inducible ER protein that mediates the degradation of heme, forming carbon monoxide, which has been implicated in anti-apoptotic signalling by blocking calcium channels (Hwang et al., 2009; Scragg et al., 2008). HO1 did indeed fractionate like a MAM protein on Optiprep gradients, and a dramatic shift towards less dense fractions was observed upon 2-bromopalmitate treatment (Figure 4.13 A). VDAC 1 and 2 are primarily localized in the outer mitochondrial membrane, but there is considerable evidence that they are also present on the ER, where they are involved in the transport of calcium and reactive oxygen species (Shoshan-Barmatz and Israelson, 2005). Using a Percoll MAM fractionation, we were able to confirm that a small population of both proteins was found on MAM (Figure 4.13 B). VDAC 1 and 2 were primarily found in fraction 6 following Optiprep fractionation of HeLa cell, and when palmitoylation was blocked, there was a small shift of both proteins from fraction 6 to fraction 5, but this was negligible in comparison with HO1 (Figure 4.13 B). GRP75 is a cytosolic chaperone that is already known to localize to MAMs, where it mediates MAM formation by connecting ER-localized IP3 receptors to mitochondrial VDAC1 (Szabadkai et al., 2006). 2-Bromopalmitate treatment did not cause a change in localization of GRP75 (Figure 4.13 C), perhaps because GRP75 is a cytosolic protein, and the transmembrane domain may be an important component of palmitoylation-mediated MAM localization. Overall, these data indicate that there may be other proteins that localize to MAM via a

palmitoylation signal, but that palmitoylation is clearly not the universal MAM targeting signal, and it is possible that it only applies to transmembrane proteins.

4.3 Discussion and Future Perspectives

The findings of this project are summarized as a model in Figure 4.14. Palmitoylation is a reversible process, and therefore the control of palmitoylation and depalmitoylation could regulate the localization of TMX and calnexin. The question of which enzymes control the equilibrium between palmitoylated/non-palmitoylated MAM proteins is therefore an important one. Addition of palmitate is catalyzed by the Palmitoyl Acyltransferase family of proteins (PATs) of which there are 23 members (Fukata and Fukata, 2010). The localizations of some of these proteins are known, but it is not known whether any specifically target to MAM. Recently, Lakkaraju et al. demonstrated that calnexin is palmitoylated by the PAT family member DHHC6 (Lakkaraju et al., 2012). Removal of palmitate is catalyzed by acylprotein thioesterases 1 and 2 (APT1 and -2) and protein palmitoyl thioesterase PPT1, but it is currently unknown which of these proteins is important in controlling calnexin's palmitoylation state.

The mechanism whereby palmitoylation targets proteins to the MAM is still an open question. Perhaps palmitoylation renders proteins more compatible with the lipids or membrane domains present at the MAM. Charollais and Van der Goot suggested that palmitoylation could orient transmembrane domains differently within a membrane, thus making them more or less compatible with an ordered lipid domain (Charollais and Van Der Goot, 2009). However, this same research group also suggests based on theoretical structure predictions that in the case of calnexin, palmitoylation may reorient the cytosolic tail, changing its ability to interact with other membrane or cytosolic proteins, and more specifically, mediating its interaction with the translocon (Lakkaraju et al., 2012). Perhaps a protein-protein interaction that is affected by calnexin's and TMX's palmitoylation status retains these two proteins at the MAM.

What does palmitoylation mean for calnexin's function? TMX's functions and binding partners are poorly understood, but calnexin has several well-described functions and many substrate proteins and binding partners. Palmitoylation could affect calnexin's functions by altering its ability to bind to other proteins (Lakkaraju et al., 2012). Palmitoylation could also affect calnexin's functions by changing its localization; either sequestering it in certain ER subdomains or excluding it from others.

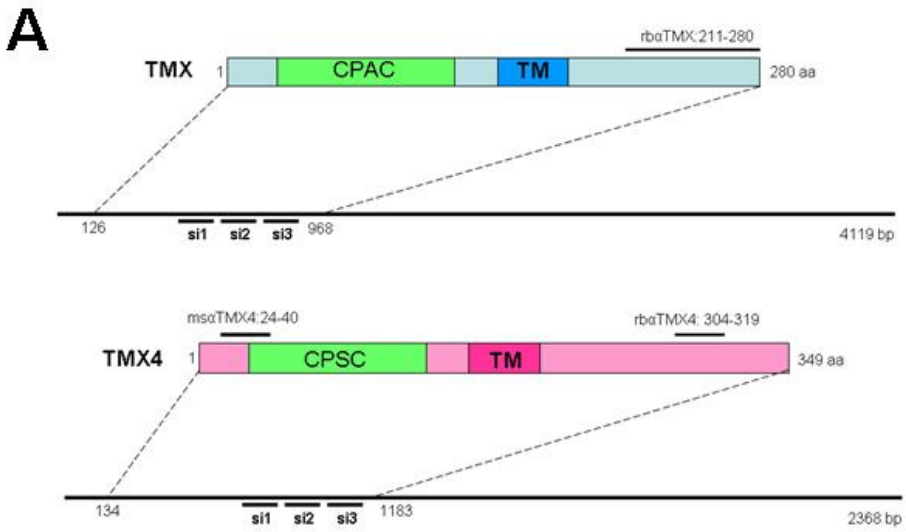
A
TMX
1
CPAC
TM
280 aa
rbαTMX:211-280
126
si1
si2
si3
968
4119 bp
TMX4
msαTMX4:24-40
rbαTMX4: 304-319
CPSC
349 aa
134
1183
2368 bp

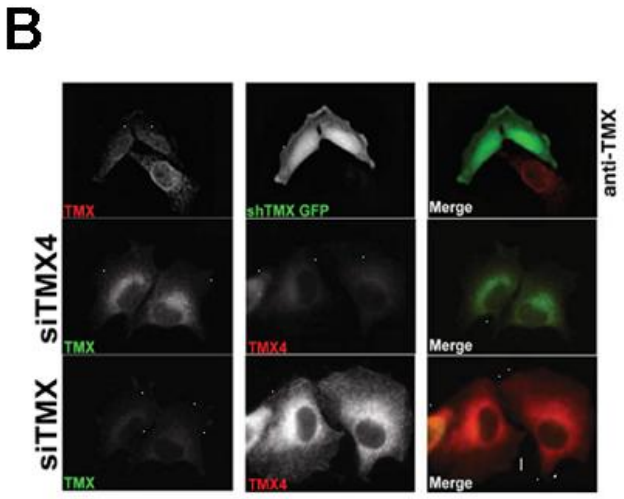
B
siTMX4
siTMX
TMX
shTMX GFP
TMX4
Merge
anti-TMX

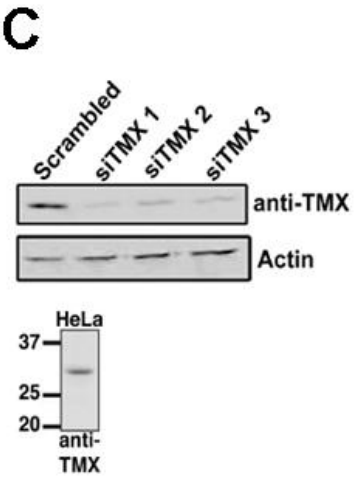
C
Scrambled
siTMX 1
siTMX 2
siTMX 3
anti-TMX
Actin
HeLa
37
25
20
anti-
TMX

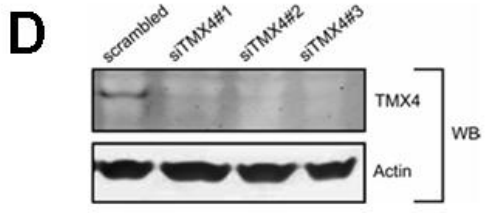
D
scrambled
siTMX4#1
siTMX4#2
siTMX4#3
TMX4
Actin
WB

Figure 4.1: Quality control of TMX and TMX4 antibodies. A: Schematic diagram of epitope sites used to generate antibodies against TMX and TMX4 proteins, as well as the target sites of the siRNAs used to knock down TMX and TMX4 siRNAs. The thioredoxin domains of TMX and TMX4 are indicated in green, and the transmembrane domains are indicated (TM). The base pair sequences targeted by siRNAs in TMX are 552-76, 799-823 and 938-62. The base pair sequences targeted by siRNAs in TMX4 are 741-67, 823-48, and 1132-56. **B**: SiRNA against TMX and TMX4, as well and shRNA against TMX, was used to knockdown TMX and TMX4 in order to test the efficacy of the rabbit anti TMX antibody in HeLa cells and mouse anti TMX 4 antibody in A375P cells for immunofluorescence microscopy. SiRNAs against TMX and TMX4 were used to similarly test the efficacies of the rabbit anti TMX (**C**) and rabbit anti TMX4 (**D**) antibodies for western blot. Actin was used as a loading control in both experiments.

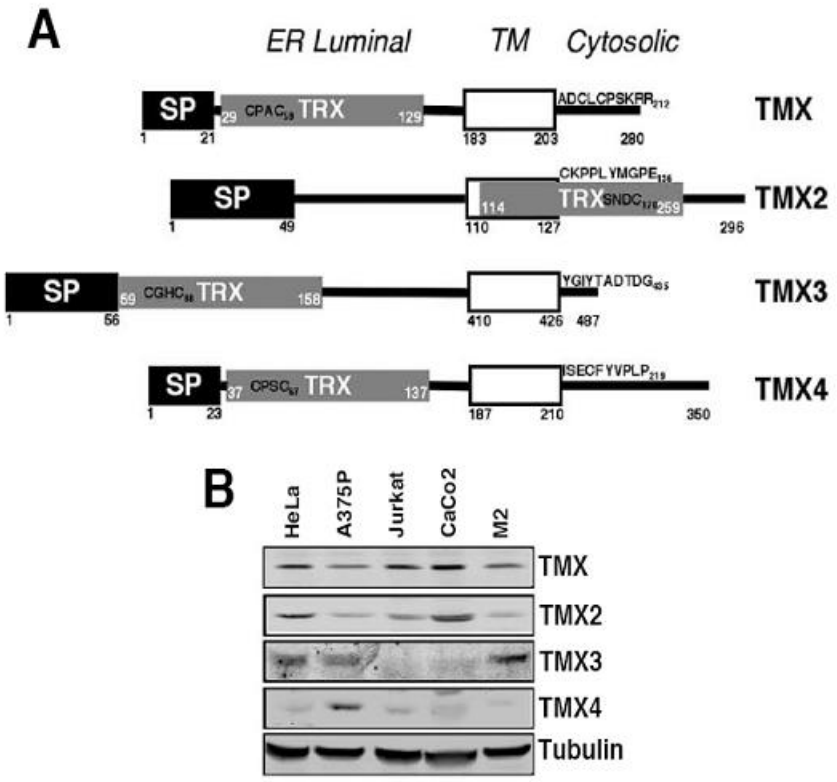

Figure 4.2: TMX family members. **A.** Schematic of the domain organization and active site and tail sequences of four TMX family members. SP = signal peptide, TRX = thioredoxin domain, TM = transmembrane domain. **B.** Expression levels of TMX family members 1-4 in a panel of cultured mammalian cancer cells. HeLa cells are cervical cancer, A375P cells are melanoma, Jurkat cells are T lymphocytes from a leukemia patient, CaCo2 are colon carcinoma, and M2 are melanoma. Tubulin was used as a loading control.

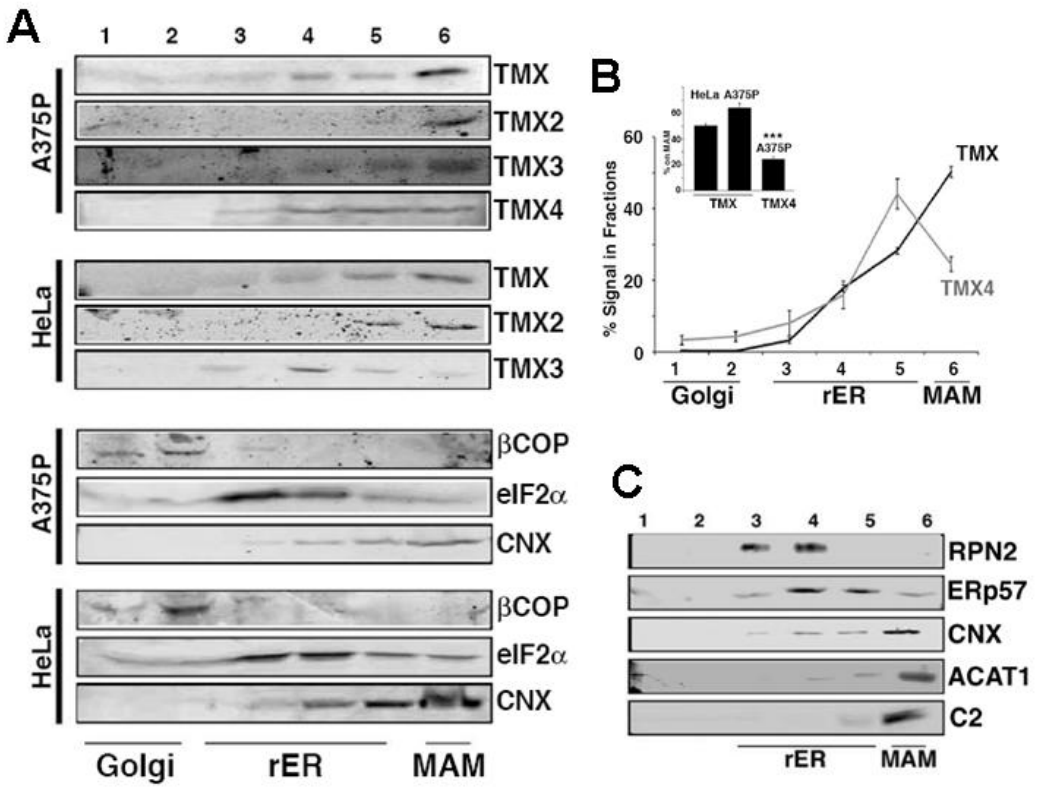

Figure 4.3: Intra-ER localization of TMX family members in A375P and HeLa cells. A. Homogenates of A375P and Hela cells were fractionated on a 10-30% discontinuous Optiprep gradient. Fractions were analyzed by SDS-PAGE and western blot. βCOP was used as a Golgi marker, eIF2α was used as a rough ER marker, and calnexin was used as a MAM marker. The percentage of TMX and TMX4 signal found by western blot in each fraction was quantified and summarized in **B.** The percentage of TMX and TMX4 found in fraction six, where MAM marker calnexin is concentrated, is also quantified. (n=3) p=0.001 between A375P TMX and TMX4. **C.** Additional markers were used to characterize the Optiprep gradient: Complex II (C2) for mitochondria, ACAT1 and calnexin (CNX) for MAM and ERp57 and ribophorin II (RPN2) for rough ER.

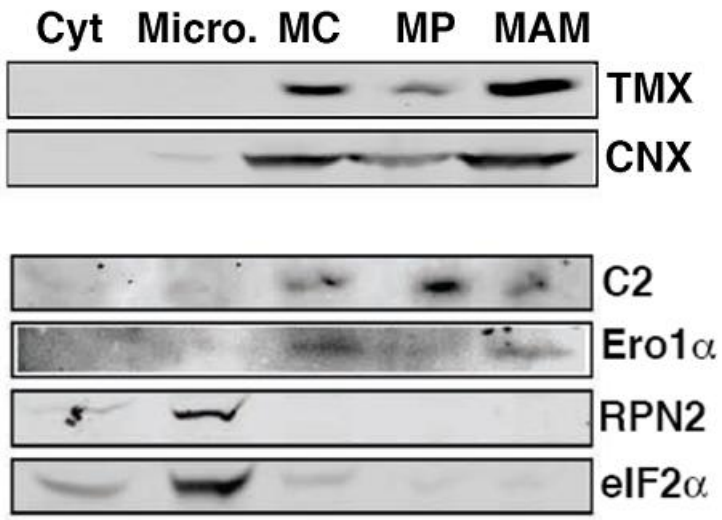

Figure 4.4: TMX localizes to MAM. Percoll MAM fractionation of HeLa cell homogenates was used to confirm TMX's MAM localization. Homogenates were separated into cytosolic (Cyt), microsomal (Micro.), crude mitochondria (MC), pure mitochondria (MP) and MAM fractions and the fractions were analyzed by SDS-PAGE and western blot. Complex II (C2) was used as a mitochondrial marker, calnexin (CNX) and Ero1α were used as MAM markers, and ribophorin 2 (RPN2) and eIF2α were used as rough ER markers.

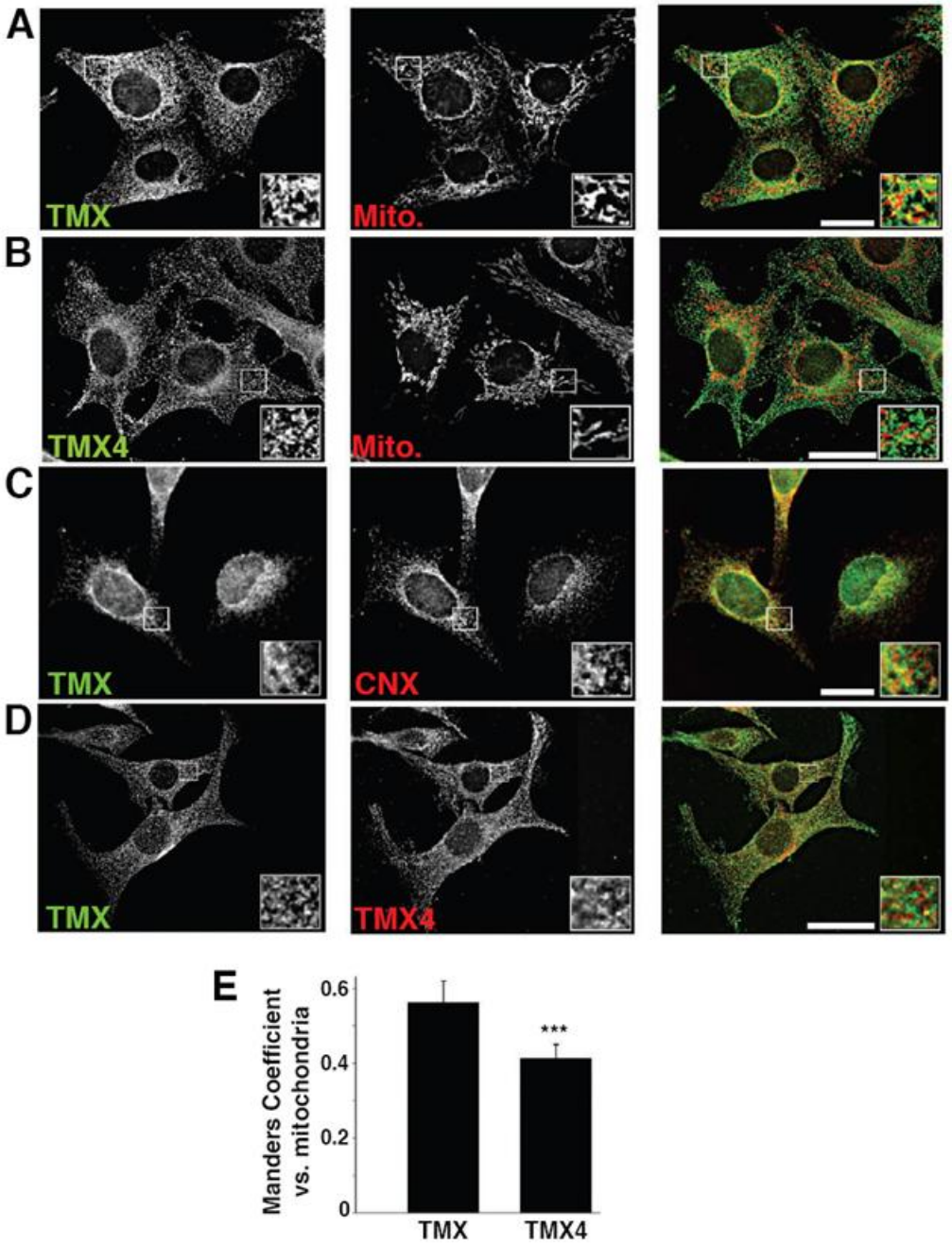

Figure 4.5: TMX colocalizes with mitotracker and MAM marker calnexin by immunofluorescence microscopy. A. Colocalization of TMX with mitotracker. **B.** Colocalization of TMX4 with mitotracker. **C.** Colocalization of TMX with calnexin. **D.** Colocalization of TMX with TMX4. **E.** The Manders coefficient represents the degree of colocalization between TMX and TMX4 with mitochondria labelled with mitotracker, as in representative images **A** and **B**. (n=7 and 8, respectively) $p<0.001$.

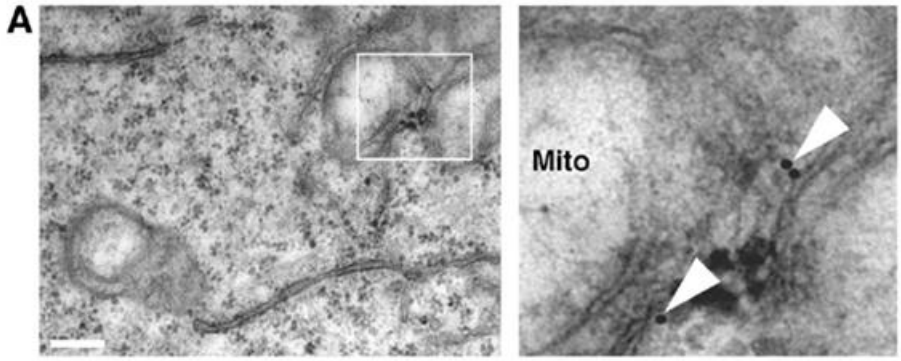

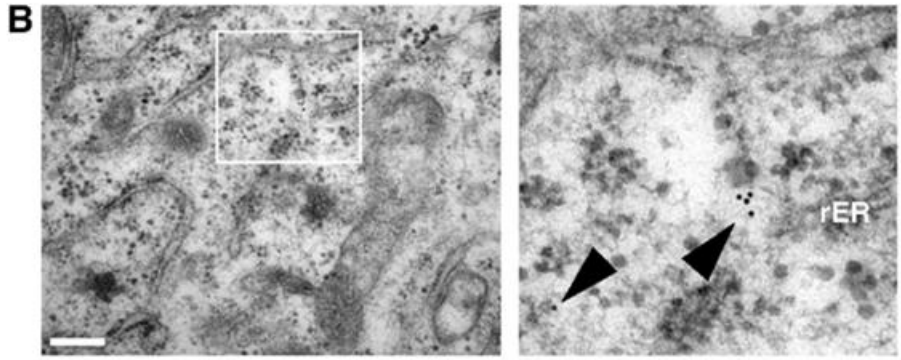

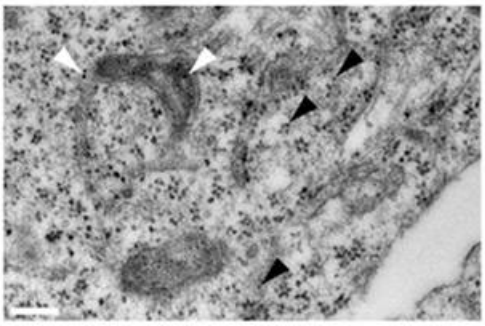

D

	rER	sER	MAM
TMX	HeLa: 33% A375P: 41%	HeLa: 12% A375P: 5%	HeLa: 55% A375P: 54%
TMX4	A375P: 76%	A375P: 7%	A375P: 17%

Figure 4.6: Immunoelectron microscopy of HeLa and A375P cells labelled with anti-TMX and TMX4 antibodies conjugated to gold particles. A. TMX immunogold labelling in HeLa cells. B. TMX4 immunogold labelling in A375P cells. C. TMX (large particles, white arrowheads) and TMX4 (small particles, black arrowheads) double labelling in A375P cells. D. Quantification of TMX and TMX4 immunogold labelling from 2 independent experiments with the localization of immunogold particles assigned to rough ER, smooth ER and MAM (ER tubules within 50 nm of mitochondria). Scale bar=200 nm. Contributed by Bobbie Schneider, Fred Hutchinson Cancer Research Center, Seattle, WA, USA.

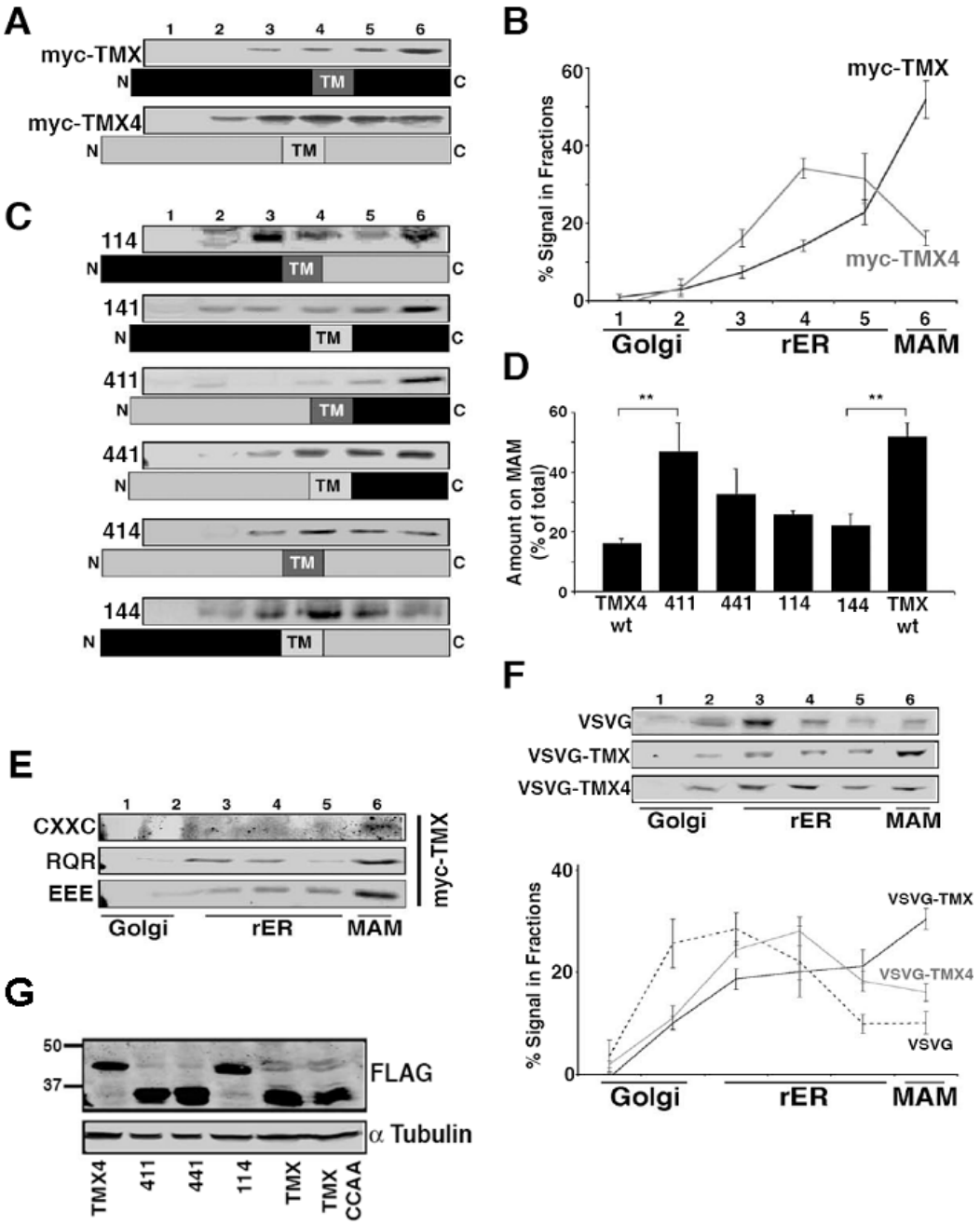
A
1 2 3 4 5 6
myc-TMX
N TM C
myc-TMX4
N TM C
B
myc-TMX
myc-TMX4
% Signal in Fractions
60
40
20
0
1 2 3 4 5 6
Golgi
rER
MAM
C
114
141
411
441
414
144
N TM C
D
Amount on MAM (% of total)
60
40
20
0
**
**
TMX4 wt
411
441
114
144
TMX wt
E
1 2 3 4 5 6
CXXC
RQR
EEE
myc-TMX
Golgi
rER
MAM
F
1 2 3 4 5 6
VSVG
VSVG-TMX
VSVG-TMX4
Golgi
rER
MAM
% Signal in Fractions
40
20
0
VSVG-TMX
VSVG-TMX4
VSVG
Golgi
rER
MAM
G
50
37
FLAG
α Tubulin
TMX4
411
441
114
TMX
TMX CCAA

Figure 4.7: The TMX transmembrane and cytosolic domains are necessary and sufficient for MAM targeting. Except where indicated, detection of chimeric mutants was performed with rabbit anti-Myc. **A.** Homogenates of HeLa cells transfected with myc-TMX and myc-TMX4 were fractionated on a 10-30% discontinuous Optiprep gradient. **B.** Quantification of the myc-TMX and myc-TMX4 signal found in each fraction. **C.** Optiprep gradient analysis of TMX/TMX4 chimera was performed as in A. Chimera were assigned a numerical code where 1 stands for TMX and 4 stands for TMX4 as follows: luminal domain/transmembrane domain/cytosolic domain. Schematic illustrations of the domain composition of each chimera are found below. **D.** Quantification of gradients in **C.** p=0.027 between TMX4 and 411, and p=0.012 between TMX and 144. **E.** Optiprep fractionation for selected TMX mutants CXXC=ΔThioredoxin site, RQR 267-9 was mutated to AAA, EEE=Asp 248-50 was mutated to AAA. **F.** Optiprep gradient fractionation of FLAG-VSVG-TMX chimeras. HeLa cells transfected with the indicated constructs were fractionated as in **C** and experiments were quantified as in **D**. **G.** Expression level analysis of TMX/TMX4 chimeras in HeLa cells by western blot. Tubulin was used as a loading control.

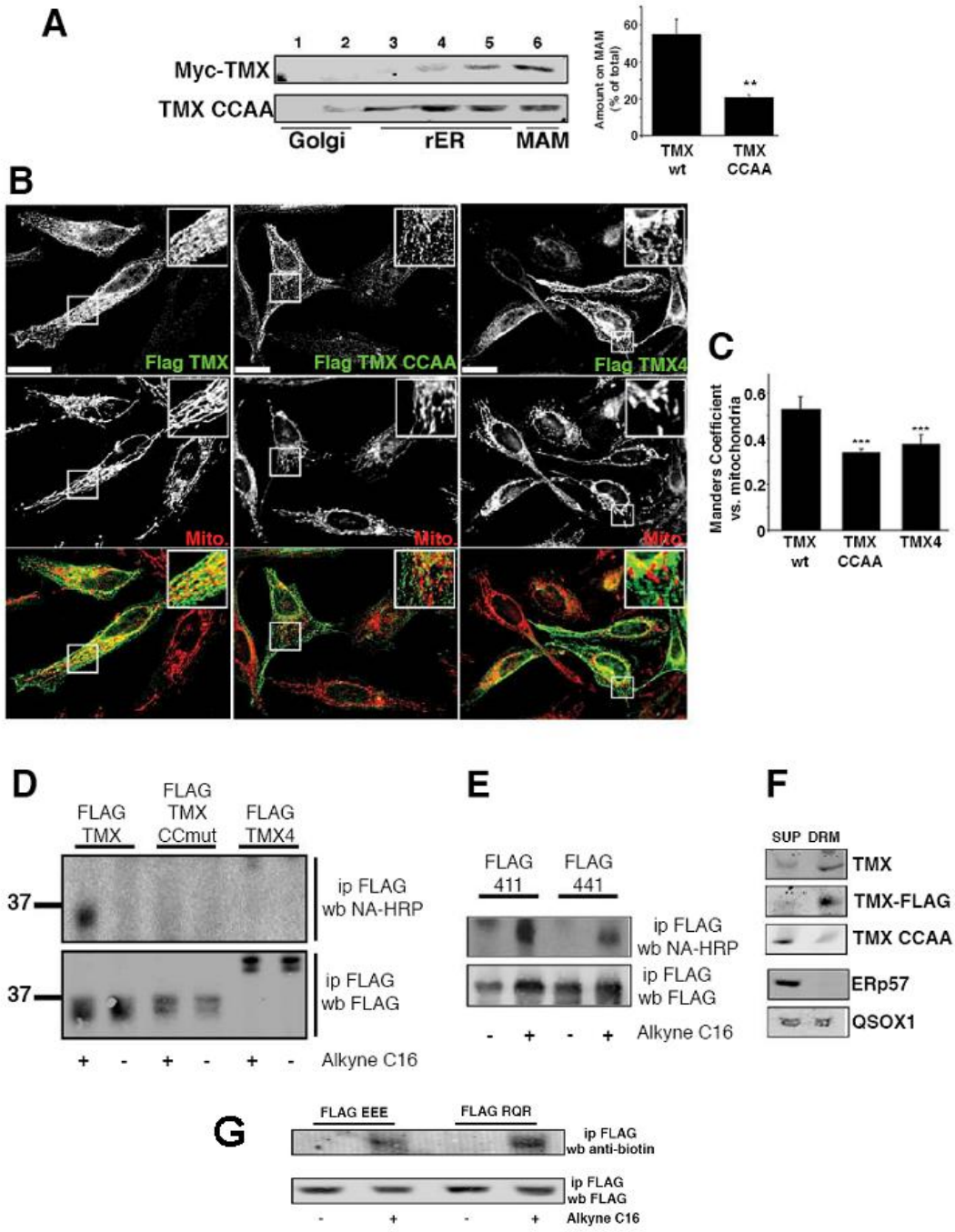
A
1 2 3 4 5 6
Myc-TMX
TMX CCAA
Golgi
rER
MAM
Amount on MAM (% of total)
60
40
20
0
**
TMX wt
TMX CCAA
B
Flag TMX
Flag TMX CCAA
Flag TMX4
Mito.
C
Manders Coefficient vs. mitochondria
0.6
0.4
0.2
0
***
TMX wt
TMX CCAA
TMX4
D
FLAG TMX
FLAG TMX CCmut
FLAG TMX4
37
ip FLAG wb NA-HRP
ip FLAG wb FLAG
+ - + - + - Alkyne C16
E
FLAG 411
FLAG 441
ip FLAG wb NA-HRP
ip FLAG wb FLAG
- + - + Alkyne C16
F
SUP DRM
TMX
TMX-FLAG
TMX CCAA
ERp57
QSOX1
G
FLAG EEE
FLAG RQR
ip FLAG wb anti-biotin
ip FLAG wb FLAG
- + - + Alkyne C16

Figure 4.8: A juxtanuclear palmitoylation signal mediates the MAM enrichment of TMX. A. Homogenates of HeLa cells transfected with wildtype myc-TMX or a myc-TMX with cysteines 205 and 207 mutated to alanines (TMX CCAA) were fractionated on a discontinuous 10-30% Optiprep gradient. A representation of 3 independent experiments is shown, and the signal for each construct in fraction six is quantified at right. $p=0.012$ between wildtype and TMX CCAA. **B.** FLAG tagged TMX wt and CCAA were expressed in HeLa cells that were processed for immunofluorescence microscopy with mitotracker and anti-FLAG antibody. Overlap between FLAG signal and mitotracker is shown at right, and quantified as a Manders coefficient in **C.** $p<0.001$. **D.** and **E.** TMX/TMX4 chimeric mutants 411 and 441 (see Figure 4.7) were transfected into HeLa cells and evaluated for incorporated alkynyl palmitate, detected by neutravidin HRP. Expression levels of the constructs were detected with anti-FLAG antibody. **F.** Detergent-resistant membrane fractionation of HeLa cells expressing FLAG-TMX and FLAG-TMX CCAA. FLAG signals and endogenous TMX were detected by western blot. ERp57 and QSOX1 were used as non-DRM enriched controls. **G.** Additonal TMX contructs were analyzed for palmitoylation as in **D** and **E**. *Panels D,E and G were done in collaboration with Megan Yap.*

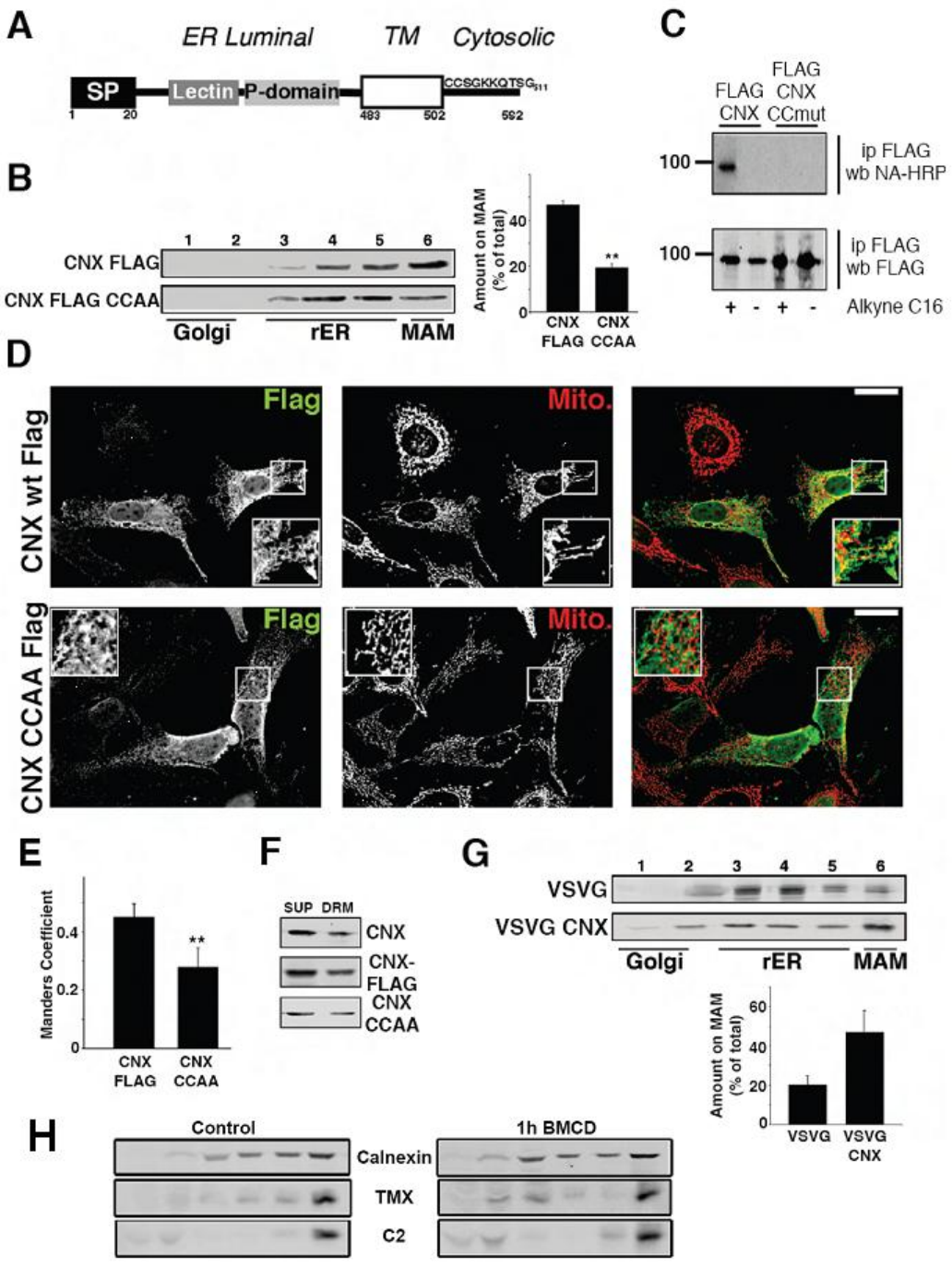
A
ER Luminal
TM
Cytosolic
SP
Lectin
P-domain
CCSGKKQTSG
1
20
483
502
592
B
CNX FLAG
CNX FLAG CCAA
1 2 3 4 5 6
Golgi
rER
MAM
Amount on MAM (% of total)
CNX FLAG
CNX CCAA
C
FLAG CNX
FLAG CNX CCmut
100
ip FLAG wb NA-HRP
ip FLAG wb FLAG
+ - + -
Alkyne C16
D
CNX wt Flag
CNX CCAA Flag
Flag
Mito.
E
Manders Coefficient
CNX FLAG
CNX CCAA
F
SUP DRM
CNX
CNX-FLAG
CNX CCAA
G
VSVG
VSVG CNX
Golgi
rER
MAM
Amount on MAM (% of total)
VSVG
VSVG CNX
H
Control
1h BMCD
Calnexin
TMX
C2

Figure 4.9: Palmitoylation mediates calnexin's MAM enrichment. A. Schematic representation of calnexin's domain structure. SP=signal peptide, TM=transmembrane domain. Amino acid positions are indicated with numbers, and the juxtamembrane amino acid sequence is indicated. **B.** Optiprep gradient fractionation of HeLa cells transfected with wildtype FLAG-calnexin or calnexin with the juxtamembrane cysteines 503 and 504 mutated to alanines (calnexin CCAA). Enrichment of these constructs on MAM membranes was determined by western blot and quantification of three independent experiments is show to the right. p=0.002 between wildtype and calnexin CCAA. **C.** Detection of alkynyl palmitate incorporation was performed as for TMX contructs in Figure 4.8. **D.** FLAG tagged CNX wt and CCAA were expressed in HeLa cells that were processed for immunofluorescence microscopy with mitotracker and anti-FLAG antibody. Scale bar=25 μm. Overlap between FLAG signal and mitotracker is shown at right, and quantified as a Manders coefficient in **E.** $p<0.0044$. **F**. Detergent-resistant membrane fractionation was performed and analyzed as in Figure 4.8. Neither endogenous calnexin nor the wildtype or CCAA calnexin constructs were enriched in DRMs. **G.** Optiprep gradient fractionation of HeLa cells tranfected with VSVG and the VSVG-calnexin chimeric construct. Distribution detected by western blot with rabbit anti-VSVG antiserum. Targeting of VSVG to MAM membranes in 3 independent experiments is quantified below. **H.** Depletion of cholesterol from membranes with β-methyl-cyclodextrin did not affect targeting of TMX or calnexin as assessed by Optiprep gradient fractionation. *Panel C was done in collaboration with Megan Yap.*

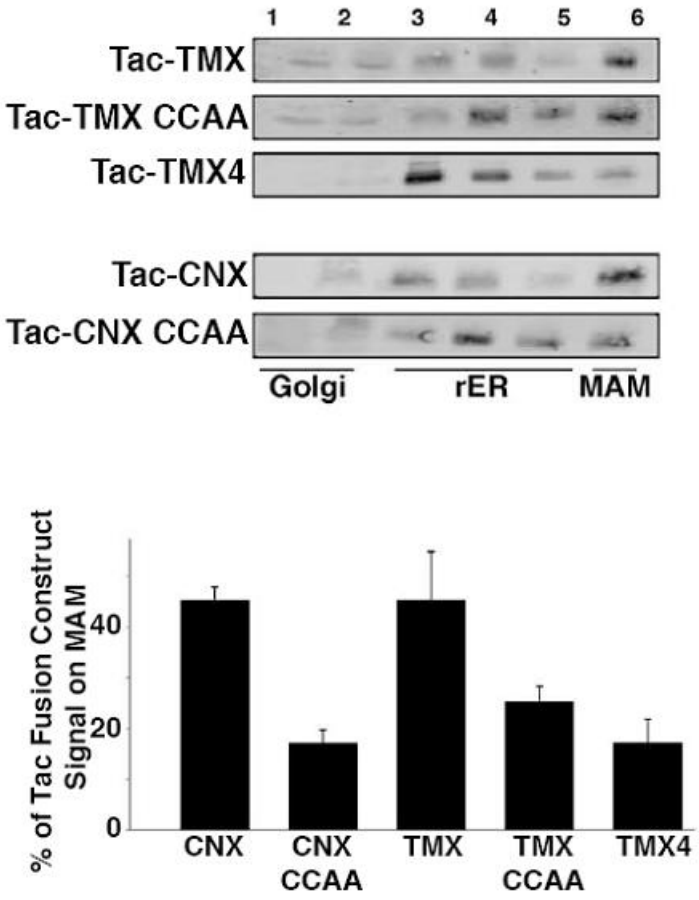

Figure 4.10: Analysis of Tac fusion construct localization by Optiprep fractionation. Fusion constructs of Tac with the transmembrane domains and cytosolic tails of calnexin, calnexin CCAA, TMX, TMX CCAA and TMX4 were expressed in HeLa cells that were homogenized and subjected to a 10-30% Optiprep density gradient fractionation. The distribution of the constructs was detected by western blot using a rabbit anti-Tac antibody. The average percent signal detected in fraction six in 3 independent experiments for each of the constructs is displayed in the chart below.

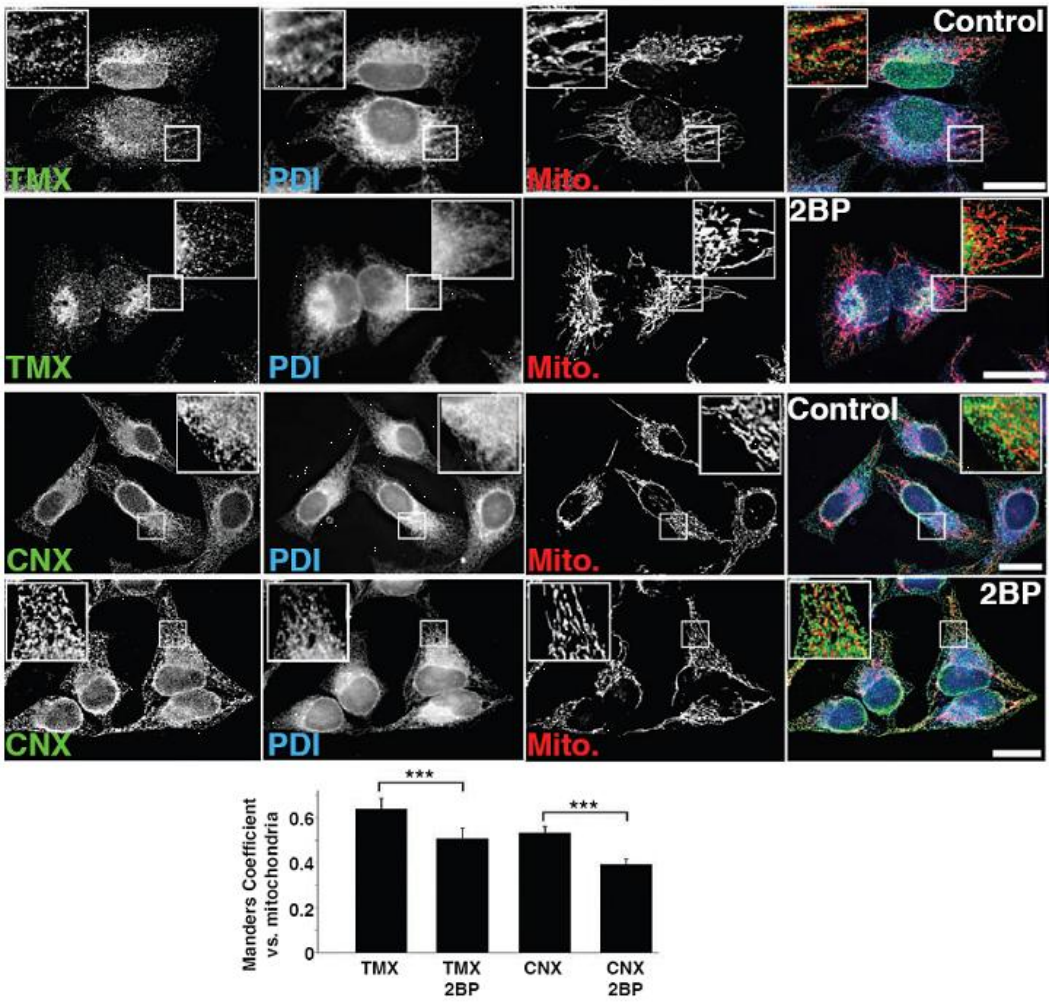

Figure 4.11: The palmitoylation inhibitor 2-Bromopalmitate reduces colocalization of TMX and calnexin signal with mitochondria. HeLa cells were treated as indicated with 2-Bromopalmitate for 4 hours before being processed for immunofluorescence microscopy. Rabbit anti-TMX, rabbit anti-calnexin, and mouse anti-PDI were used to detect the indicated proteins, and mitotracker was used to visualize mitochondria. Scale bar=25 μm and framed inset picture show a magnified area. Right-most images of each row show the overlap of TMX or calnexin with mitotracker and PDI, which was quantified using a Manders coefficient. $p<0.001$ for the comparisons indicated.

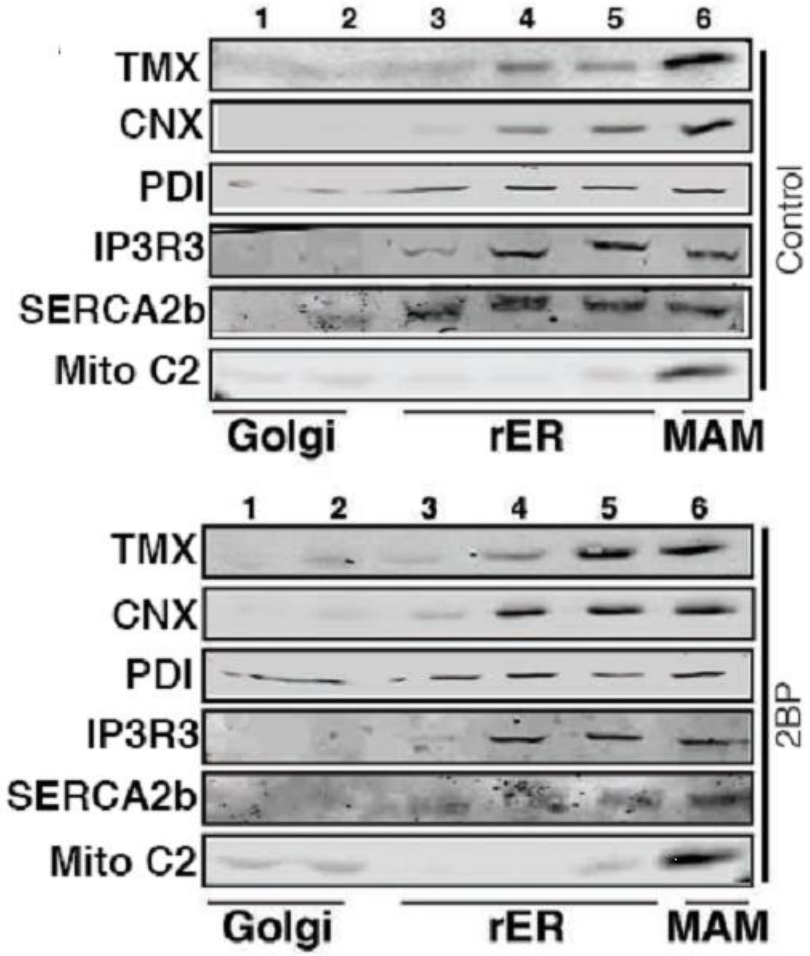

Figure 4.12: 2-Bromopalmitate decreases co-fractionation of calnexin and TMX with MAM markers. Control HeLa cells or HeLa cells treated for 4 hours with 2-Bromopalmitate were fractionated on a 10-30% discontinuous Optiprep gradient. Enrichment of calnexin and TMX in MAM fraction 6 was determined by western blot, with ER proteins PDI, IP_3R3, SERCA2b and mitochondrial Complex II (C2) serving as controls for MAM integrity. Exposure times were adjusted such that the most intense band appeared black.

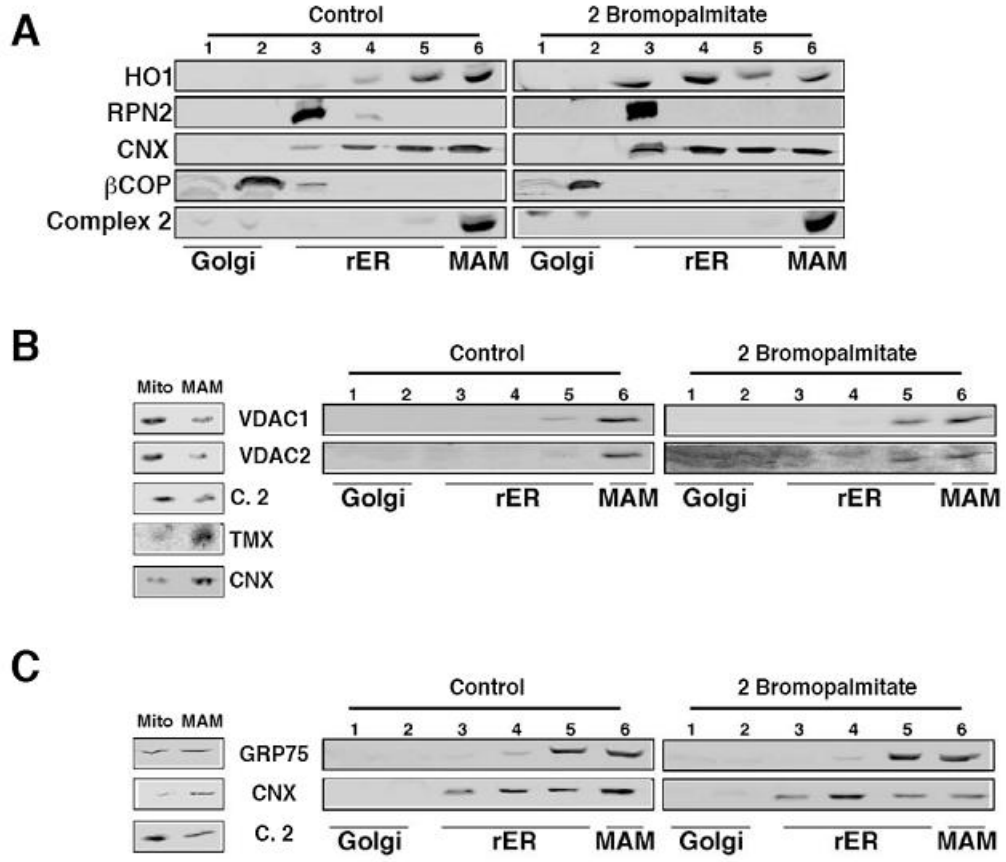

Figure 4.13: Palmitoylation also affects the intra-ER localization of MAM protein Hemeoxygenase-1 (HO1) and VDAC1/2 but not GRP75. A. Control B16 cells or cells treated for 4 hours with 2-Bromopalmitate were fractionated on a discontinuous 10-30% Optiprep gradient. Enrichment of HO1 on MAM membranes was determined by western blot, and detection of ribophorin 2 (RPN2, rough ER), calnexin (CNX, MAM), bCOP (Golgi) and complex II (CII, mitochondria) served as a control for MAM intergrity. **B.** Left gels: Percoll fractionation of mitochondria and MAM using HeLa cells. VDAC 1 and 2 cofractionate mostly with mitochondrial marker complex II (CII) but show some cofractionation with MAM markers TMX and calnexin (CNX). Right gels: Optiprep fractionation of control HeLa cells and cells treated with 2-Bromopalmitate for 4 hours. **C.** Left gels: Percoll fractionation of HeLa cells shows GRP75 signal evenly detected in MAM and mitochondrial fraction indicated by calnexin and complex II. Right gels: Optiprep gradient fractionation performed as above. No change in GRP75 localization was observed despite the expected shift in calnexin's localization (lower right).

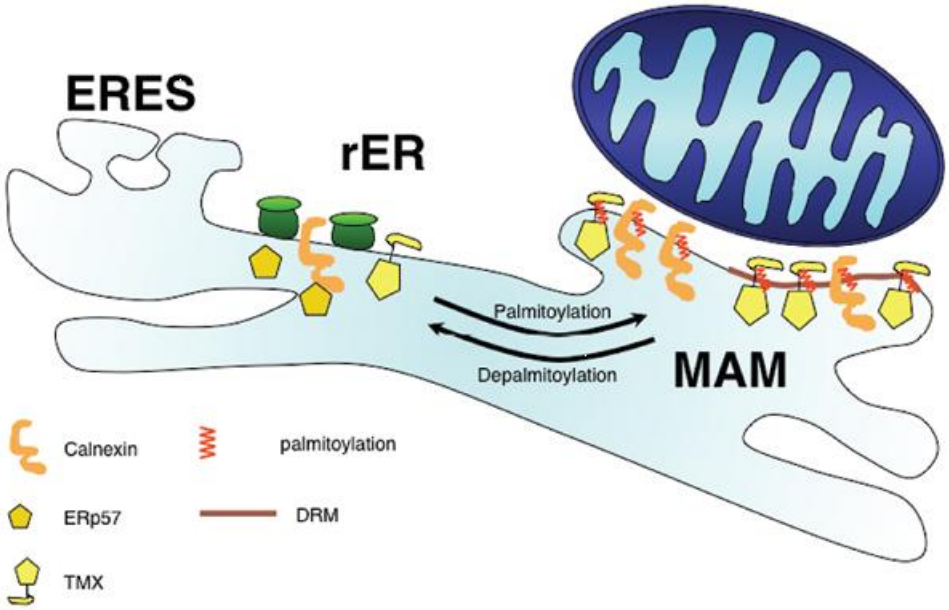

Figure 4.14: Model depicting how palmitoylation regulates the intra-ER localizations of TMX and calnexin. Palmitoylated calnexin and TMX localize to the mitochondria associated membrane (MAM). Furthermore, TMX also localizes to detergent resistant membranes within the MAM depending on its palmitoylation state. Depalmitoylated TMX and calnexin cofractionate with rough ER proteins such as ERp57, ribophorin I and eIF2α, which associates with ribosomes.

Chapter 5: Palmitoylation affects calnexin's chaperone and calcium signalling functions

Chapter 5: Palmitoylation affects calnexin's chaperone and calcium signalling functions

5.1 Introduction and Rationale

Calnexin is a lectin chaperone, and its primary role in the ER is to perform quality control of secreted glycoproteins. As newly synthesized glycoproteins emerge into the ER lumen, an oligosaccharide is attached and subsequently trimmed by ER glucosidases to the monoglucosylated oligosaccharide that is recognized by calnexin (Rutkevich and Williams, 2011). Binding of nascent glycoproteins to calnexin serves many important functions; it slows down folding and prevents aggregation of misfolded proteins, and retains folding intermediates in the ER, where other chaperones help to correctly fold them. Upon release from calnexin, the glycoprotein may fold rapidly and correctly and be exported to the Golgi apparatus or, in the case of a protein that does not immediately fold correctly, it will be reglucosylated and returned to the calnexin cycle (Dejgaard et al., 2004). Proteins that have been trapped in the calnexin cycle for a prolonged period are eventually subject to retrotranslocation from the ER to the cytosol and degradation by the proteasome, a process known as ER Associated Degradation (ERAD) (Lederkremer, 2009).

Importantly, binding to calnexin also brings misfolded glycoproteins into proximity with another chaperone, ERp57, which is responsible for disulphide bond isomerisation. ERp57 is an oxidoreductase that is a member of the Protein Disulphide Isomerase (PDI) family (Rutkevich and Williams, 2011). Studies have shown that a certain subset of disulphide-bonded, heavily glycosylated proteins depend specifically on this partnership for efficient folding and subsequent trafficking through the secretory system (Jessop et al., 2007; Rutkevich et al., 2010). Like PDI, ERp57 contains two active sites consisting of a pair of cysteines flanking any two amino acids (C-X-X-C) that can switch between the disulphide, or oxidized, and dithiol, or reduced forms. ERp57 is thought to be primarily in a reduced form in the ER, meaning that it can act as an

electron donor, and catalyze the breakage and isomerisation of disulphide bonds, rather than the formation of new disulphide bonds (Jessop and Bulleid, 2004). The first cysteine of the active site interacts with cysteine pairs in client proteins and forms a mixed disulphide intermediate that is resolved by the intervention of the second cysteine of ERp57's catalytic domain. The disulphide bond can either be broken or shuffled into a new disulphide bond with another cysteine in the substrate protein. If the disulphide bond is broken, then ERp57's active site becomes oxidized. There is evidence that glutathione then acts as an electron donor to recycle ERp57 to its reduced, active, form (Jessop and Bulleid, 2004).

Apart from its best known role as a lectin chaperone responsible for the quality control of glycoprotein production in the ER, calnexin also has lesser-known roles in calcium signalling. Calnexin has been found to be a modulator of SERCA2b function (Roderick et al., 2000), by downregulating SERCA2b's calcium pumping activity. This modulation is dependent on the phosphorylation of ser583 in calnexin's cytosolic domain. Calnexin has three phosphorylation sites in its cytosolic tail: two membrane-proximal casein kinase 2 (CK2) sites on Ser554 and Ser564 (Cala et al., 1993; Ou et al., 1992) that control its interaction with PACS-2 (Chapter 3) and a more distal ERK site on ser583 (Chevet et al., 1999). Interestingly, calnexin has also been shown to play a role in calcium signalling in the *Drosophila* eye that controls cell survival (Rosenbaum et al., 2006).

As we and others have shown that calnexin is MAM-localized (Lynes et al., 2012; Wieckowski et al., 2009), and calcium signalling is one of the main functions of the MAM, we wanted to test whether the control of calcium signalling could be one of calnexin's roles at the MAM. Although phosphorylation and PACS-2 interaction was found to be important for calnexin's MAM localization (Chapter 3), both we and others identified a palmitoylation motif that also contributed to its MAM targeting (Ferrera et al., 2008; Lakkaraju et al., 2012; Lynes et al., 2012). Little is known about how palmitoylation might affect calnexin's protein-protein interactions and functions. Given the fact that calnexin has both a calcium

signalling role as well as a protein folding role in the ER, we hypothesized that palmitoylation might act as a switch between calnexin's folding and calcium handling roles. As palmitoylation is also a dynamic post-translational modification, we decided to test whether it could be controlled by ER stress.

5.2 Results

5.2.1 ER stress affects calnexin's localization and its interaction with ER binding partners

Using a differential centrifugation fractionation to separate a crude mitochondrial pellet (containing mitochondria, MAM, and rER) from microsomes, Delom et al. showed that upon ER-stress, calnexin shifted from heavy membranes to light microsomal membranes, consisting of ER, Golgi and plasma membrane (Delom et al., 2007), suggesting that calnexin's MAM localization might change depending on ER stress. We first confirmed that calnexin's localization changed after a 4 hour tunicamycin stress treatment using a simple fractionation of HeLa cells (Figure 5.1 A). Tunicamycin induces ER stress by blocking the transfer of sugar groups to N-linked glycoproteins, causing them to accumulate in the ER (McDowell and Schwarz, 1988). Although PDI localization did not change, calnexin was indeed redistributed to the light membrane pellet after tunicamycin-induced ER stress. We then used an Optiprep gradient fractionation to further clarify this localization change (Figure 5.1 B). After a 4 hour tunicamycin treatment, calnexin relocalized from the 6th MAM/mitochondria fraction, marked by FACL4 (Lewin et al., 2001), to ER fractions indicated by PDI staining. In order to verify that this localization change was due to ER stress and not a non-specific effect of tunicamycin, the experiment was repeated with the ER stressor thapsigargin, which reduces ER calcium levels by blocking SERCA2b pumps. Similar results were obtained using these alternative methods of inducing ER stress (Figure 5.2). Calnexin's change in localization after ER stress was also confirmed by immunofluorescence microscopy. HeLa cells were treated with tunicamycin for 4 hours, and then stained with a calnexin antibody and mitotracker. Tunicamycin-treated cells had a reduced colocalization with

mitochondria in comparison with control cells, confirming that tunicamycin dislodged calnexin from the MAM (Figure 5.1 C).

5.2.2 ER stress regulates calnexin's palmitoylation state

Since calnexin's change in localization upon ER stress induced by tunicamycin, DTT and thapsigargin was very similar to the localization change we observed after blocking palmitoylation, we hypothesized that ER stress might be affecting calnexin's palmitoylation state. FLAG-Calnexin was immunoprecipitated from ω-alkynyl-palmitate labelled HeLa cells that had been treated with tunicamycin for 4 hours, and a click chemistry reaction was performed to detect the incorporation of the palmitatoylation probe. Tunicamycin significantly reduced calnexin's palmitoylation (Figure 5.3 A). In order to confirm this result, the experiment was repeated, this time with a 4 hour DTT treatment. Even more strikingly, a palmitoylation signal could no longer be detected for calnexin after DTT treatment (Figure 5.3 A). This could be because DTT might affect the cysteines in calnexin's palmitoylation motif; however, since the motif is in the cytosolic environment, the cysteines are already expected to be reduced. Since ER stress had already been shown to regulate calnexin's phosphorylation state (Roderick et al., 2000), this raised the question of whether the localization changes observed in this study and by others (Delom et al., 2007) were mediated by reduced phosphorylation or reduced palmitoylation. HeLa cells were treated with tunicamycin for 1, 4, or 16 hours, and lysates for each of these timepoints were tested by western blot for total calnexin levels, as well as with phospho-specific calnexin antibodies (see Materials and Methods, Table 2.1.5). While the changes we observed in calnexin's localization and palmitoylation occurred 4 hours after stress treatment, it was not until after 16 hours of tunicamycin treatment that a decrease in phosphorylation on serines 564 and 583 was observed (Figure 5.3 B). Furthermore, phosphorylation on serine 583 was unchanged in a mutant of calnexin where palmitoylation was abrogated (calnexin CCAA) or in calnexin mutants where serines 554 and 564 were mutated to alanines or aspartic acid (calnexin SSAA and SSDD). This result led to the conclusion that the

relocalization of calnexin from MAM to rER was as a result of depalmitoylation, and not dephosphorylation.

5.2.3 Calnexin's palmitoylation state affects its interaction with binding partners SERCA2b

Lakkaraju et al suggested that palmitoylation might impact calnexin's ability to bind to other proteins by re-orienting its cytosolic tail with respect to the ER membrane (Lakkaraju et al., 2012). The interaction between calnexin and SERCA2b occurs via calnexin's cytosolic tail (Roderick et al., 2000) and is already known to be controlled by phosphorylation of calnexin's ser583. Binding of calnexin to SERCA2b decreases its calcium pumping function (Bollo et al., 2010; Roderick et al., 2000). We wondered whether palmitoylation might also impact calnexin's ability to bind SERCA2b. We first compared the localizations of calnexin and SERCA2b by Optiprep gradient fractionation (Figure 5.4 A) and by differential centrifugation fractionation (Figure 5.4 A). While calnexin was found in fraction 6, corresponding to MAMs, and relocalized to rER fractions after various ER stress treatments, SERCA2b was found on lighter membranes corresponding to rER under control conditions and did not relocalize upon ER stress. This finding was confirmed using a differential centrifugation fractionation. Since calnexin cofractionated with SERCA2b after ER stress treatments, but not under control conditions, we hypothesized that the interaction between depalmitoylated calnexin and SERCA2b might increase. This hypothesis was tested with a coimmunoprecipitation experiment. HeLa cells were transiently transfected with either wildtype FLAG tagged calnexin, or the FLAG-Calnexin CCAA mutant construct. FLAG tagged proteins were immunoprecipitated, and probed by Western blot for coimmunoprecipitating endogenous SERCA2b. Surprisingly, despite the fact that depalmitoylated calnexin cofractionated with SERCA2b, its interaction with SERCA2b was greatly reduced (Figure 5.4 B). The interaction between endogenous calnexin and SERCA2b was also tested following ER stress treatments. HeLa cells were treated with DTT and tunicamycin for four hours, after which calnexin was immunoprecipitated and

examined by Western blot for coimmunoprecipitating SERCA2b. Consistent with the results from the previous experiment, the interaction between calnexin and SERCA2b was weaker after both 4 hour ER stress treatments, when calnexin is depalmitoylated, but not yet dephosphorylated (Figure 5.4 C).

As the interaction between calnexin and SERCA2b has previously been shown to be regulated by dephosphorylation of calnexin's ser583, we tested the CCAA mutant, SSAA and SSDD CK2 phosphorylation site mutants had decreased levels of phosphorylation on ser583. These mutants were transiently transfected into HeLa cells and the lysates were probed by Western blot for total calnexin and phosphorylated ser583 levels (Figure 5.5). None of the mutants showed a change in phospho-ser583 with respect to wildtype, confirming that the reduction in interaction seen between calnexin CCAA and SERCA2b was due to the abrogation of palmitoylation.

5.2.4 Calnexin's palmitoylation state alters ER calcium signalling to mitochondria

Calnexin's interaction with the ER calcium pump SERCA2b changed depending on its palmitoylation state, and calnexin has an inhibitory effect on SERCA2b. This raised the question of whether palmitoylation could be another switch mechanism, like ser563 phosphorylation, that regulates calnexin's inhibition of SERCA2b pumps. We therefore decided to assess whether the calnexin CCAA mutation affected calcium homeostasis and ER-mitochondria calcium signalling. Calnexin knockout mouse embryonic fibroblast (MEF) cells are slightly less susceptible to ER stress-induced apoptosis than wildtype MEFs (Groenendyk et al., 2006; Zuppini et al., 2002), although no changes in cytosolic calcium levels were measured after agonist stimulation of IP3 receptors (Kraus et al., 2010; Zuppini et al., 2002). The defect in apoptosis induction was instead attributed to calnexin's ability to recruit caspase-8 or caspase-12 to the ER surface for Bap-31 cleavage (Groenendyk et al., 2006; Zuppini et al., 2002). However, changes in

mitochondrial uptake of calcium after stimulation of IP3 receptors or ER stress were not examined.

Calnexin knockout MEFs were transiently transfected with FLAG-tagged wildtype calnexin or calnexin CCAA. Both constructs were expressed at similar levels in the cells (Figure 5.6 D). The cells were loaded with the fluorescent calcium-dependent probe Fluo8, which measures cytosolic calcium levels. The cells were then treated with thapsigargin, which blocks the reuptake of calcium from the cytosol into the ER via SERCA2b pumps, for 5 minutes, and its effect on cytosolic calcium levels was measured by Fluo8 fluorescence as detected by flow cytometry. Confirming results obtained by Kraus et al. (2010), no differences in the release of calcium into the cytosol were observed between the cnx -/- MEFs or those transiently transfected with wildtype or CCAA mutant calnexin (Figure 5.6 A). Mitochondria can also act as calcium buffers, and take up a large amount of calcium from the cytosol (de Brito and Scorrano, 2008). Therefore, we next repeated the experiment with a mitochondrially-targeted calcium sensitive fluorescent probe, Rhod2 (Fonteriz et al., 2010), to determine whether the expression of wildtype calnexin or the CCAA mutant affected calcium uptake by mitochondria after SERCA2b pumps were disabled by thapsigargin treatment. Mitochondrial calcium more than doubled in calnexin knockout cells after thapsigargin treatment, and interestingly, this response was blunted in cells transfected with wildtype calnexin, but not calnexin CCAA (Figure 5.6 B).

Bravo et al. reported that a 4 hour tunicamycin treatment more than doubled the percentage of mitochondria that make close contacts with the ER. In addition, they showed that in cells treated with tunicamycin and stimulated with thapsigargin or histamine to release calcium from the ER, the uptake of calcium by mitochondria was greater than in untreated control cells (Bravo et al., 2011). We decided to test whether these observations were dependent on calnexin, or more specifically MAM-localized calnexin. Calnexin -/- cells were transiently transfected with either wildtype or CCAA calnexin constructs, and subjected to

tunicamycin treatment for 4 hours. The uptake of calcium into mitochondria after histamine stimulation of IP_3 receptors was measured using Rhod2 signal detected by flow cytometry, as in the previous experiments. In calnexin knockout cells as well as cells transfected with calnexin CCAA, there was no difference in calcium uptake by mitochondria after tunicamycin treatment. However, when cells were transfected with wildtype calnexin, calcium uptake by mitochondria under normal conditions was reduced, and there was a large increase in mitochondrial calcium uptake after tunicamycin treatment, as observed by Bravo et al. (Figure 5.6 C). This observation suggests that MAM-localized, palmitoylated calnexin is required for the increased mitochondrial calcium uptake after ER stress.

Uptake of calcium into mitochondria can have several different effects. Calcium is needed as a cofactor in many of the enzymatic reactions of the TCA cycle, which drives the electron transport chain, thus creating a proton gradient across the mitochondrial membrane (Poburko and Demaurex, 2012; Robb-Gaspers et al., 1998). However, other groups have shown that the mechanisms of uptake of calcium into the mitochondria can actually have the effect of reducing mitochondrial membrane potential (Loew et al., 1994; Talbot et al., 2007). The mitochondrial membrane potential of calnexin knockout MEFs, and knockout MEFS expressing wildtype calnexin or calnexin CCAA, was measured by flow cytometry using a tetramethylrhodamine (TMRM) probe, which is more readily sequestered by active mitochondria (Perry et al., 2011). Overexpression of wildtype calnexin in calnexin -/- MEFs reduced the proportion of TMRM positive cells measured by flow cytometry, however, overexpressing the calnexin CCAA mutant had no effect on mitochondrial membrane potential (Figure 5.6 C).

5.2.5 Calnexin's palmitoylation state affects its interaction with binding partner ERp57. Surface expression levels of client protein LDL-R depend on calnexin's palmitoylation state

We decided to test whether the palmitoylation state of calnexin impacted calnexin's relationship with ERp57. ERp57 cofractionates with rER markers on

an Optiprep gradient (Figure 4.3 C) but is mainly found in heavy membranes in a differential centrifugation fractionation (Figure 5.7 A). Like calnexin, ERp57 redistributes to the light membrane fraction upon tumicamycin stress (Figure 5.7 A). Next, the interaction between calnexin and ERp57 during ER stress was evaluated by a coimmunoprecipitation experiment. HeLa cells were stressed with reducing agent DTT or with tunicamycin for 4 hours, and calnexin was immunoprecipitated from the cells lysates. Calnexin and coimmunoprecipitating ERp57 were detected by western blot. Compared to control cells, more ERp57 was pulled down with calnexin in cells treated with DTT and tunicamycin, suggesting that ER stress increases the interaction between calnexin and ERp57 (Figure 5.7 B).

We hypothesized that depalmitoylated calnexin might interact more strongly with ERp57 than its wildtype counterpart, since depalmitoylated calnexin and ERp57 are both found in the same fractions of the Optiprep gradient and furthermore, both move from heavy to light membranes after tunicamycin treatment. As opposed to SERCA2b whose interaction with calnexin weakens after ER stress (Figure 5.4 C), ERp57's interaction with calnexin increased. HeLa cells were transfected with FLAG-tagged wildtype and CCAA mutant calnexin, which were immunoprecipitated from lysates using a FLAG antibody. Immunoprecipitates were analyzed by Western blot for FLAG and coimmunoprecipitating ERp57. In agreement with our findings that ER stress treatments depalmitoylate calnexin and that ER stress increased calnexin's interaction with ERp57, the calnexin CCAA mutant pulled down more than 1.5 fold more ERp57 than wildtype calnexin (Figure 5.7 C).

In order to evaluate whether the increased binding of depalmitoylated calnexin with ERp57 had functional consequences for protein folding, a reporter protein was selected. The low-density lipoprotein receptor (LDL-R) is expressed in clathrin coated pits on the cell surface, and binds and internalizes low-density lipoproteins in complex with cholesterol, thus helping to regulate cholesterol

homeostasis (Brown and Goldstein, 1979). We hypothesized that since palmitoylation affects calnexin's binding to ERp57 and that LDL-R maturation relies on both calnexin and ERp57 (Jessop et al., 2007; McCormick et al., 2005), calnexin's palmitoylation state might affect surface levels of LDL-R. We selected LDL-R due to its high number of potential N-linked glycans (5) and 30 disulphide bonds. We evaluated surface LDL-R in calnexin knockout AKO cells, as compared to AKO cells overexpressing wildtype and CCAA mutant calnexin, by biotinylating the cell surface proteins, then quenching the biotinylation reaction and pulling down biotinylated proteins using streptavidin beads. Biotinylated LDL-R was then compared to total LDL-R from whole cell lysates from each of the experimental conditions. Calnexin knockout cells overexpressing wildtype calnexin had similar levels of cell surface LDL-R as control cells; however, cells overexpressing the calnexin CCAA mutant had reduced levels of surface LDL-R (Figure 5.7 D). The total level of LDL-R in cell lysates was unchanged across all the experimental conditions. This experiment was repeated in HeLa cells treated with 2-bromopalmitate to depalmitoylate calnexin, and similar results were obtained with treated cells having less surface LDL-R (Figure 5.7 E). These results are consistent with the observation that overexpression of chaperone proteins often slows the progress of client proteins through the secretory system, decreasing their rate of secretion or surface expression, as is the case for ERp57 and cell surface expression of the human gonadotropin releasing hormone receptor (hGnRHR) (Ayala Yanez and Conn, 2010).

5.3 Discussion and Future Perspectives

ER stress depalmitoylates calnexin and relocalizes it from the MAM to rER membranes. Depalmitoylation due to ER stress also coincided with a decreased interaction with SERCA2b, despite the increased cofractionation of calnexin with SERCA2b on the Optiprep gradient. Our data indicated that expressing calnexin in cxn -/- cells reduces mitochondrial uptake of calcium upon thapsigargin treatment. However, expressing calnexin CCAA had no effect on mitochondrial calcium uptake. One possible explanation is that calnexin knockout cells have

generally higher SERCA2b activities because calnexin is not there to repress SERCA2b's activity, and there is therefore more calcium stored in the ER to be released. Since calnexin CCAA binds less strongly to SERCA2b (Figure 5.4), cells expressing calnexin CCAA act like the calnexin -/- control cells. It is also possible that calnexin changes the structure of the MAM, perhaps by acting as part of a tethering complex, in such a way as to regulate the surface area of ER in contact with mitochondria, or the distance between the ER and outer mitochondrial membrane at MAMs, and that non-MAM localized calnexin CCAA is unable to perform this function.

Tunicamycin treatment as well as other stressors increases the number of ER-mitochondria contacts, and decreases the gap between ER and mitochondria at contact sites (Bravo et al., 2011; Csordas et al., 2006). We observed that the concomitant increase in mitochondrial calcium uptake is dependent on palmitoylated calnexin (Figure 5.6), which raises the question of whether palmitoylated calnexin is also required for the changes in MAM structure observed after ER stress treatments. This question could be addressed with an electron microscopy experiment to compare MAM structures in cells depleted of calnexin or overexpressing wildtype or CCAA mutant calnexin, before and after tunicamycin treatment or another ER stress.

Depalmitoylation of calnexin due to ER stress also coincided with an increased interaction between calnexin and the PDI-related disulphide bond isomerase ERp57, suggesting that depalmitoylation could possible upregulate calnexin's quality control function. There have been several reports suggesting that calnexin interacts directly with translocon and ribosome complexes (Boisrame et al., 2002) and that it may be involved in retrotranslocation of misfolded proteins at the ER quality control compartment (ERQC), which is a compartment of the ER dedicated to degradation of misfolded proteins (Kamhi-Nesher et al., 2001). Lakkaraju et al. (2010) reported that depalmitoylated calnexin interacted poorly with the translocon and with glycoproteins in general. However, we evaluated the

effect of expressing calnexin and calnexin CCAA in calnexin deficient MEFs on the maturation of a specific glycoprotein receptor, LDL-R, that also required the PDI-related chaperone ERp57 for proper folding, due to its numerous disulphide bonds. Calnexin CCAA, which interacts more strongly with ERp57, but not wildtype calnexin, retained LDL-R and slowed its progress to the cell surface, which is consistent with an increased chaperone function (Ayala Yanez and Conn, 2010). Many questions remain, for example, does LDL-R in calnexin-deficient cells have spurious disulphide bonds? It is also unclear how ER stress, and the concomitant reduction of calnexin palmitoylation, might affect LDL-R maturation in calnexin-deficient cells compared to cells expressing wildtype or CCAA mutant calnexin. Our data suggest that depalmitoylated calnexin may play a role in the quality control of disulphide bond-rich glycoproteins in the ER, but this specific role has yet to be elucidated.

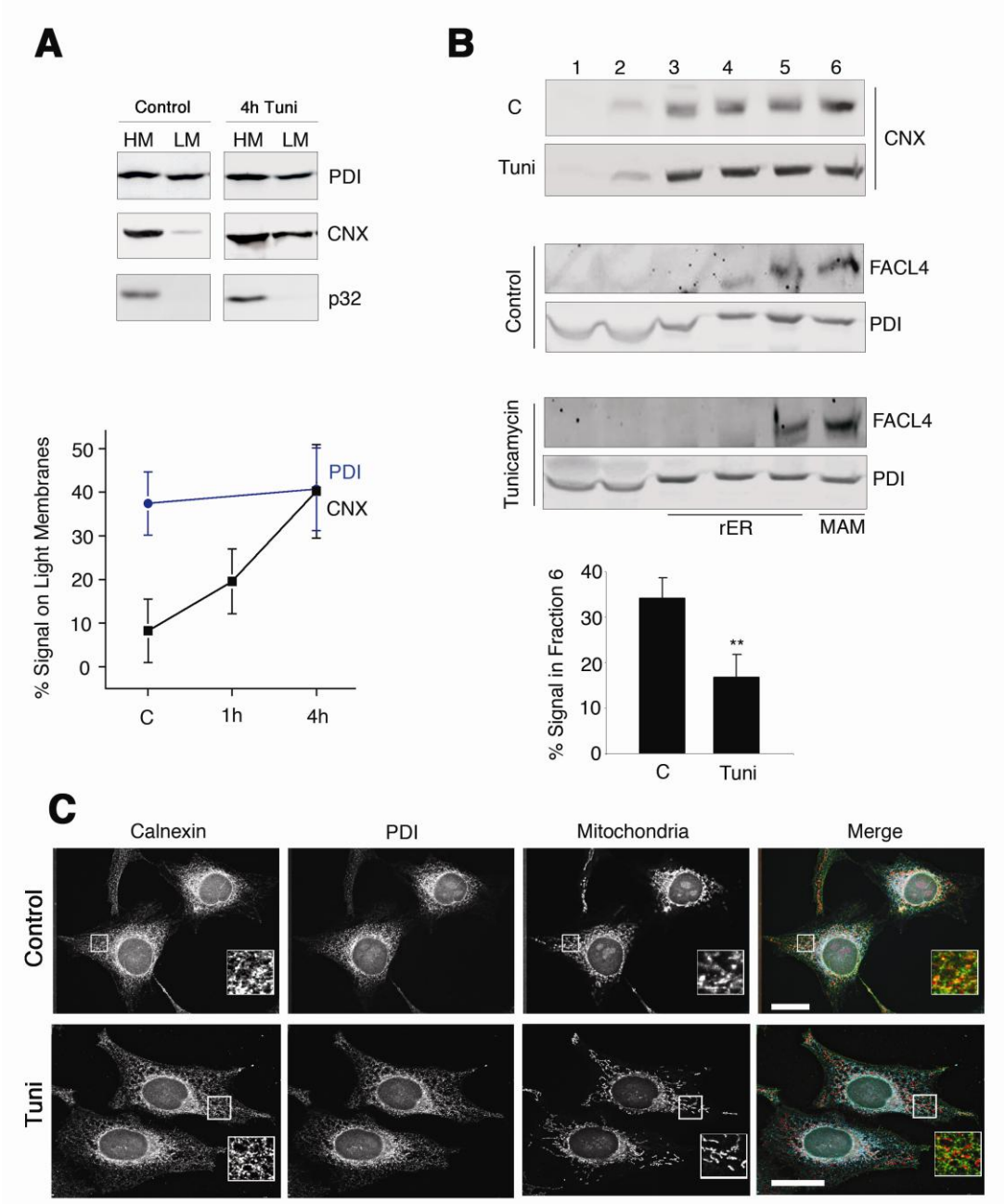
A
Control
4h Tuni
HM
LM
HM
LM
PDI
CNX
p32
% Signal on Light Membranes
50
40
30
20
10
0
PDI
CNX
C
1h
4h
B
1
2
3
4
5
6
C
Tuni
CNX
Control
FACL4
PDI
Tunicamycin
FACL4
PDI
rER
MAM
% Signal in Fraction 6
40
30
20
10
0
**
C
Tuni
C
Calnexin
PDI
Mitochondria
Merge
Control
Tuni

Figure 5.1: Calnexin changes localization following ER stress. A. Differential gradient fractionation was performed with homogenates of control HeLa cells and cells treated for 4 hours with 10 μM tunicamycin HM=10 000g pellet, LM=100 000g pellet. Equal proportions of fractions were analyzed by western blot for calnexin, PDI (ER), and p32 (mitochondria). Quantification of three independent experiments is displayed below. **B.** Optiprep gradient fractionation of control HeLa cells and cells treated or 4 hours with 10 μM tunicamycin. FACL4 and PDI are used to control for MAM membranes ER membranes respectively. The percentage of calnexin signal in fraction 6, co-sedimenting with FACL4 is quantified below. n=3, P=0.035 **C.** Calnexin's colocalization with mitochondria depends on ER stress. Control HeLa cells and cells treated with 10 μM Tunicamycin were processed for immunofluorescence microscopy and analyzed for the signals of calnexin, PDI and mitochondria (mitotracker). The merged images are shown on the right with a magnified area of calnexin and mitotracker signals. Scale bar= 25 μm. ***A** and **C** contributed by Thomas Simmen*.

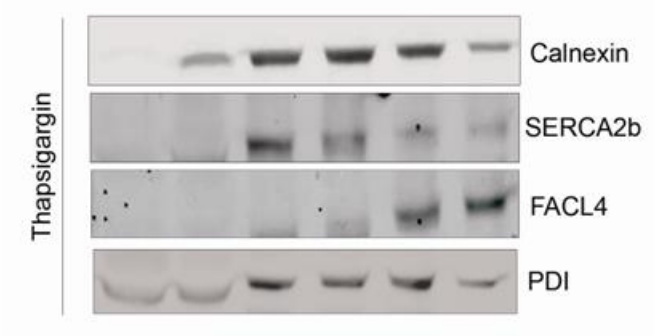

Figure 5.2: Thapsigargin treatment also displaces calnexin from MAM. HeLa cells were treated with 1.5 μM thapsigargin for 4 hours and homogenized and fractionated as in Figure 5.1 B. Fractions were analyzed by western blot and FACL4 was used as a MAM marker, and PDI as an ER marker. Please refer to Figure 5.1 B for control.

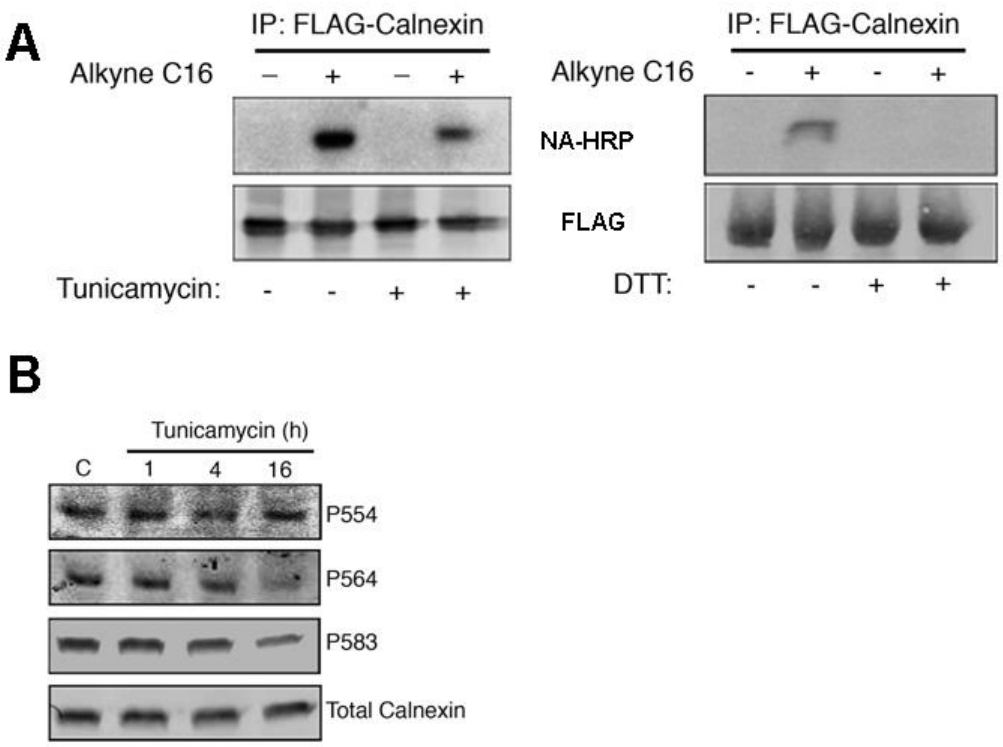

Figure 5.3: Analysis of calnexin phosphorylation and palmitoylation during an ER stress time course. A. Calnexin palmitoylation is reduced during ER stress. HeLa cells were incubated for 4h with 10 μM Tunicamycin or with 5 mM DTT and incorporation of alkynyl palmitate was measured using click chemistry as described in Methods. FLAG antibody was used to assess the expression level of wildtype calnexin. *Done in collaboration with Megan Yap.* **B.** Phosphorylation of calnexin's 3 phosphorylation sites is individually altered during an ER stress time course. Lysates of HeLa cells treated for the indicated times with 10 μM Tunicamycin and analyzed via Western blot using phospho-specific antibodies against the three known sites serine 554, 564, 583.

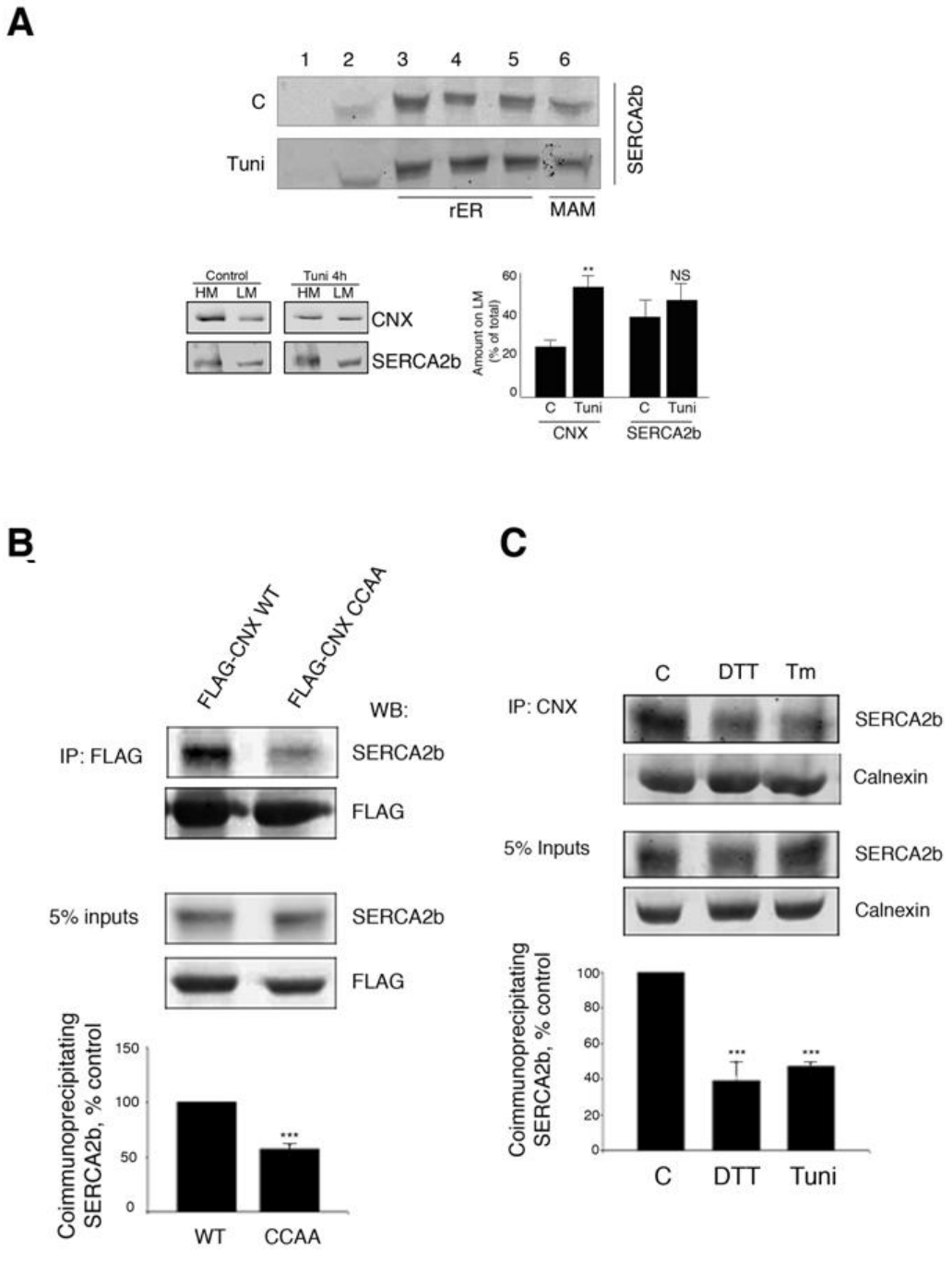
A
1 2 3 4 5 6
C
Tuni
SERCA2b
rER
MAM
Control
Tuni 4h
HM LM
HM LM
CNX
SERCA2b
Amount on LM (% of total)
60
40
20
0
**
NS
C Tuni
C Tuni
CNX
SERCA2b
B
FLAG-CNX WT
FLAG-CNX CCAA
WB:
IP: FLAG
SERCA2b
FLAG
5% inputs
SERCA2b
FLAG
Coimmunoprecipitating SERCA2b, % control
150
100
50
0
***
WT
CCAA
C
C DTT Tm
IP: CNX
SERCA2b
Calnexin
5% Inputs
SERCA2b
Calnexin
Coimmunoprecipitating SERCA2b, % control
100
80
60
40
20
0
***
***
C DTT Tuni

Figure 5.4: ER stress and palmitoylation affect calnexin's interaction with SERCA2b. A. SERCA2b localization is not affected by tunicamycin stress. Homogenized HeLa cell lysates were separated by Optiprep gradient fractionation following a 4h treatment with 10 μM tunicamycin (Tuni). Fractions were analyzed as indicated by SDS-PAGE and western blot for SERCA2b. Homogenized HeLa cell lysates were separated into heavy and light membranes as in Figure 5.1 following a 4h treatment with 10 μM Tunicamycin (Tuni). Membrane fractions were analyzed as indicated by SDS-PAGE and Western Blot for calnexin and SERCA2b. The graph shows the calnexin and SERCA2b amounts in the heavy membrane fraction from 3 independent experiments (Statistics: P=0.013 for calnexin, P=0.395 for SERCA2b). *Contributed by Carolina Ortiz* **B.** Calnexin-SERCA2b co-immunoprecipitation following ER stress. HeLa cells were treated for 4 h with either 5 mM Dithiothreitol (DTT) or 10 μM Tunicamycin (Tuni). DSP-crosslinked lysates (5% inputs) and calnexin immunoprecipitates were analyzed for calnexin and co-immunoprecipitating SERCA2b. The graph shows results from 3 independent experiments (Statistics: p=0.0073 for DTT, p<0.001 for Tunicamycin). **C.** Calnexin wildtype and CCAA were expressed in AKO calnexin -/- MEFs and immunoprecipitated with FLAG antibody. DSP-crosslinked lysates (5% inputs) and FLAG immunoprecipitates were analyzed for FLAG-tagged calnexin and co-immunoprecipitating SERCA2b. The graph shows results from 3 independent experiments. P=0.006.

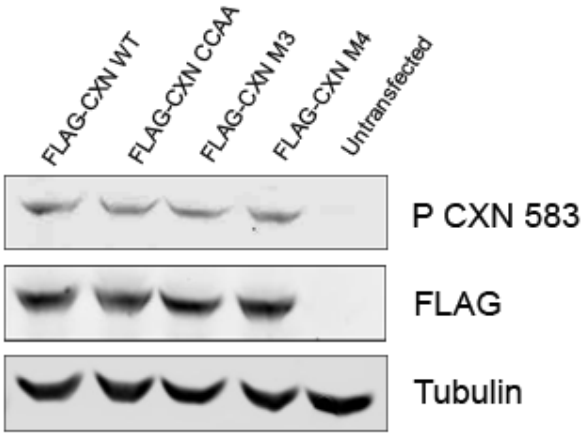

Figure 5.5: Serine 583 phosphorylation of calnexin mutants. Lysates of HeLa cells transfected with the indicated calnexin constructs were analyzed for the phosphorylation levels of serine 583 by western blot with a phosphospecific antibody. The FLAG and Tubulin antibodies show equal expression and loading of the different constructs.

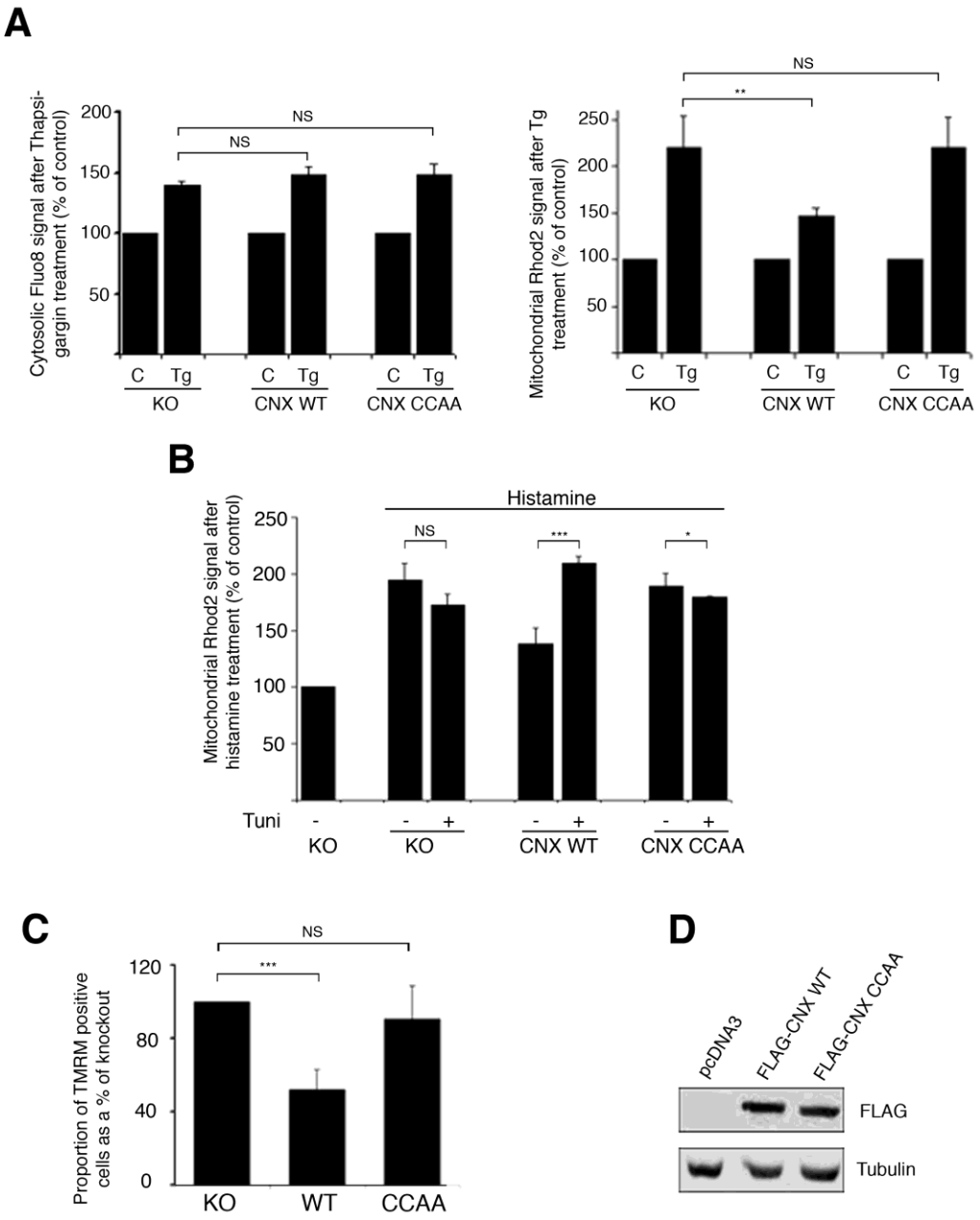
A
Cytosolic Fluo8 signal after Thapsi-gargin treatment (% of control)
200
150
100
50
NS
NS
C
Tg
KO
CNX WT
CNX CCAA
Mitochondrial Rhod2 signal after Tg treatment (% of control)
250
200
150
100
50
NS
**
B
Mitochondrial Rhod2 signal after histamine treatment (% of control)
Histamine
NS
***
*
Tuni
-
+
C
Proportion of TMRM positive cells as a % of knockout
120
80
40
0
KO
WT
CCAA
D
pcDNA3
FLAG-CNX WT
FLAG-CNX CCAA
FLAG
Tubulin

Figure 5.6: Palmitoylated calnexin regulates ER calcium signaling. A. Measurement of cytosolic and mitochondrial calcium following thapsigargin-mediated ER calcium release. Calnexin knockout (ko) MEFs and ko cells transfected with FLAG-tagged wild type or CCAA calnexin were loaded with Fluo8 (left) and Rhod2 (right). Cells were then treated with 1.5 μM thapsigargin and probe fluorescence was recorded before and after thapsigargin treatment by flow cytometry (n=3 for both experiments, left panel: P=0.8419 for calnexin wild type, P=0.8816 for calnexin CCAA; right panel: P=0.02 for calnexin wild type, P=0.8583 for calnexin CCAA). **B.** Measurement of mitochondrial calcium following histamine-mediated ER calcium release. Calnexin knockout (ko) MEFs and ko cells transfected with FLAG-tagged wild type or CCAA calnexin were loaded with Rhod2. Cells were then treated with 50 μM histamine and probe fluorescence was recorded before and after histamine treatment by flow cytometry (n=3, P=0.2581 for calnexin knockout, P<0.001 for calnexin wild type, P=0.088 for calnexin CCAA). **C.** Measurement of mitochondrial membrane potential. Calnexin knockout (ko) MEFs and ko cells transfected with FLAG-tagged wild type or CCAA calnexin were loaded with TMRM and probe fluorescence was recorded by flow cytometry (n=3, P=0.001 for calnexin wild type, P=0.4135 for calnexin CCAA). **D.** Calnexin expression levels of representative cells from flow cytometry experiments. Calnexin knockout (ko) MEFs and ko cells transfected with FLAG-tagged wild type or CCAA calnexin were lysed and processed for Western blot using the FLAG antibody. Tubulin was used as a loading control. *This figure was done in collaboration with Arun Raturi.*

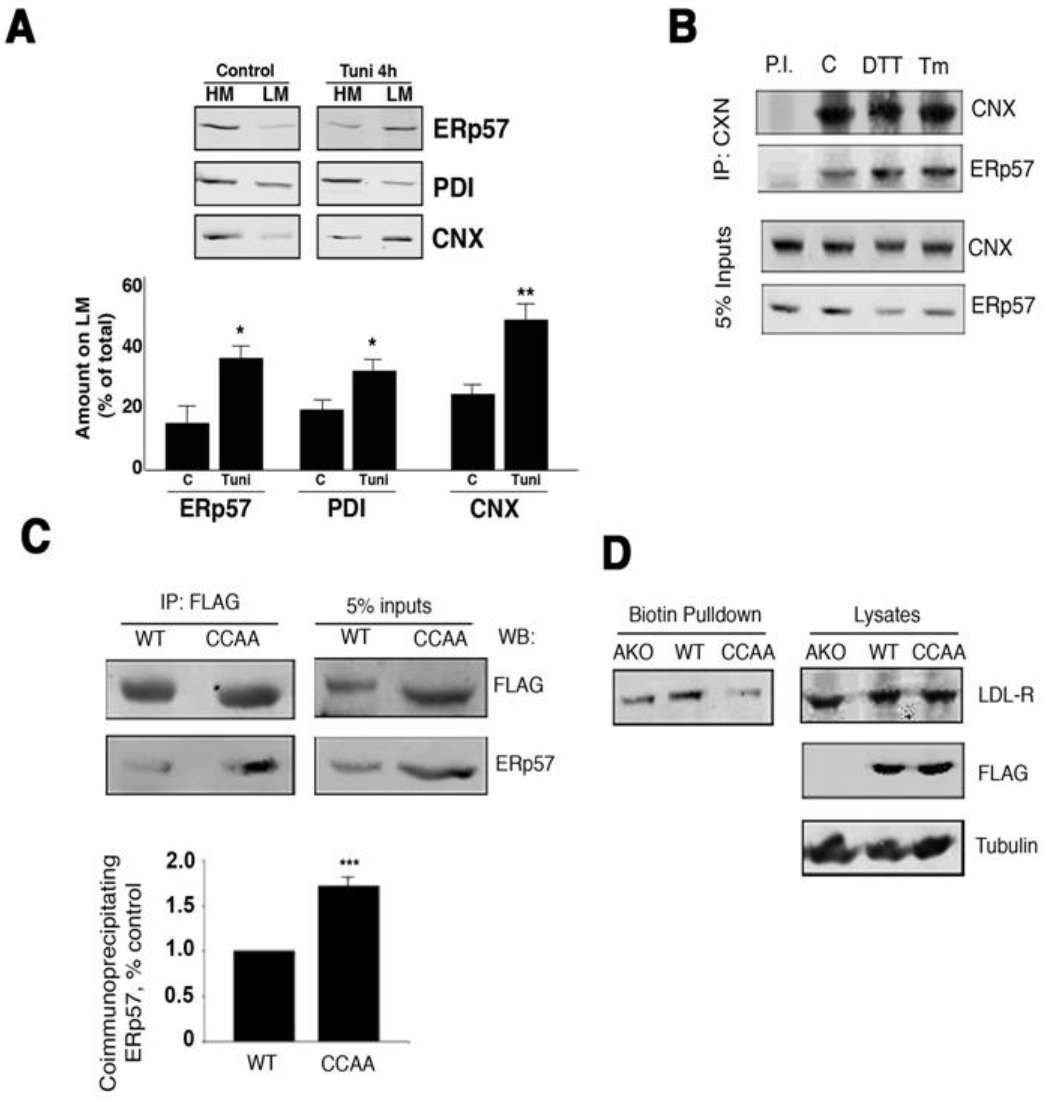
A
Control
Tuni 4h
HM
LM
HM
LM
ERp57
PDI
CNX
Amount on LM (% of total)
60
40
20
0
*
*
**
C
Tuni
C
Tuni
C
Tuni
ERp57
PDI
CNX
B
P.I.
C
DTT
Tm
IP: CXN
CNX
ERp57
5% Inputs
CNX
ERp57
C
IP: FLAG
5% inputs
WT
CCAA
WT
CCAA
WB:
FLAG
ERp57
Coimmunoprecipitating ERp57, % control
2.0
1.5
1.0
0.5
0
***
WT
CCAA
D
Biotin Pulldown
Lysates
AKO
WT
CCAA
AKO
WT
CCAA
LDL-R
FLAG
Tubulin

Figure 5.7: ER stress and palmitoylation affect calnexin's interaction with ERp57. A. Homogenized HeLa cell lysates were separated into heavy (10 000g pellet) and light (100 000g pellet) membranes by differential centrifugation fractionation following a 4h treatment with 10 μM Tunicamycin (Tuni). Membrane fractions were analyzed as indicated by SDS-PAGE and Western Blot for ERp57, PDI and calnexin. The graph shows the ERp57, PDI and calnexin amounts in the light membrane fraction from 3 independent experiments. p=0.056 for ERp57, p=0.088 for PDI, p=0.013 for calnexin. *Contributed by Carolina Ortiz* **B.** Calnexin-ERp57 co-immunoprecipitation following ER stress. HeLa cells were treated for 4 h with either 5 mM Dithiothreitol (DTT) or 10 μM Tunicamycin (Tuni). DSP-crosslinked lysates (5% inputs) and calnexin immunoprecipitates were analyzed for calnexin and co-immunoprecipitating ERp57. **C.** HeLa cells were transfected with FLAG-tagged wild type or CCAA calnexin. DSP-crosslinked lysates (5% inputs) and FLAG immunoprecipitates were analyzed for FLAG-tagged calnexin and co-immunoprecipitating ERp57. The graph shows results from 3 independent experiments. p=0.003. **D**. LDLR surface biotinylation. Calnexin -/- MEFs and cells transfected with FLAG-tagged wild type or CCAA calnexin were lysed and processed for Western blot using the LDLR antibody. In parallel, the same set of cells was processed for surface biotinylation as described in Materials & Methods and probed for biotinylated surface LDLR. **E**. Control HeLa cells and cells treated with 2-Bromopalmitate for 4 hours were analyzed as in **D.**

Chapter 6: Perspectives

Chapter 6: Perspectives

6.1 Summary of Results

The goal of this thesis project was to identify novel proteins at the MAM, the subdomain of the ER responsible for communication via calcium and lipid exchange with mitochondria. Furthermore, we also wished to determine how these proteins target to MAM, and what role they play in the MAM's functions. To summarize the findings of this thesis, we found that calnexin is a MAM protein whose localization partially depends on PACS-2, and more specifically the phosphorylation state of PACS-2 binding site (Chapter 3). We then turned our attention to TMX and TMX4, two members of the PDI family of oxidoreductase chaperone proteins. We hypothesized that since TMX and TMX4 share a PACS-2 interaction sequence with calnexin, and that several PDI family members have been implicated in calcium signalling, one of the MAM's main functions, TMX and TMX4 may localize to MAM as well. We discovered that TMX localizes to MAM but TMX4 does not, even though the proteins are very similar. Chimeric TMX/TMX4 mutants revealed that a motif present in a combination of TMX's transmembrane and cytosolic domains controls MAM localization. We identified this motif as a juxtamembrane cytosolic palmitoylation site that TMX and calnexin share, whereupon we confirmed that palmitoylation targets calnexin and TMX to MAM (Chapter 4). We also identified 3 other proteins, VDAC1 and 2 and HO1, which are also MAM-targeted via palmitoylation.

We next wanted to determine the significance of calnexin's targeting to MAM. In the second project we demonstrated that calnexin becomes depalmitoylated and therefore loses its MAM targeting after ER stress. Furthermore, depalmitoylation and ER stress decreased calnexin's interactions with binding partner SERCA2b, which had consequences for calcium handling in the cell. We found that upon release of calcium from the ER, the presence of calnexin reduced the uptake of calcium into mitochondria. Increased mitochondrial calcium uptake was previously observed in cells that had been treated with tunicamycin prior to

agonist-stimulated release of calcium from the IP3 receptors. We demonstrated that calnexin knockout MEFs did not respond to tunicamycin stress in this way, and that the effect could be rescued by wildtype, but not non-palmitoylatable calnexin. Interestingly, non-palmitoylatable calnexin interacted better with ERp57, a PDI-related protein that mediates disulphide bond formation in glycoproteins. Calnexin also interacted better with its protein folding partner ERp57 during ER stress, when we showed calnexin's palmitoylation is reduced. We therefore examined the maturation of LDL receptor, a substrate of both calnexin and ERp57 that is normally expressed on the cell surface. We found that when non-palmitoylatable calnexin was overexpressed in calnexin knockout cells, or when palmitoylation was pharmacologically blocked, the amount of LDL receptor on the cell surface decreased, which could indicate that the chaperone or folding function of the calnexin increases when calnexin is not palmitoylated.

6.2 Palmitoylation acts as a switch that regulates calnexin's interactions and functions

Phosphorylation has already been shown to be regulated by tunicamycin-induced ER stress and play a role in calnexin's subcellular localization (Delom et al., 2007). Furthermore, phosphorylation on serine 583 regulates calnexin's interaction with SERCA2b, which serves to decrease SERCA2b's calcium pumping function (Roderick et al., 2000). We observed that palmitoylation also plays a major role in calnexin's intra-ER localization, as depalmitoylated calnexin loses its localization to MAMs (Chapter 4). We hypothesized that ER stress could also modulate calnexin's localization by changing its palmitoylation status. In Figure 5.1 and 5.2, we show that 4 hours of tunicamycin and thapsigargin-induced ER stress indeed provoke the loss of calnexin's MAM targeting, as well as the depalmitoylation of calnexin. We also show that the loss of palmitoylation due to tunicamycin stress occurs at a 4 hour timepoint, whereas the dephosphorylation of calnexin's serine 583 does not occur until a 16 hour timepoint. Therefore the change in localization that we observed at 4 hours must be due to the

depalmitoylation of calnexin, and not its dephosphorylation that occurs at a later timepoint.

We also demonstrate that at this 4 hour timepoint, there is a major decrease in calnexin's interaction with SERCA2b. The non-palmitoylatable calnexin mutant also has a decreased interaction with SERCA2b, which could have consequences for calcium signalling in the cell. Although release of calcium from the ER into the cytosol was the same in cells that did not express calnexin, cells that expressed wildtype calnexin and cells that expressed non-palmitoylatable calnexin, we noticed that cells expressing wildtype calnexin had less mitochondrial uptake of calcium after release of calcium from the ER. Overexpressing non-palmitoylatable calnexin (CCAA) in calnexin knockout cells had no effect on the mitochondrial uptake of calcium. What effect does ER stress have on calcium signalling at the MAM? Bravo et al. (2011) reported that a 4 hour tunicamycin treatment increased the number of mitochondria that make close contacts with the ER. Furthermore, they showed that tunicamycin treatment increased the uptake of calcium by mitochondria when cells were stimulated with thapsigargin or histamine to release calcium from the ER. We therefore asked whether calnexin was necessary for these two phenomena to occur. We repeated the experiment with calnexin knockout cells, and cells overexpressing wildtype calnexin or calnexin CCAA. We were able to reproduce the results of Bravo et al. with cells overexpressing wildtype calnexin, but in calnexin knockout cells or cells overexpressing calnexin CCAA, we did not observe an increase in mitochondrial uptake of calcium after tunicamycin treatment. In fact, the uptake of calcium by mitochondria in calnexin knockout cells or cell overexpressing calnexin CCAA was already quite high prior to tunicamycin treatment. There are several possible interpretations of our calcium data; calnexin's interaction with SERCA2b might affect calcium stores in the ER, or calnexin may negatively modulate the formation of MAMs themselves. This possibility is further explored in section 6.4. Lastly, Lakkaraju et al. (2012) have demonstrated that depalmitoylated calnexin loses its interaction with the translocon. As calcium leakage through the

translocon has been reported during polypeptide translocation (Van Coppenolle et al. 2004), it is possible that calnexin's involvement in calcium homeostasis is mediated by its interaction with the translocon. In summary, our data provide a possible mechanism for the observations of Bravo et al., and show that palmitoylation of calnexin is key to its role in modulating calcium transfer at MAMs.

What then is the role of depalmitoylated calnexin in the cell? Based on our Optiprep gradient fractionation data showing that depalmitoylated calnexin co-fractionates with rough ER markers, including its known chaperone partner ERp57, we hypothesized that depalmitoylated calnexin might be important for protein folding and quality control. Furthermore, Kamhi-Nesher et al. (2001) have shown that calnexin migrates to the ER quality control compartment (ERQC) upon ER stress. We demonstrated that following ER stress, calnexin interacts more strongly with ERp57. We also showed that non-palmitoylatable calnexin interacts better with ERp57 than its wildtype counterpart. In order to verify whether this increased interaction translates into an increased folding capacity for the calnexin-ERp57 partnership, we chose to examine the surface expression of the LDL receptor, a client protein of both calnexin and ERp57. When calnexin CCAA was overexpressed in calnexin knockout cells, or palmitoylation was blocked by an inhibitor, less LDL receptor appeared on the cell surface, which could indicate slower maturation of the receptor due to increased interaction with calnexin/ERp57. Many questions remain regarding the function and localization of depalmitoylated calnexin. Although Lakkaraju et al. (2012) reported that depalmitoylated calnexin interacts poorly with glycoproteins in general, we have demonstrated that depalmitoylation increases the function of calnexin and ERp57 and affects the maturation of at least one glycoprotein, LDL-R. It would be interesting to test whether this holds true with other glycoproteins. Furthermore, it would be interesting to test whether depalmitoylated calnexin targets preferentially to the ERQC in ER-stressed cells.

6.3 What is the mechanism by which ER stress can regulate palmitoylation?

ER stress is defined as the accumulation of unfolded proteins in the endoplasmic reticulum, which in turn triggers the unfolded protein response (UPR). The UPR is initiated by the receptor proteins PERK, Ire1 and ATF6 on the ER membrane, which normally associate with the ER chaperone BiP (Szegezdi et al., 2006). When BiP disassociates from these receptors in favour of binding to unfolded proteins, the receptors oligomerize and become active. Receptors can also become activated when they are bound by unfolded proteins themselves (Gardner and Walter, 2011). The UPR is a series of signalling pathways that first aims to resolve the accumulation of unfolded proteins, culminating in the suppression of translation, the upregulation of chaperone proteins, and the upregulation of genes involved in protein degradation. If this is unsuccessful, the UPR can also signal for apoptosis (Szegezdi et al., 2006). Cell death due to ER stress and protein aggregation is a feature of many neurodegenerative diseases (Wang and Kaufman, 2012), as well as diabetes (Papa, 2012). Interestingly, calnexin's palmitoylation is reduced by ER stress and this in turn regulates calnexin's binding partners and activities. As calnexin has been shown to relocalize to the ER quality control compartment (ERQC), where proteins are retrotranslocated and degraded at times of ER stress (Kamhi-Nesher et al., 2001), perhaps depalmitoylation triggered by ER stress serves as a relocalization signal. Further supporting an increased role for depalmitoylated calnexin in quality control and protein folding, we observed that ER stress-mediated depalmitoylation increased calnexin's interaction with ERp57.

Palmitoylation is a reversible process, which is regulated by a 23-member family of DHHC domain-containing palmitoyl acyl transferases, or DHHC PATs, which palmitoylate proteins (Fukata et al., 2006). Acyl protein thioesterases (APT) 1 and 2 (Dekker et al., 2010) regulate the depalmitoylation of proteins. A third protein, protein palmitoyl thioesterase 1 (PPT1) also mediates depalmitoylation, but its function is restricted to lysosomes (Kim et al., 2006). Changes in protein palmitoylation are therefore as a result of a disruption in the equilibrium between

palmitoylation and depalmitoylation reactions. The PAT that regulates calnexin's palmitoylation is DHHC6 (Lakkaraju et al., 2012), but the protein that mediates its depalmitoylation has not yet been identified. An APT1 inhibitor, palmostatin B, has been developed (Dekker et al., 2010), which could be used to test whether calnexin's palmitoylation levels are regulated by APT1. Since calnexin's palmitoylation decreases during ER stress, it could be as a result of either a decrease in DHHC6 function, or an increase in APT1 or APT2 function. Further experiments will be required to understand how ER stress regulates calnexin's palmitoylation. It would be interesting to study whether UPR signalling downregulates the transcription of DHHC6 or perhaps mediates its degradation. For example, Li et al. found that the PAT family member DHHC5, which is involved in learning and memory, is rapidly degraded upon differentiation of neurons, which suggests that differentiation signals can regulate palmitoylation through the regulation of PAT expression (Li et al., 2012). Furthermore, it remains to be investigated whether ER stress globally affects the palmitoylation of proteins at MAM, or whether this effect is specific to calnexin. As we have identified several other palmitoylated MAM proteins (Lynes et al., 2012) (Chapter 4), we could test whether ER stress affects TMX's palmitoylation, or that of VDAC 1 or 2, or Hemeoxygenase1.

6.4 Does calnexin play a role in MAM formation or lipid transfer at the MAM?

Our observations of calnexin's effect on calcium signalling could be due to calnexin playing a structural role in MAM formation, or simply because of its regulatory effect on SERCA2b. If calnexin affects MAM structure, does palmitoylation status affect this role? We could assess this using EM of cells with or without calnexin or expressing wildtype vs. non-palmitoylatable calnexin. We could also modify the dimerization-dependent fluorophore system that our lab developed in conjunction with the Campbell lab (Deparment of Biological Sciences, University of Alberta) (Alford et al., 2012) to test whether calnexin knockout affects MAM structure. In this assay, a mitochondrial protein, TOM20,

is fused with one monomer of the fluorophore, and a MAM protein is fused with the other. Only in the case of dimerization does fluorescence occur, indicating that the mitochondrial and MAM proteins were close enough to allow dimerization of the fluorescent monomers.

Based on our calcium transfer data, calnexin may play a role in negatively regulating MAM formation. It is therefore entirely possible that its absence would lead to an increase in aminoglycerophospholipid synthesis, which depends on transfer of aminoglycerophospholipid precursors between the MAM and mitochondria (Shiao et al., 1995). In fact, other MAM tethering structures such as ERMES and MFN2 tethers have been shown to be involved in lipid transfer (Area-Gomez et al., 2012; Kornmann et al., 2009). When presenilins 1 and 2, which negatively regulate MAM tethering, are knocked out, lipid transfer and synthesis increases (Area-Gomez et al., 2012). If calnexin does play a role in MAM structure, it would then be interesting to test whether its absence affects lipid transfer. Furthermore, it would be interesting to test whether palmitoylation of calnexin affects lipid transfer at the MAM, in the same way it is necessary for calnexin's function in calcium signalling modulation.

6.5 Palmitoylation is a novel MAM targeting mechanism that applies to several MAM localized proteins. How does this mechanism fit in with the other known MAM targeting mechanisms?

Table 6.1 summarizes the various proteins that specifically localize to MAMs and have either a well characterized function there or a known targeting motif. The mechanisms of MAM localization that have been described for different proteins are extremely varied, but two main themes emerge. One group of proteins seems to target to MAM through an interaction with mitochondria, which is exemplified by the following three proteins. DGAT2 has a cytosolic mitochondrial targeting sequence that is necessary for its localization to MAMs (Stone et al., 2009). ER-localized MFN2, on the other hand, forms a homodimer with its mitochondrial counterpart to localize to MAMs (de Brito and Scorrano, 2008), and similarly, the

ER protein Bap31 forms a complex with mitochondrial Fis1 at MAMs (Iwasawa et al., 2011). The other group of proteins relies on the lipid composition of the MAM, which is higher in cholesterol and sphingolipids (Hayashi and Fujimoto, 2010), for targeting information. This group includes the Sigma1 receptor and viral pUL37x1/vMIA protein, which lose either their MAM localization or their DRM association, respectively, when cholesterol is extracted from membranes (Hayashi and Fujimoto, 2010; Williamson et al., 2011).

We identified a group of proteins, calnexin, TMX, VDAC 1 and 2, and Hemeoxygenase1, which localize to MAM via a palmitoylation signal (Lynes et al., 2012) (Chapter 4). Like Sigma1 receptor and pUL37x1/vMIA, TMX was found to localize to detergent-resistant domains of the membrane, however calnexin did not (Figures 4.8F and 4.9F). This could reflect the extent of MAM localization of the two proteins, as calnexin does not cofractionate with MAM markers to the same degree as TMX. Charollais and Van der Goot suggested that palmitoylation of membrane proteins could cause change their association with lipid domains in the membrane by tilting the transmembrane helix to better fit across the width of the membrane or by directly interacting with lipids in membrane rafts (Charollais and Van Der Goot, 2009). Although neither the localization of TMX nor that of calnexin changed when membranes were depleted of cholesterol (Figure 4.9 H), perhaps another component of the MAM membrane could be retaining them there.

Alternatively, palmitoylation can also alter the protein-protein interactions by reducing the accessibility of a protein domain or altering its conformation (Charollais and Van Der Goot, 2009). Indeed, we found that depalmitoylated calnexin interacts less with SERCA2b and more with ERp57, and Lakkaraju et al. (2012) found that depalmitoylated calnexin interacts poorly with the translocon. Perhaps altered protein-protein interactions could be responsible for depalmitoylated calnexin's and TMX's change in localization. Since depalmitoylated calnexin's departure from MAMs coincides with a decrease in its

interaction with SERCA2b, it may be possible that SERCA2b is retaining calnexin at the MAM. This could be tested by analyzing calnexin's localization in cells where SERCA2b expression had been knocked down by RNAi. It is not currently known whether palmitoylation affects TMX's protein-protein interactions, and indeed, very little is known about possible TMX interactors at all, which will be further discussed in the next section.

Table 6.1 MAM-localized proteins and their targeting mechanisms

	Protein	**MAM function**	**Targeting mechanism**	**Reference**
Chaperones	Calnexin	SERCA2b modulation, calcium signalling/homeostasis	Palmitoylation	(Lynes et al., 2012)
	TMX	Unknown	Palmitoylation	(Lynes et al., 2012)
	Sigma1 receptor	Stabilizing IP3 receptors, modulation of calcium signalling	Association with lipid rafts, cholesterol	(Hayashi and Fujimoto, 2010; Hayashi and Su, 2007)
	Ero1a	Stimulation of IP3 receptors; oxidative protein folding	Requires oxidizing conditions	(Gilady et al.,2010)
	GRP75	Tethering complex	Association with IP3R and VDAC	(Szabadkai et al., 2006)
Lipid Synthesis/ Transfer	ACAT1	Cholesterol ester synthesis	Unknown	(Rusinol et al., 1994)
	FACL4	Ligates fatty acids to coA	Unknown	(Lewin et al., 2001)
	PSS1/PSS2	Synthesis of PtdSer	Unknown	(Stone and Vance, 2000)
	DGAT2	Lipid droplet formation	Cytosolic mitochondrial targeting sequence	(Stone et al., 2009)
Tethering proteins/ MAM structure	PS1/PS2	Counteracts MFN2's tethering role	May be raft-associated	(Area-Gomez et al., 2009; Area-Gomez et al., 2012)
	MFN2	Tethering, calcium signalling	Homodimerization with mitochondrial MFN2	(de Brito and Scorrano, 2008)
	Mmm1p	ER member of ERMES complex; Tethering	Association with mitochondrial ERMES members?	(Kornmann et al., 2009)
Viral proteins	pUL37x1	Traffic through MAM on their way to mitochondria	Association with lipid rafts, cholesterol	(Bozidis et al., 2008; Williamson et al.,2011)
	HIV Vpr		Unknown	(Huang et al., 2012)
Miscellaneous	Bap31	Apoptosis induction	Association with Fis1 (ARCosome)	(Iwasawa et al., 2011)

6.6 What is the function of TMX at the MAM?

TMX cofractionates with MAM markers to a greater extent than calnexin does, but very little is known about TMX's function in general, let alone its function at the MAM. TMX is a member of the PDI family of oxidoreductases, a 23-member group whose members share one or more thioredoxin-like catalytic domains comprising a CXXC motif and one or more substrate-binding domains. However, unlike PDI, TMX lacks a substrate binding domain and has an unusual active site sequence, CPAC instead of the CXHC motif found in PDI. Ellgaard and Ruddock predict that these differences may cast some doubt on TMX's ability to act as an efficient oxidoreductase (Ellgaard and Ruddock, 2005). In an *in vitro* assay, TMX was shown to be able to refold RNase, demonstrating that it does have a functional catalytic site (Matsuo et al., 2004). Two studies have shown that like ERp57, TMX is primarily reduced in vivo (Matsuo et al., 2009; Roth et al., 2009), which means that it is capable of isomerising or breaking, but not forming, disulphide bonds (Jessop and Bulleid, 2004). However although major histocompatibility complex class 1 heavy chain (MHC class 1 HC) was identified as a potential substrate for TMX, TMX is not essential for MHC class 1 assembly *in vivo* (Matsuo et al., 2009). TMX did, however, bind more MHC class 1 HC during ER stress, preventing its retrotranslocation and proteasomal degradation (Matsuo et al., 2009). The MHC class 1 HC was identified as a TMX substrate using a substrate trapping strategy where the second cysteine of TMX's thioredoxin site was mutated to alanine, which prevents redox reactions from being completed and stabilizes the intermediate complex formed between TMX and its substrate (Matsuo et al., 2009). Although at least four other TMX-substrate intermediate complexes were formed, the identity of the other substrates remains unknown. Repeating this experiment and identifying more TMX substrates could give important clues as to the function of TMX.

Matsuo et al. also showed that TMX binds to calnexin, and that this interaction is dependent on TMX's transmembrane domain, but not its cytosolic domain or its

active site (Matsuo et al., 2009). They also reported that blocking the recognition of glycoproteins by calnexin using castanospermine reduced the formation of TMX-substrate complexes, implying that calnexin's function is important for TMX's substrate-binding capabilities. These data suggest that TMX and calnexin may work in tandem, as ERp57 and calnexin do (Jessop et al., 2007). As TMX does not have a substrate-binding domain, perhaps calnexin functions as a scaffold to bring TMX into proximity with its substrates. Another intriguing possibility is that like other PDI family members ERp57 and ERp44, TMX may modulate calcium handling proteins at the ER in response to ER luminal redox conditions (Higo et al., 2005; Li and Camacho, 2004). Further coimmunoprecipitation experiments could be used in order to determine whether TMX interacts with SERCA2b or the IP_3 receptor. In conjunction with calcium sensitive dyes or organelle-targeted calcium sensitive proteins, fluorescence microscopy and flow cytometry could be used to compare the calcium handling properties of cells that do not express TMX to cells overexpressing TMX or its non-palmitoylatable counterpart, TMX CCAA.

DHHC6 has been identified as the PAT that mediates calnexin's palmitoylation (Lakkaraju et al. 2012). It is not known whether DHHC6 specifically localizes to MAMs, or whether DHHC6 could also be responsible for TMX's palmitoylation. The PAT that palmitoylates TMX could be identified using a similar strategy to the one used for calnexin. TMX palmitoylation could be observed after siRNA knockdown and overexpression of DHHC PAT family members to determine which PAT palmitoylates TMX. It is also unknown what palmitoylation and the MAM localization of TMX mean for TMX's function. As TMX and calnexin interact (Matsuo et al., 2009) and both proteins rely on palmitoylation to localize to MAM, it is likely that palmitoylation is important for this interaction. As more of TMX's functions become clear, it will be interesting to evaluate how palmitoylation plays a role by knocking down TMX and evaluating whether its functions can be rescued by the wildtype or non-palmitoylatable mutants.

6.7 Optiprep gradient fractionation adds to the various existing methods of studying MAM

Several techniques for studying the MAM existed prior to this work. These included techniques to study MAM structure and protein targeting to MAM by electron and immunofluorescence microscopy, as well as biochemical fractionations to study the protein and lipid composition of MAM. In addition, microscopical and flow cytometry techniques have been used in conjunction with calcium-sensitive dyes and proteins to analyze calcium signalling at the MAM. Finally, lipid biosynthesis assays can be used to analyze lipid transfer between the ER and mitochondria at MAMs. Each of these techniques has its own particular strengths and weaknesses, as discussed in the introduction to this thesis.

For our study, we required a biochemical fractionation method that could separate MAM from other ER compartments. The Percoll MAM fractionation separates MAM from mitochondria very well, but it is difficult to separate rough ER from MAM markers when adapting the protocol for use with cultured mammalian cells. The protocol was also developed for use with liver tissue and requires a lot of starting material in order to be able to identify the MAM band by eye. We therefore decided to develop a new fractionation method based on the Optiprep density medium in the hopes of obtaining better resolution of MAM and rough ER and that reduced the amount of starting material necessary in order to be able to analyze transfected cells expressing mutant constructs. The Optiprep gradient fractionation method described in Methods and in Chapter 3 achieved both goals, which allowed us to analyze mutants of calnexin, TMX and TMX4. The separation of MAM from rough ER is evidenced by separation of marker proteins. Rough ER markers Ribophorin I and II, Sec61 and eIF2a sediment mainly in fractions 3 and 4, whereas MAM markers ACAT1 and FACL4 co sediment with mitochondria in fractions 5 and 6. One drawback of the Optiprep fractionation is the lack of resolution of MAM and mitochondria, which could be improved by taking more fractions, or altering the percentage of Optiprep used. This problem can also be circumvented by using additional assays to ensure the proteins of

interest are targeted exclusively to ER and not to mitochondria, either by immunofluorescence microscopy or by performing a Percoll fractionation. In fact, most proteins that have been conclusively demonstrated to target to MAM have consistently been isolated there using more than one experimental technique. Calnexin, for example has been found at MAMs by Percoll fractionation (Lynes et al., 2012; Wieckowski et al., 2009), Optiprep fractionation (Myhill et al., 2008), immunofluorescence microscopy (Lynes et al. 2012) and calcium signalling assays (this thesis, Chapter 5).

6.8 Conclusions

Our understanding of the apposition between the ER and mitochondrial membranes, first observed more than 50 years ago by electron microscopy, has increased exponentially in more recent years. Due to the development of new microscopical and biochemical techniques for studying the structure and function of MAM, more is known about the lipid and protein composition of the MAM, how it is formed and how it is involved in cellular processes such as calcium and lipid trafficking. In this thesis I have developed a new protocol for separating MAM from rough ER. Furthermore, I have identified two new MAM targeting mechanisms, PACS-2 interaction and palmitoylation, and elucidated the calcium signalling function of calnexin at the MAM. This thesis also provides evidence of palmitoylation being a switch-like mechanism that regulates not only calnexin's intra-ER localization but also its protein-protein interactions and functions. Understanding protein targeting to MAM and MAM structure and formation will help us to understand MAM's role in disease. The MAM has been shown to play a role in a number of human diseases, including pulmonary hypertension (Sutendra et al. 2011), Alzheimer Disease (Area-Gomez et al., 2009; Area-Gomez et al. 2012), viral illnesses (Bozidis et al., 2008; Huang et al. 2012), and cancer (Pinton et al. 2011). Given the MAM's central role in apoptotic calcium trafficking and signalling it is not surprising that MAM is involved in neurodegenerative disease and cancer, where these processes are often

misregulated. My findings will help to explain the pathogenesis of these diseases, and perhaps provide novel avenues for their treatment.

The formation of ER-mitochondria contact sites has been shown to increase upon ER stress (Bravo et al., 2011; Csordas et al., 2006), which has consequences for the calcium-signalling function of MAM and mitochondrial function, but the mechanism whereby ER stress exerts this influence is unknown. Several MAM tethering complexes have been identified, but it is unclear whether or how they can be regulated. Furthermore, the MAM targeting mechanisms for many proteins with well-established MAM localizations and functions remain unknown. A better understanding of how MAM is regulated, including how tethering complexes are formed and broken and how proteins target to MAM, will give us a clearer picture of how ER and mitochondria communicate and, eventually, how this communication in disrupted in disease.

Chapter 7: References

Abrami, L., B. Kunz, I. Iacovache, and F.G. van der Goot. 2008. Palmitoylation and ubiquitination regulate exit of the Wnt signaling protein LRP6 from the endoplasmic reticulum. *Proceedings of the National Academy of Sciences of the United States of America*. 105:5384-5389.

Achleitner, G., B. Gaigg, A. Krasser, E. Kainersdorfer, S.D. Kohlwein, A. Perktold, G. Zellnig, and G. Daum. 1999. Association between the endoplasmic reticulum and mitochondria of yeast facilitates interorganelle transport of phospholipids through membrane contact. *European journal of biochemistry / FEBS*. 264:545-553.

Albert, P.R., and M. Tiberi. 2001. Receptor signaling and structure: insights from serotonin-1 receptors. *Trends in endocrinology and metabolism: TEM*. 12:453-460.

Alford, S.C., Y. Ding, T. Simmen, and R.E. Campbell. 2012. Dimerization-Dependent Green and Yellow Fluorescent Proteins. *ACS Synthetic Biology*.

Anderson, D.J., and M.W. Hetzer. 2007. Nuclear envelope formation by chromatin-mediated reorganization of the endoplasmic reticulum. *Nature cell biology*. 9:1160-1166.

Anelli, T., M. Alessio, A. Bachi, L. Bergamelli, G. Bertoli, S. Camerini, A. Mezghrani, E. Ruffato, T. Simmen, and R. Sitia. 2003. Thiol-mediated protein retention in the endoplasmic reticulum: the role of ERp44. *The EMBO journal*. 22:5015-5022.

Annaert, W.G., L. Levesque, K. Craessaerts, I. Dierinck, G. Snellings, D. Westaway, P.S. George-Hyslop, B. Cordell, P. Fraser, and B. De Strooper. 1999. Presenilin 1 controls gamma-secretase processing of amyloid precursor protein in pre-golgi compartments of hippocampal neurons. *The Journal of cell biology*. 147:277-294.

Area-Gomez, E., A.J. de Groof, I. Boldogh, T.D. Bird, G.E. Gibson, C.M. Koehler, W.H. Yu, K.E. Duff, M.P. Yaffe, L.A. Pon, and E.A. Schon. 2009. Presenilins are enriched in endoplasmic reticulum membranes associated with mitochondria. *The American journal of pathology*. 175:1810-1816.

Area-Gomez, E., M. Del Carmen Lara Castillo, M.D. Tambini, C. Guardia-Laguarta, A.J. de Groof, M. Madra, J. Ikenouchi, M. Umeda, T.D. Bird, S.L. Sturley, and E.A. Schon. 2012. Upregulated function of mitochondria-associated ER membranes in Alzheimer disease. *The EMBO journal*. 31:4106-4123.

Arnoult, D., L.M. Bartle, A. Skaletskaya, D. Poncet, N. Zamzami, P.U. Park, J. Sharpe, R.J. Youle, and V.S. Goldmacher. 2004. Cytomegalovirus cell death suppressor vMIA blocks Bax- but not Bak-mediated apoptosis by binding and sequestering Bax at mitochondria. *Proceedings of the National Academy of Sciences of the United States of America*. 101:7988-7993.

Ayala Yanez, R., and P.M. Conn. 2010. Protein disulfide isomerase chaperone ERP-57 decreases plasma membrane expression of the human GnRH receptor. *Cell biochemistry and function*. 28:66-73.

Bannykh, S.I., T. Rowe, and W.E. Balch. 1996. The organization of endoplasmic reticulum export complexes. *The Journal of cell biology*. 135:19-35.

Barile, M., C. Brizio, D. Valenti, C. De Virgilio, and S. Passarella. 2000. The riboflavin/FAD cycle in rat liver mitochondria. *European journal of biochemistry / FEBS*. 267:4888-4900.

Bass, R., L.W. Ruddock, P. Klappa, and R.B. Freedman. 2004. A major fraction of endoplasmic reticulum-located glutathione is present as mixed disulfides with protein. *The Journal of biological chemistry*. 279:5257-5262.

Bathori, G., G. Csordas, C. Garcia-Perez, E. Davies, and G. Hajnoczky. 2006. Ca2+-dependent control of the permeability properties of the mitochondrial outer membrane and voltage-dependent anion-selective channel (VDAC). *The Journal of biological chemistry*. 281:17347-17358.

Beck, R., M. Rawet, F.T. Wieland, and D. Cassel. 2009. The COPI system: molecular mechanisms and function. *FEBS letters*. 583:2701-2709.

Bernardi, P., and A. Rasola. 2007. Calcium and cell death: the mitochondrial connection. *Sub-cellular biochemistry*. 45:481-506.

Berridge, M.J. 2009. Inositol trisphosphate and calcium signalling mechanisms. *Biochimica et biophysica acta*. 1793:933-940.

Berthiaume, L., S.M. Peseckis, and M.D. Resh. 1995. Synthesis and use of iodo-fatty acid analogs. *Methods in enzymology*. 250:454-466.

Bezprozvanny, I., and M.P. Mattson. 2008. Neuronal calcium mishandling and the pathogenesis of Alzheimer's disease. *Trends in neurosciences*. 31:454-463.

Bhattacharyya, D., and B.S. Glick. 2007. Two mammalian Sec16 homologues have nonredundant functions in endoplasmic reticulum (ER) export and transitional ER organization. *Molecular biology of the cell*. 18:839-849.

Bickel, P.E., J.T. Tansey, and M.A. Welte. 2009. PAT proteins, an ancient family of lipid droplet proteins that regulate cellular lipid stores. *Biochimica et biophysica acta*. 1791:419-440.

Blumental-Perry, A., C.J. Haney, K.M. Weixel, S.C. Watkins, O.A. Weisz, and M. Aridor. 2006. Phosphatidylinositol 4-phosphate formation at ER exit sites regulates ER export. *Developmental cell*. 11:671-682.

Boehning, D., R.L. Patterson, L. Sedaghat, N.O. Glebova, T. Kurosaki, and S.H. Snyder. 2003. Cytochrome c binds to inositol (1,4,5) trisphosphate receptors, amplifying calcium-dependent apoptosis. *Nature cell biology*. 5:1051-1061.

Boisrame, A., M. Chasles, A. Babour, J.M. Beckerich, and C. Gaillardin. 2002. Sbh1p, a subunit of the Sec61 translocon, interacts with the chaperone calnexin in the yeast Yarrowia lipolytica. *Journal of cell science*. 115:4947-4956.

Bollo, M., R.M. Paredes, D. Holstein, N. Zheleznova, P. Camacho, and J.D. Lechleiter. 2010. Calcineurin interacts with PERK and dephosphorylates calnexin to relieve ER stress in mammals and frogs. *PloS one*. 5:e11925.

Bononi, A., S. Missiroli, F. Poletti, J.M. Suski, C. Agnoletto, M. Bonora, E. De Marchi, C. Giorgi, S. Marchi, S. Patergnani, A. Rimessi, M.R. Wieckowski, and P. Pinton. 2012. Mitochondria-associated membranes (MAMs) as hotspot Ca(2+) signaling units. *Advances in experimental medicine and biology*. 740:411-437.

Bozidis, P., C.D. Williamson, and A.M. Colberg-Poley. 2008. Mitochondrial and secretory human cytomegalovirus UL37 proteins traffic into mitochondrion-associated membranes of human cells. *Journal of virology*. 82:2715-2726.

Braakman, I., J. Helenius, and A. Helenius. 1992. Role of ATP and disulphide bonds during protein folding in the endoplasmic reticulum. *Nature*. 356:260-262.

Bravo, R., J.M. Vicencio, V. Parra, R. Troncoso, J.P. Munoz, M. Bui, C. Quiroga, A.E. Rodriguez, H.E. Verdejo, J. Ferreira, M. Iglewski, M. Chiong, T. Simmen, A. Zorzano, J.A. Hill, B.A. Rothermel, G. Szabadkai, and S. Lavandero. 2011. Increased ER-mitochondrial coupling promotes mitochondrial respiration and bioenergetics during early phases of ER stress. *Journal of cell science*. 124:2143-2152.

Breckenridge, D.G., M. Germain, J.P. Mathai, M. Nguyen, and G.C. Shore. 2003a. Regulation of apoptosis by endoplasmic reticulum pathways. *Oncogene*. 22:8608-8618.

Breckenridge, D.G., M. Nguyen, S. Kuppig, M. Reth, and G.C. Shore. 2002. The procaspase-8 isoform, procaspase-8L, recruited to the BAP31 complex at the endoplasmic reticulum. *Proceedings of the National Academy of Sciences of the United States of America*. 99:4331-4336.

Breckenridge, D.G., M. Stojanovic, R.C. Marcellus, and G.C. Shore. 2003b. Caspase cleavage product of BAP31 induces mitochondrial fission through endoplasmic reticulum calcium signals, enhancing cytochrome c release to the cytosol. *The Journal of cell biology*. 160:1115-1127.

Brough, D., M.J. Schell, and R.F. Irvine. 2005. Agonist-induced regulation of mitochondrial and endoplasmic reticulum motility. *The Biochemical journal*. 392:291-297.

Brown, M.S., and J.L. Goldstein. 1979. Receptor-mediated endocytosis: insights from the lipoprotein receptor system. *Proceedings of the National Academy of Sciences of the United States of America*. 76:3330-3337.

Bui, M., S.Y. Gilady, R.E. Fitzsimmons, M.D. Benson, E.M. Lynes, K. Gesson, N.M. Alto, S. Strack, J.D. Scott, and T. Simmen. 2010. Rab32 modulates apoptosis onset and mitochondria-associated membrane (MAM) properties. *The Journal of biological chemistry*. 285:31590-31602.

Cabibbo, A., M. Pagani, M. Fabbri, M. Rocchi, M.R. Farmery, N.J. Bulleid, and R. Sitia. 2000. ERO1-L, a human protein that favors disulfide bond formation in the endoplasmic reticulum. *The Journal of biological chemistry*. 275:4827-4833.

Cala, S.E., C. Ulbright, J.S. Kelley, and L.R. Jones. 1993. Purification of a 90-kDa protein (Band VII) from cardiac sarcoplasmic reticulum. Identification as calnexin and localization of casein kinase II phosphorylation sites. *The Journal of biological chemistry*. 268:2969-2975.

Camacho, P., and J.D. Lechleiter. 1995. Calreticulin inhibits repetitive intracellular Ca2+ waves. *Cell*. 82:765-771.

Cardenas, C., R.A. Miller, I. Smith, T. Bui, J. Molgo, M. Muller, H. Vais, K.H. Cheung, J. Yang, I. Parker, C.B. Thompson, M.J. Birnbaum, K.R. Hallows, and J.K. Foskett. 2010. Essential regulation of cell bioenergetics by constitutive InsP3 receptor Ca2+ transfer to mitochondria. *Cell*. 142:270-283.

Charollais, J., and F.G. Van Der Goot. 2009. Palmitoylation of membrane proteins (Review). *Molecular membrane biology*. 26:55-66.

Chevet, E., H.N. Wong, D. Gerber, C. Cochet, A. Fazel, P.H. Cameron, J.N. Gushue, D.Y. Thomas, and J.J. Bergeron. 1999. Phosphorylation by CK2 and MAPK enhances calnexin association with ribosomes. *The EMBO journal*. 18:3655-3666.

Copeland, D.E., and A.J. Dalton. 1959. An association between mitochondria and the endoplasmic reticulum in cells of the pseudobranch gland of a teleost. *The Journal of biophysical and biochemical cytology*. 5:393-396.

Coppock, D.L., and C. Thorpe. 2006. Multidomain flavin-dependent sulfhydryl oxidases. *Antioxidants & redox signaling*. 8:300-311.

Csordas, G., C. Renken, P. Varnai, L. Walter, D. Weaver, K.F. Buttle, T. Balla, C.A. Mannella, and G. Hajnoczky. 2006. Structural and functional features and significance of the physical linkage between ER and mitochondria. *The Journal of cell biology*. 174:915-921.

Csordas, G., A.P. Thomas, and G. Hajnoczky. 1999. Quasi-synaptic calcium signal transmission between endoplasmic reticulum and mitochondria. *The EMBO journal*. 18:96-108.

Cupers, P., M. Bentahir, K. Craessaerts, I. Orlans, H. Vanderstichele, P. Saftig, B. De Strooper, and W. Annaert. 2001. The discrepancy between presenilin subcellular localization and gamma-secretase processing of amyloid precursor protein. *The Journal of cell biology*. 154:731-740.

D'Angelo, G., M. Vicinanza, and M.A. De Matteis. 2008. Lipid-transfer proteins in biosynthetic pathways. *Current opinion in cell biology*. 20:360-370.

Dallner, G., S. Orrenius, and A. Bergstrand. 1963. Isolation and properties of rough and smooth vesicles from rat liver. *The Journal of cell biology*. 16:426-430.

de Brito, O.M., and L. Scorrano. 2008. Mitofusin 2 tethers endoplasmic reticulum to mitochondria. *Nature*. 456:605-610.

De Stefani, D., A. Bononi, A. Romagnoli, A. Messina, V. De Pinto, P. Pinton, and R. Rizzuto. 2012. VDAC1 selectively transfers apoptotic Ca2+ signals to mitochondria. *Cell death and differentiation*. 19:267-273.

De Stefani, D., A. Raffaello, E. Teardo, I. Szabo, and R. Rizzuto. 2011. A forty-kilodalton protein of the inner membrane is the mitochondrial calcium uniporter. *Nature*. 476:336-340.

Dejgaard, S., J. Nicolay, M. Taheri, D.Y. Thomas, and J.J. Bergeron. 2004. The ER glycoprotein quality control system. *Current issues in molecular biology*. 6:29-42.

Dekker, F.J., O. Rocks, N. Vartak, S. Menninger, C. Hedberg, R. Balamurugan, S. Wetzel, S. Renner, M. Gerauer, B. Scholermann, M. Rusch, J.W. Kramer, D. Rauh, G.W. Coates, L. Brunsveld, P.I. Bastiaens, and H. Waldmann. 2010. Small-molecule inhibition of APT1 affects Ras localization and signaling. *Nature chemical biology*. 6:449-456.

Delom, F., D. Fessart, and E. Chevet. 2007. Regulation of calnexin sub-cellular localization modulates endoplasmic reticulum stress-induced apoptosis in MCF-7 cells. *Apoptosis*. 12:293-305.

Depeint, F., W.R. Bruce, N. Shangari, R. Mehta, and P.J. O'Brien. 2006. Mitochondrial function and toxicity: role of the B vitamin family on mitochondrial energy metabolism. *Chemico-biological interactions*. 163:94-112.

Di Bisceglie, A.M. 1998. Hepatitis C. *Lancet*. 351:351-355.

Dowal, L., W. Yang, M.R. Freeman, H. Steen, and R. Flaumenhaft. 2011. Proteomic analysis of palmitoylated platelet proteins. *Blood*. 118:e62-73.

Dromparis, P., G. Sutendra, and E.D. Michelakis. 2010. The role of mitochondria in pulmonary vascular remodeling. *Journal of molecular medicine*. 88:1003-1010.

Duden, R. 2003. ER-to-Golgi transport: COP I and COP II function (Review). *Molecular membrane biology*. 20:197-207.

Egea, P.F., R.M. Stroud, and P. Walter. 2005. Targeting proteins to membranes: structure of the signal recognition particle. *Current opinion in structural biology*. 15:213-220.

Ehehalt, R., P. Keller, C. Haass, C. Thiele, and K. Simons. 2003. Amyloidogenic processing of the Alzheimer beta-amyloid precursor protein depends on lipid rafts. *The Journal of cell biology*. 160:113-123.

Ellgaard, L., and L.W. Ruddock. 2005. The human protein disulphide isomerase family: substrate interactions and functional properties. *EMBO reports*. 6:28-32.

Elliott, J.G., J.D. Oliver, and S. High. 1997. The thiol-dependent reductase ERp57 interacts specifically with N-glycosylated integral membrane proteins. *The Journal of biological chemistry*. 272:13849-13855.

Farese, R.V., Jr., and T.C. Walther. 2009. Lipid droplets finally get a little R-E-S-P-E-C-T. *Cell*. 139:855-860.

Ferrera, D., M. Panigada, S. Porcellini, and F. Grassi. 2008. Recombinase-deficient T cell development by selective accumulation of CD3 into lipid rafts. *European journal of immunology*. 38:1148-1156.

Filippin, L., P.J. Magalhaes, G. Di Benedetto, M. Colella, and T. Pozzan. 2003. Stable interactions between mitochondria and endoplasmic reticulum allow rapid accumulation of calcium in a subpopulation of mitochondria. *The Journal of biological chemistry*. 278:39224-39234.

Fonteriz, R.I., S. de la Fuente, A. Moreno, C.D. Lobaton, M. Montero, and J. Alvarez. 2010. Monitoring mitochondrial [Ca(2+)] dynamics with rhod-2, ratiometric pericam and aequorin. *Cell calcium*. 48:61-69.

Forrester, M.T., D.T. Hess, J.W. Thompson, R. Hultman, M.A. Moseley, J.S. Stamler, and P.J. Casey. 2011. Site-specific analysis of protein S-acylation by resin-assisted capture. *Journal of lipid research*. 52:393-398.

Fransson, S., A. Ruusala, and P. Aspenstrom. 2006. The atypical Rho GTPases Miro-1 and Miro-2 have essential roles in mitochondrial trafficking. *Biochemical and biophysical research communications*. 344:500-510.

Fregeau, M.O., Y. Regimbald-Dumas, and G. Guillemette. 2011. Positive regulation of inositol 1,4,5-trisphosphate-induced Ca2+ release by mammalian target of rapamycin (mTOR) in RINm5F cells. *Journal of cellular biochemistry*. 112:723-733.

Friedman, J.R., L.L. Lackner, M. West, J.R. DiBenedetto, J. Nunnari, and G.K. Voeltz. 2011. ER tubules mark sites of mitochondrial division. *Science (New York, N.Y.* 334:358-362.

Fujimoto, M., T. Hayashi, and T.P. Su. 2012. The role of cholesterol in the association of endoplasmic reticulum membranes with mitochondria. *Biochemical and biophysical research communications*. 417:635-639.

Fukata, Y., D.S. Bredt, and M. Fukata. 2006. Protein Palmitoylation by DHHC Protein Family.

Fukata, Y., and M. Fukata. 2010. Protein palmitoylation in neuronal development and synaptic plasticity. *Nature reviews. Neuroscience*. 11:161-175.

Galteau, M.M., B. Antoine, and H. Reggio. 1985. Epoxide hydrolase is a marker for the smooth endoplasmic reticulum in rat liver. *The EMBO journal*. 4:2793-2800.

Gardner, B.M., and P. Walter. 2011. Unfolded proteins are Ire1-activating ligands that directly induce the unfolded protein response. *Science (New York, N.Y.* 333:1891-1894.

Gilady, S.Y., M. Bui, E.M. Lynes, M.D. Benson, R. Watts, J.E. Vance, and T. Simmen. 2010. Ero1alpha requires oxidizing and normoxic conditions to localize to the mitochondria-associated membrane (MAM). *Cell stress & chaperones*. 15:619-629.

Giorgi, C., K. Ito, H.K. Lin, C. Santangelo, M.R. Wieckowski, M. Lebiedzinska, A. Bononi, M. Bonora, J. Duszynski, R. Bernardi, R. Rizzuto, C. Tacchetti, P. Pinton, and P.P. Pandolfi. 2010. PML regulates apoptosis at endoplasmic reticulum by modulating calcium release. *Science (New York, N.Y.* 330:1247-1251.

Goedert, M., and M.G. Spillantini. 2006. A century of Alzheimer's disease. *Science (New York, N.Y.* 314:777-781.

Grimm, S. 2012. The ER-mitochondria interface: the social network of cell death. *Biochimica et biophysica acta*. 1823:327-334.

Groenendyk, J., A. Zuppini, G. Shore, M. Opas, R.C. Bleackley, and M. Michalak. 2006. Caspase 12 in calnexin-deficient cells. *Biochemistry*. 45:13219-13226.

Guerin, R., G. Arseneault, S. Dumont, and L.A. Rokeach. 2008. Calnexin is involved in apoptosis induced by endoplasmic reticulum stress in the fission yeast. *Molecular biology of the cell*. 19:4404-4420.

Gunteski-Hamblin, A.M., J. Greeb, and G.E. Shull. 1988. A novel Ca2+ pump expressed in brain, kidney, and stomach is encoded by an alternative transcript of the slow-twitch muscle sarcoplasmic reticulum Ca-ATPase gene. Identification of cDNAs encoding Ca2+ and other cation-transporting ATPases using an oligonucleotide probe derived from the ATP-binding site. *The Journal of biological chemistry*. 263:15032-15040.

Hales, C.N., J.P. Luzio, J.A. Chandler, and L. Herman. 1974. Localization of calcium in the smooth endoplasmic reticulum of rat isolated fat cells. *Journal of cell science*. 15:1-15.

Hamman, B.D., L.M. Hendershot, and A.E. Johnson. 1998. BiP maintains the permeability barrier of the ER membrane by sealing the lumenal end of the translocon pore before and early in translocation. *Cell*. 92:747-758.

Hayashi, T., and M. Fujimoto. 2010. Detergent-resistant microdomains determine the localization of sigma-1 receptors to the endoplasmic reticulum-mitochondria junction. *Molecular pharmacology*. 77:517-528.

Hayashi, T., and T.P. Su. 2007. Sigma-1 receptor chaperones at the ER-mitochondrion interface regulate Ca(2+) signaling and cell survival. *Cell*. 131:596-610.

Heckman, K.L., and L.R. Pease. 2007. Gene splicing and mutagenesis by PCR-driven overlap extension. *Nature protocols*. 2:924-932.

Higgins, J.A. 1974. Studies on the biogenesis of smooth endoplasmic reticulum membranes in hepatocytes of phenobarbital-treated rats. II. The site of phospholipid synthesis in the initial phase of membrane proliferation. *The Journal of cell biology*. 62:635-646.

Higo, T., M. Hattori, T. Nakamura, T. Natsume, T. Michikawa, and K. Mikoshiba. 2005. Subtype-specific and ER lumenal environment-dependent regulation of inositol 1,4,5-trisphosphate receptor type 1 by ERp44. *Cell*. 120:85-98.

Hodges, B.D., and C.C. Wu. 2010. Proteomic insights into an expanded cellular role for cytoplasmic lipid droplets. *Journal of lipid research*. 51:262-273.

Hoepfner, D., D. Schildknegt, I. Braakman, P. Philippsen, and H.F. Tabak. 2005. Contribution of the endoplasmic reticulum to peroxisome formation. *Cell*. 122:85-95.

Horibe, T., M. Gomi, D. Iguchi, H. Ito, Y. Kitamura, T. Masuoka, I. Tsujimoto, T. Kimura, and M. Kikuchi. 2004. Different contributions of the three CXXC motifs of human protein-disulfide isomerase-related protein to isomerase activity and oxidative refolding. *The Journal of biological chemistry*. 279:4604-4611.

Hu, J., Y. Shibata, P.P. Zhu, C. Voss, N. Rismanchi, W.A. Prinz, T.A. Rapoport, and C. Blackstone. 2009. A class of dynamin-like GTPases involved in the generation of the tubular ER network. *Cell*. 138:549-561.

Huang, C.Y., S.F. Chiang, T.Y. Lin, S.H. Chiou, and K.C. Chow. 2012. HIV-1 Vpr triggers mitochondrial destruction by impairing Mfn2-mediated ER-mitochondria interaction. *PloS one*. 7:e33657.

Hughes, H., A. Budnik, K. Schmidt, K.J. Palmer, J. Mantell, C. Noakes, A. Johnson, D.A. Carter, P. Verkade, P. Watson, and D.J. Stephens. 2009. Organisation of human ER-exit sites: requirements for the localisation of Sec16 to transitional ER. *Journal of cell science*. 122:2924-2934.

Hwang, C., A.J. Sinskey, and H.F. Lodish. 1992. Oxidized redox state of glutathione in the endoplasmic reticulum. *Science (New York, N.Y.* 257:1496-1502.

Hwang, H.W., J.R. Lee, K.Y. Chou, C.S. Suen, M.J. Hwang, C. Chen, R.C. Shieh, and L.Y. Chau. 2009. Oligomerization is crucial for the stability and function of heme oxygenase-1 in the endoplasmic reticulum. *The Journal of biological chemistry*. 284:22672-22679.

Ishihara, N., Y. Eura, and K. Mihara. 2004. Mitofusin 1 and 2 play distinct roles in mitochondrial fusion reactions via GTPase activity. *Journal of cell science*. 117:6535-6546.

Ivan, V., G. de Voer, D. Xanthakis, K.M. Spoorendonk, V. Kondylis, and C. Rabouille. 2008. Drosophila Sec16 mediates the biogenesis of tER sites upstream of Sar1 through an arginine-rich motif. *Molecular biology of the cell*. 19:4352-4365.

Iwasawa, R., A.L. Mahul-Mellier, C. Datler, E. Pazarentzos, and S. Grimm. 2011. Fis1 and Bap31 bridge the mitochondria-ER interface to establish a platform for apoptosis induction. *The EMBO journal*. 30:556-568.

Jessop, C.E., and N.J. Bulleid. 2004. Glutathione directly reduces an oxidoreductase in the endoplasmic reticulum of mammalian cells. *The Journal of biological chemistry*. 279:55341-55347.

Jessop, C.E., S. Chakravarthi, N. Garbi, G.J. Hammerling, S. Lovell, and N.J. Bulleid. 2007. ERp57 is essential for efficient folding of glycoproteins sharing common structural domains. *The EMBO journal*. 26:28-40.

Kalantari, F., J.J. Bergeron, and T. Nilsson. 2010. Biogenesis of lipid droplets--how cells get fatter. *Molecular membrane biology*. 27:462-468.

Kalies, K.U., T.A. Rapoport, and E. Hartmann. 1998. The beta subunit of the Sec61 complex facilitates cotranslational protein transport and interacts with the signal peptidase during translocation. *The Journal of cell biology*. 141:887-894.

Kamhi-Nesher, S., M. Shenkman, S. Tolchinsky, S.V. Fromm, R. Ehrlich, and G.Z. Lederkremer. 2001. A novel quality control compartment derived from the endoplasmic reticulum. *Molecular biology of the cell*. 12:1711-1723.

Kang, R., J. Wan, P. Arstikaitis, H. Takahashi, K. Huang, A.O. Bailey, J.X. Thompson, A.F. Roth, R.C. Drisdel, R. Mastro, W.N. Green, J.R. Yates, 3rd, N.G. Davis, and A. El-Husseini. 2008. Neural palmitoyl-proteomics reveals dynamic synaptic palmitoylation. *Nature*. 456:904-909.

Kim, S.J., Z. Zhang, E. Hitomi, Y.C. Lee, and A.B. Mukherjee. 2006. Endoplasmic reticulum stress-induced caspase-4 activation mediates apoptosis and neurodegeneration in INCL. *Human molecular genetics*. 15:1826-1834.

Klappa, P., H.C. Hawkins, and R.B. Freedman. 1997. Interactions between protein disulphide isomerase and peptides. *European journal of biochemistry / FEBS*. 248:37-42.

Kleizen, B., and I. Braakman. 2004. Protein folding and quality control in the endoplasmic reticulum. *Current opinion in cell biology*. 16:343-349.

Knarr, G., M.J. Gething, S. Modrow, and J. Buchner. 1995. BiP binding sequences in antibodies. *The Journal of biological chemistry*. 270:27589-27594.

Kornmann, B., E. Currie, S.R. Collins, M. Schuldiner, J. Nunnari, J.S. Weissman, and P. Walter. 2009. An ER-mitochondria tethering complex revealed by a synthetic biology screen. *Science (New York, N.Y.* 325:477-481.

Kornmann, B., C. Osman, and P. Walter. 2011. The conserved GTPase Gem1 regulates endoplasmic reticulum-mitochondria connections. *Proceedings of the National Academy of Sciences of the United States of America*. 108:14151-14156.

Kornmann, B., and P. Walter. 2010. ERMES-mediated ER-mitochondria contacts: molecular hubs for the regulation of mitochondrial biology. *Journal of cell science*. 123:1389-1393.

Kostiuk, M.A., B.O. Keller, and L.G. Berthiaume. 2009. Non-radioactive detection of palmitoylated mitochondrial proteins using an azido-palmitate analogue. *Methods in enzymology*. 457:149-165.

Kozlov, G., P. Maattanen, D.Y. Thomas, and K. Gehring. 2010. A structural overview of the PDI family of proteins. *The FEBS journal*. 277:3924-3936.

Kozutsumi, Y., M. Segal, K. Normington, M.J. Gething, and J. Sambrook. 1988. The presence of malfolded proteins in the endoplasmic reticulum signals the induction of glucose-regulated proteins. *Nature*. 332:462-464.

Kraus, A., J. Groenendyk, K. Bedard, T.A. Baldwin, K.H. Krause, M. Dubois-Dauphin, J. Dyck, E.E. Rosenbaum, L. Korngut, N.J. Colley, S. Gosgnach, D. Zochodne, K. Todd, L.B. Agellon, and M. Michalak. 2010. Calnexin deficiency leads to dysmyelination. *The Journal of biological chemistry*. 285:18928-18938.

Kuge, O., Y. Yamakawa, and M. Nishijima. 2001. Enhancement of transport-dependent decarboxylation of phosphatidylserine by S100B protein in permeabilized Chinese hamster ovary cells. *The Journal of biological chemistry*. 276:23700-23706.

Kuhn, B., A. Schmid, C. Harteneck, T. Gudermann, and G. Schultz. 1996. G proteins of the Gq family couple the H2 histamine receptor to phospholipase C. *Molecular endocrinology (Baltimore, Md*. 10:1697-1707.

Lakkaraju, A.K., L. Abrami, T. Lemmin, S. Blaskovic, B. Kunz, A. Kihara, M. Dal Peraro, and F.G. van der Goot. 2012. Palmitoylated calnexin is a key component of the ribosome-translocon complex. *The EMBO journal*. 31:1823-1835.

Lam, K.K., M. Davey, B. Sun, A.F. Roth, N.G. Davis, and E. Conibear. 2006. Palmitoylation by the DHHC protein Pfa4 regulates the ER exit of Chs3. *The Journal of cell biology*. 174:19-25.

Lambert, G., B. Becker, R. Schreiber, A. Boucherot, M. Reth, and K. Kunzelmann. 2001. Control of cystic fibrosis transmembrane conductance regulator expression by BAP31. *The Journal of biological chemistry*. 276:20340-20345.

Lederkremer, G.Z. 2009. Glycoprotein folding, quality control and ER-associated degradation. *Current opinion in structural biology*. 19:515-523.

Lee, I., and W. Hong. 2006. Diverse membrane-associated proteins contain a novel SMP domain. *Faseb J*. 20:202-206.

Lee, R.G., M.C. Willingham, M.A. Davis, K.A. Skinner, and L.L. Rudel. 2000. Differential expression of ACAT1 and ACAT2 among cells within liver, intestine, kidney, and adrenal of nonhuman primates. *Journal of lipid research*. 41:1991-2001.

Levine, T., and C. Rabouille. 2005. Endoplasmic reticulum: one continuous network compartmentalized by extrinsic cues. *Current opinion in cell biology*. 17:362-368.

Lewin, T.M., J.H. Kim, D.A. Granger, J.E. Vance, and R.A. Coleman. 2001. Acyl-CoA synthetase isoforms 1, 4, and 5 are present in different subcellular membranes in rat liver and can be inhibited independently. *The Journal of biological chemistry*. 276:24674-24679.

Li, G., M. Mongillo, K.T. Chin, H. Harding, D. Ron, A.R. Marks, and I. Tabas. 2009. Role of ERO1-alpha-mediated stimulation of inositol 1,4,5-triphosphate receptor activity in endoplasmic reticulum stress-induced apoptosis. *The Journal of cell biology*. 186:783-792.

Li, J., and A.S. Lee. 2006. Stress induction of GRP78/BiP and its role in cancer. *Current molecular medicine*. 6:45-54.

Li, Y., and P. Camacho. 2004. Ca2+-dependent redox modulation of SERCA 2b by ERp57. *The Journal of cell biology*. 164:35-46.

Li, Y., B.R. Martin, B.F. Cravatt, and S.L. Hofmann. 2012. DHHC5 protein palmitoylates flotillin-2 and is rapidly degraded on induction of neuronal differentiation in cultured cells. *The Journal of biological chemistry*. 287:523-530.

Loew, L.M., W. Carrington, R.A. Tuft, and F.S. Fay. 1994. Physiological cytosolic Ca2+ transients evoke concurrent mitochondrial depolarizations. *Proceedings of the National Academy of Sciences of the United States of America*. 91:12579-12583.

Lynes, E.M., M. Bui, M.C. Yap, M.D. Benson, B. Schneider, L. Ellgaard, L.G. Berthiaume, and T. Simmen. 2012. Palmitoylated TMX and calnexin target to the mitochondria-associated membrane. *The EMBO journal*. 31:457-470.

Manders, E.M., R. Hoebe, J. Strackee, A.M. Vossepoel, and J.A. Aten. 1996. Largest contour segmentation: a tool for the localization of spots in confocal images. *Cytometry*. 23:15-21.

Manthey, K.C., Y.C. Chew, and J. Zempleni. 2005. Riboflavin deficiency impairs oxidative folding and secretion of apolipoprotein B-100 in HepG2 cells, triggering stress response systems. *The Journal of nutrition*. 135:978-982.

Marchant, J.S. 2005. Cellular signalling: STIMulating calcium entry. *Curr Biol*. 15:R493-495.

Marchetti, P., M. Bugliani, R. Lupi, L. Marselli, M. Masini, U. Boggi, F. Filipponi, G.C. Weir, D.L. Eizirik, and M. Cnop. 2007. The endoplasmic reticulum in pancreatic beta cells of type 2 diabetes patients. *Diabetologia*. 50:2486-2494.

Marelli, M., J.J. Smith, S. Jung, E. Yi, A.I. Nesvizhskii, R.H. Christmas, R.A. Saleem, Y.Y. Tam, A. Fagarasanu, D.R. Goodlett, R. Aebersold, R.A. Rachubinski, and J.D. Aitchison. 2004. Quantitative mass spectrometry reveals a role for the GTPase Rho1p in actin organization on the peroxisome membrane. *The Journal of cell biology*. 167:1099-1112.

Mast, F.D., A. Fagarasanu, B. Knoblach, and R.A. Rachubinski. 2010. Peroxisome biogenesis: something old, something new, something borrowed. *Physiology (Bethesda, Md*. 25:347-356.

Matsuo, Y., H. Masutani, A. Son, S. Kizaka-Kondoh, and J. Yodoi. 2009. Physical and functional interaction of transmembrane thioredoxin-related protein with major histocompatibility complex class I heavy chain: redox-based protein quality control and its potential relevance to immune responses. *Molecular biology of the cell*. 20:4552-4562.

Mavinakere, M.S., C.D. Williamson, V.S. Goldmacher, and A.M. Colberg-Poley. 2006. Processing of human cytomegalovirus UL37 mutant glycoproteins in the endoplasmic reticulum lumen prior to mitochondrial importation. *Journal of virology*. 80:6771-6783.

May, D., A. Itin, O. Gal, H. Kalinski, E. Feinstein, and E. Keshet. 2005. Ero1-L alpha plays a key role in a HIF-1-mediated pathway to improve disulfide bond formation and VEGF secretion under hypoxia: implication for cancer. *Oncogene*. 24:1011-1020.

McCormick, L.M., R. Urade, Y. Arakaki, A.L. Schwartz, and G. Bu. 2005. Independent and cooperative roles of N-glycans and molecular chaperones in the folding and disulfide bond formation of the low-density lipoprotein (LDL) receptor-related protein. *Biochemistry*. 44:5794-5803.

McDowell, W., and R.T. Schwarz. 1988. Dissecting glycoprotein biosynthesis by the use of specific inhibitors. *Biochimie*. 70:1535-1549.

McFie, P.J., S.L. Banman, S. Kary, and S.J. Stone. 2011. Murine diacylglycerol acyltransferase-2 (DGAT2) can catalyze triacylglycerol synthesis and promote lipid droplet formation independent of its localization to the endoplasmic reticulum. *The Journal of biological chemistry*. 286:28235-28246.

McGraw, C.F., A.V. Somlyo, and M.P. Blaustein. 1980. Localization of calcium in presynaptic nerve terminals. An ultrastructural and electron microprobe analysis. *The Journal of cell biology*. 85:228-241.

Meldolesi, J., and T. Pozzan. 1998. The endoplasmic reticulum Ca2+ store: a view from the lumen. *Trends in biochemical sciences*. 23:10-14.

Mellad, J.A., D.T. Warren, and C.M. Shanahan. 2011. Nesprins LINC the nucleus and cytoskeleton. *Current opinion in cell biology*. 23:47-54.

Michalak, M., J.M. Robert Parker, and M. Opas. 2002. Ca2+ signaling and calcium binding chaperones of the endoplasmic reticulum. *Cell calcium*. 32:269-278.

Miyawaki, A., J. Llopis, R. Heim, J.M. McCaffery, J.A. Adams, M. Ikura, and R.Y. Tsien. 1997. Fluorescent indicators for Ca2+ based on green fluorescent proteins and calmodulin. *Nature*. 388:882-887.

Moussalli, M., S.W. Pipe, H.P. Hauri, W.C. Nichols, D. Ginsburg, and R.J. Kaufman. 1999. Mannose-dependent endoplasmic reticulum (ER)-Golgi intermediate compartment-53-mediated ER to Golgi trafficking of coagulation factors V and VIII. *The Journal of biological chemistry*. 274:32539-32542.

Myhill, N., E.M. Lynes, J.A. Nanji, A.D. Blagoveshchenskaya, H. Fei, K.C. Simmen, T.J. Cooper, G. Thomas, and T. Simmen. 2008. The Subcellular Distribution of Calnexin is Mediated by PACS-2. *Molecular biology of the cell*.

Nakagawa, T., H. Zhu, N. Morishima, E. Li, J. Xu, B.A. Yankner, and J. Yuan. 2000. Caspase-12 mediates endoplasmic-reticulum-specific apoptosis and cytotoxicity by amyloid-beta. *Nature*. 403:98-103.

Nguyen, T.T., A. Lewandowska, J.Y. Choi, D.F. Markgraf, M. Junker, M. Bilgin, C.S. Ejsing, D.R. Voelker, T.A. Rapoport, and J.M. Shaw. 2012. Gem1 and ERMES do not directly affect phosphatidylserine transport from ER to mitochondria or mitochondrial inheritance. *Traffic (Copenhagen, Denmark)*. 13:880-890.

Okazaki, Y., H. Ohno, K. Takase, T. Ochiai, and T. Saito. 2000. Cell surface expression of calnexin, a molecular chaperone in the endoplasmic reticulum. *The Journal of biological chemistry*. 275:35751-35758.

Olson, M.L., S. Chalmers, and J.G. McCarron. 2010. Mitochondrial Ca2+ uptake increases Ca2+ release from inositol 1,4,5-trisphosphate receptor clusters in smooth muscle cells. *The Journal of biological chemistry*. 285:2040-2050.

Orso, G., D. Pendin, S. Liu, J. Tosetto, T.J. Moss, J.E. Faust, M. Micaroni, A. Egorova, A. Martinuzzi, J.A. McNew, and A. Daga. 2009. Homotypic fusion of ER membranes requires the dynamin-like GTPase atlastin. *Nature*. 460:978-983.

Osibow, K., S. Frank, R. Malli, R. Zechner, and W.F. Graier. 2006. Mitochondria maintain maturation and secretion of lipoprotein lipase in the endoplasmic reticulum. *The Biochemical journal*. 396:173-182.

Ou, W.J., D.Y. Thomas, A.W. Bell, and J.J. Bergeron. 1992. Casein kinase II phosphorylation of signal sequence receptor alpha and the associated membrane chaperone calnexin. *The Journal of biological chemistry*. 267:23789-23796.

Pagani, M., M. Fabbri, C. Benedetti, A. Fassio, S. Pilati, N.J. Bulleid, A. Cabibbo, and R. Sitia. 2000. Endoplasmic reticulum oxidoreductin 1-lbeta (ERO1-Lbeta), a human gene induced in the course of the unfolded protein response. *The Journal of biological chemistry*. 275:23685-23692.

Palade, G. 1975. Intracellular aspects of the process of protein synthesis. *Science (New York, N.Y.* 189:867.

Palade, G.E., and P. Siekevitz. 1956. Liver microsomes; an integrated morphological and biochemical study. *The Journal of biophysical and biochemical cytology*. 2:171-200.

Pani, B., H.L. Ong, X. Liu, K. Rauser, I.S. Ambudkar, and B.B. Singh. 2008. Lipid rafts determine clustering of STIM1 in endoplasmic reticulum-plasma membrane junctions and regulation of store-operated Ca2+ entry (SOCE). *The Journal of biological chemistry*. 283:17333-17340.

Papa, F.R. 2012. Endoplasmic reticulum stress, pancreatic beta-cell degeneration, and diabetes. *Cold Spring Harbor perspectives in medicine*. 2:a007666.

Pathre, P., K. Shome, A. Blumental-Perry, A. Bielli, C.J. Haney, S. Alber, S.C. Watkins, G. Romero, and M. Aridor. 2003. Activation of phospholipase D by the small GTPase Sar1p is required to support COPII assembly and ER export. *The EMBO journal*. 22:4059-4069.

Perry, S.W., J.P. Norman, J. Barbieri, E.B. Brown, and H.A. Gelbard. 2011. Mitochondrial membrane potential probes and the proton gradient: a practical usage guide. *BioTechniques*. 50:98-115.

Pinton, P., C. Giorgi, and P.P. Pandolfi. 2011. The role of PML in the control of apoptotic cell fate: a new key player at ER-mitochondria sites. *Cell death and differentiation*. 18:1450-1456.

Pinton, P., C. Giorgi, R. Siviero, E. Zecchini, and R. Rizzuto. 2008. Calcium and apoptosis: ER-mitochondria Ca2+ transfer in the control of apoptosis. *Oncogene*. 27:6407-6418.

Poburko, D., and N. Demaurex. 2012. Regulation of the mitochondrial proton gradient by cytosolic Ca(2)(+) signals. *Pflugers Arch*. 464:19-26.

Poncet, D., N. Larochette, A.L. Pauleau, P. Boya, A.A. Jalil, P.F. Cartron, F. Vallette, C. Schnebelen, L.M. Bartle, A. Skaletskaya, D. Boutolleau, J.C. Martinou, V.S. Goldmacher, G. Kroemer, and N. Zamzami. 2004. An anti-apoptotic viral protein that recruits Bax to mitochondria. *The Journal of biological chemistry*. 279:22605-22614.

Prakriya, M., S. Feske, Y. Gwack, S. Srikanth, A. Rao, and P.G. Hogan. 2006. Orai1 is an essential pore subunit of the CRAC channel. *Nature*. 443:230-233.

Priller, C., T. Bauer, G. Mitteregger, B. Krebs, H.A. Kretzschmar, and J. Herms. 2006. Synapse formation and function is modulated by the amyloid precursor protein. *J Neurosci*. 26:7212-7221.

Prins, D., J. Groenendyk, N. Touret, and M. Michalak. 2011. Modulation of STIM1 and capacitative Ca2+ entry by the endoplasmic reticulum luminal oxidoreductase ERp57. *EMBO reports*. 12:1182-1188.

Protchenko, O., R. Rodriguez-Suarez, R. Androphy, H. Bussey, and C.C. Philpott. 2006. A screen for genes of heme uptake identifies the FLC family required for import of FAD into the endoplasmic reticulum. *The Journal of biological chemistry*. 281:21445-21457.

Radhakrishnan, A., J.L. Goldstein, J.G. McDonald, and M.S. Brown. 2008. Switch-like control of SREBP-2 transport triggered by small changes in ER cholesterol: a delicate balance. *Cell metabolism*. 8:512-521.

Raychaudhuri, S., Y.J. Im, J.H. Hurley, and W.A. Prinz. 2006. Nonvesicular sterol movement from plasma membrane to ER requires oxysterol-binding protein-related proteins and phosphoinositides. *The Journal of cell biology*. 173:107-119.

Regimbald-Dumas, Y., M.O. Fregeau, and G. Guillemette. 2011. Mammalian target of rapamycin (mTOR) phosphorylates inositol 1,4,5-trisphosphate receptor type 2 and increases its Ca(2+) release activity. *Cellular signalling*. 23:71-79.

Resh, M.D. 2006. Use of analogs and inhibitors to study the functional significance of protein palmitoylation. *Methods (San Diego, Calif.* 40:191-197.

Rizzuto, R., M. Brini, M. Murgia, and T. Pozzan. 1993. Microdomains with high Ca2+ close to IP3-sensitive channels that are sensed by neighboring mitochondria. *Science (New York, N.Y.* 262:744-747.

Rizzuto, R., P. Pinton, W. Carrington, F.S. Fay, K.E. Fogarty, L.M. Lifshitz, R.A. Tuft, and T. Pozzan. 1998. Close contacts with the endoplasmic reticulum as determinants of mitochondrial Ca2+ responses. *Science (New York, N.Y.* 280:1763-1766.

Robb-Gaspers, L.D., P. Burnett, G.A. Rutter, R.M. Denton, R. Rizzuto, and A.P. Thomas. 1998. Integrating cytosolic calcium signals into mitochondrial metabolic responses. *The EMBO journal*. 17:4987-5000.

Roderick, H.L., J.D. Lechleiter, and P. Camacho. 2000. Cytosolic phosphorylation of calnexin controls intracellular Ca(2+) oscillations via an interaction with SERCA2b. *The Journal of cell biology*. 149:1235-1248.

Roos, J., P.J. DiGregorio, A.V. Yeromin, K. Ohlsen, M. Lioudyno, S. Zhang, O. Safrina, J.A. Kozak, S.L. Wagner, M.D. Cahalan, G. Velicelebi, and K.A. Stauderman. 2005. STIM1, an essential and conserved component of store-operated Ca2+ channel function. *The Journal of cell biology*. 169:435-445.

Rosenbaum, E.E., R.C. Hardie, and N.J. Colley. 2006. Calnexin is essential for rhodopsin maturation, Ca2+ regulation, and photoreceptor cell survival. *Neuron*. 49:229-241.

Ross, M.E., R. Mahfouz, M. Onciu, H.C. Liu, X. Zhou, G. Song, S.A. Shurtleff, S. Pounds, C. Cheng, J. Ma, R.C. Ribeiro, J.E. Rubnitz, K. Girtman, W.K. Williams, S.C. Raimondi, D.C. Liang, L.Y. Shih, C.H. Pui, and J.R. Downing. 2004. Gene expression profiling of pediatric acute myelogenous leukemia. *Blood*. 104:3679-3687.

Roth, D., E. Lynes, J. Riemer, H.G. Hansen, N. Althaus, T. Simmen, and L. Ellgaard. 2009. A di-arginine motif contributes to the ER-localization of the type I transmembrane ER oxidoreductase TMX4. *The Biochemical journal*.

Ruddock, L.W., and M. Molinari. 2006. N-glycan processing in ER quality control. *Journal of cell science*. 119:4373-4380.

Rusinol, A.E., Z. Cui, M.H. Chen, and J.E. Vance. 1994. A unique mitochondria-associated membrane fraction from rat liver has a high capacity for lipid synthesis and contains pre-Golgi secretory proteins including nascent lipoproteins. *The Journal of biological chemistry*. 269:27494-27502.

Rutkevich, L.A., M.F. Cohen-Doyle, U. Brockmeier, and D.B. Williams. 2010. Functional relationship between protein disulfide isomerase family members during the oxidative folding of human secretory proteins. *Molecular biology of the cell*. 21:3093-3105.

Rutkevich, L.A., and D.B. Williams. 2011. Participation of lectin chaperones and thiol oxidoreductases in protein folding within the endoplasmic reticulum. *Current opinion in cell biology*. 23:157-166.

Salaun, C., J. Greaves, and L.H. Chamberlain. 2010. The intracellular dynamic of protein palmitoylation. *The Journal of cell biology*. 191:1229-1238.

Sano, R., I. Annunziata, A. Patterson, S. Moshiach, E. Gomero, J. Opferman, M. Forte, and A. d'Azzo. 2009. GM1-ganglioside accumulation at the mitochondria-associated ER membranes links ER stress to Ca(2+)-dependent mitochondrial apoptosis. *Molecular cell*. 36:500-511.

Schon, E.A., and E. Area-Gomez. 2012. Mitochondria-associated ER membranes in Alzheimer disease. *Molecular and cellular neurosciences*.

Schulz, I., F. Thevenod, and M. Dehlinger-Kremer. 1989. Modulation of intracellular free Ca2+ concentration by IP3-sensitive and IP3-insensitive nonmitochondrial Ca2+ pools. *Cell calcium*. 10:325-336.

Schulz, T.A., and W.A. Prinz. 2007. Sterol transport in yeast and the oxysterol binding protein homologue (OSH) family. *Biochimica et biophysica acta*. 1771:769-780.

Schumacher, M.M., J.Y. Choi, and D.R. Voelker. 2002. Phosphatidylserine transport to the mitochondria is regulated by ubiquitination. *The Journal of biological chemistry*. 277:51033-51042.

Scragg, J.L., M.L. Dallas, J.A. Wilkinson, G. Varadi, and C. Peers. 2008. Carbon monoxide inhibits L-type Ca2+ channels via redox modulation of key cysteine residues by mitochondrial reactive oxygen species. *The Journal of biological chemistry*. 283:24412-24419.

Sharom, F.J. 2011. Flipping and flopping--lipids on the move. *IUBMB life*. 63:736-746.

Sharon-Friling, R., J. Goodhouse, A.M. Colberg-Poley, and T. Shenk. 2006. Human cytomegalovirus pUL37x1 induces the release of endoplasmic reticulum calcium stores. *Proceedings of the National Academy of Sciences of the United States of America*. 103:19117-19122.

Shiao, Y.J., B. Balcerzak, and J.E. Vance. 1998. A mitochondrial membrane protein is required for translocation of phosphatidylserine from mitochondria-associated membranes to mitochondria. *The Biochemical journal*. 331 (Pt 1):217-223.

Shiao, Y.J., G. Lupo, and J.E. Vance. 1995. Evidence that phosphatidylserine is imported into mitochondria via a mitochondria-associated membrane and that the majority of mitochondrial phosphatidylethanolamine is derived from decarboxylation of phosphatidylserine. *The Journal of biological chemistry*. 270:11190-11198.

Shibata, Y., T. Shemesh, W.A. Prinz, A.F. Palazzo, M.M. Kozlov, and T.A. Rapoport. 2010. Mechanisms determining the morphology of the peripheral ER. *Cell*. 143:774-788.

Shioda, N., K. Ishikawa, H. Tagashira, T. Ishizuka, H. Yawo, and K. Fukunaga. 2012. Expression of a truncated form of the endoplasmic reticulum chaperone protein, sigma1 receptor, promotes mitochondrial energy depletion and apoptosis. *The Journal of biological chemistry*. 287:23318-23331.

Shoshan-Barmatz, V., and A. Israelson. 2005. The voltage-dependent anion channel in endoplasmic/sarcoplasmic reticulum: characterization, modulation and possible function. *The Journal of membrane biology*. 204:57-66.

Shuttleworth, T.J., J.L. Thompson, and O. Mignen. 2007. STIM1 and the noncapacitative ARC channels. *Cell calcium*. 42:183-191.

Simmen, T., J.E. Aslan, A.D. Blagoveshchenskaya, L. Thomas, L. Wan, Y. Xiang, S.F. Feliciangeli, C.H. Hung, C.M. Crump, and G. Thomas. 2005. PACS-2 controls endoplasmic reticulum-mitochondria communication and Bid-mediated apoptosis. *The EMBO journal*. 24:717-729.

Simmen, T., M. Nobile, J.S. Bonifacino, and W. Hunziker. 1999. Basolateral sorting of furin in MDCK cells requires a phenylalanine-isoleucine motif together with an acidic amino acid cluster. *Molecular and cellular biology*. 19:3136-3144.

Sitia, R., and I. Braakman. 2003. Quality control in the endoplasmic reticulum protein factory. *Nature*. 426:891-894.

Sitia, R., and J. Meldolesi. 1992. Endoplasmic reticulum: a dynamic patchwork of specialized subregions. *Molecular biology of the cell*. 3:1067-1072.

Sleight, R.G., and R.E. Pagano. 1983. Rapid appearance of newly synthesized phosphatidylethanolamine at the plasma membrane. *The Journal of biological chemistry*. 258:9050-9058.

Soni, K.G., G.A. Mardones, R. Sougrat, E. Smirnova, C.L. Jackson, and J.S. Bonifacino. 2009. Coatomer-dependent protein delivery to lipid droplets. *Journal of cell science*. 122:1834-1841.

Stefani, M., and G. Liguri. 2009. Cholesterol in Alzheimer's disease: unresolved questions. *Current Alzheimer research*. 6:15-29.

Stone, S.J., M.C. Levin, P. Zhou, J. Han, T.C. Walther, and R.V. Farese, Jr. 2009. The endoplasmic reticulum enzyme DGAT2 is found in mitochondria-associated membranes and has a mitochondrial targeting signal that promotes its association with mitochondria. *The Journal of biological chemistry*. 284:5352-5361.

Stone, S.J., and J.E. Vance. 2000. Phosphatidylserine synthase-1 and -2 are localized to mitochondria-associated membranes. *The Journal of biological chemistry*. 275:34534-34540.

Sutendra, G., P. Dromparis, P. Wright, S. Bonnet, A. Haromy, Z. Hao, M.S. McMurtry, M. Michalak, J.E. Vance, W.C. Sessa, and E.D. Michelakis. 2011. The role of Nogo and the mitochondria-endoplasmic reticulum unit in pulmonary hypertension. *Science translational medicine*. 3:88ra55.

Suzuki, R., S. Sakamoto, T. Tsutsumi, A. Rikimaru, K. Tanaka, T. Shimoike, K. Moriishi, T. Iwasaki, K. Mizumoto, Y. Matsuura, T. Miyamura, and T. Suzuki. 2005. Molecular determinants for subcellular localization of hepatitis C virus core protein. *Journal of virology*. 79:1271-1281.

Szabadkai, G., K. Bianchi, P. Varnai, D. De Stefani, M.R. Wieckowski, D. Cavagna, A.I. Nagy, T. Balla, and R. Rizzuto. 2006. Chaperone-mediated coupling of endoplasmic reticulum and mitochondrial Ca2+ channels. *The Journal of cell biology*. 175:901-911.

Szabadkai, G., and R. Rizzuto. 2004. Participation of endoplasmic reticulum and mitochondrial calcium handling in apoptosis: more than just neighborhood? *FEBS letters*. 567:111-115.

Szabadkai, G., A.M. Simoni, M. Chami, M.R. Wieckowski, R.J. Youle, and R. Rizzuto. 2004. Drp-1-dependent division of the mitochondrial network blocks intraorganellar Ca2+ waves and protects against Ca2+-mediated apoptosis. *Molecular cell*. 16:59-68.

Szegezdi, E., S.E. Logue, A.M. Gorman, and A. Samali. 2006. Mediators of endoplasmic reticulum stress-induced apoptosis. *EMBO reports*. 7:880-885.

Tagliavacca, L., T. Anelli, C. Fagioli, A. Mezghrani, E. Ruffato, and R. Sitia. 2003. The making of a professional secretory cell: architectural and functional changes in the ER during B lymphocyte plasma cell differentiation. *Biological chemistry*. 384:1273-1277.

Takahashi, T., J.M. Lasker, A.S. Rosman, and C.S. Lieber. 1993. Induction of cytochrome P-4502E1 in the human liver by ethanol is caused by a corresponding increase in encoding messenger RNA. *Hepatology (Baltimore, Md*. 17:236-245.

Takei, K., H. Stukenbrok, A. Metcalf, G.A. Mignery, T.C. Sudhof, P. Volpe, and P. De Camilli. 1992. Ca2+ stores in Purkinje neurons: endoplasmic reticulum subcompartments demonstrated by the heterogeneous distribution of the InsP3 receptor, Ca(2+)-ATPase, and calsequestrin. *J Neurosci*. 12:489-505.

Talbot, J., J.N. Barrett, E.F. Barrett, and G. David. 2007. Stimulation-induced changes in NADH fluorescence and mitochondrial membrane potential in lizard motor nerve terminals. *The Journal of physiology*. 579:783-798.

Tam, Y.Y., A. Fagarasanu, M. Fagarasanu, and R.A. Rachubinski. 2005. Pex3p initiates the formation of a preperoxisomal compartment from a subdomain of the endoplasmic reticulum in Saccharomyces cerevisiae. *The Journal of biological chemistry*. 280:34933-34939.

Toulmay, A., and W.A. Prinz. 2012. A conserved membrane-binding domain targets proteins to organelle contact sites. *Journal of cell science*. 125:49-58.

Tu, B.P., and J.S. Weissman. 2002. The FAD- and O(2)-dependent reaction cycle of Ero1-mediated oxidative protein folding in the endoplasmic reticulum. *Molecular cell*. 10:983-994.

Tu, B.P., and J.S. Weissman. 2004. Oxidative protein folding in eukaryotes: mechanisms and consequences. *The Journal of cell biology*. 164:341-346.

Vance, J.E. 1990. Phospholipid synthesis in a membrane fraction associated with mitochondria. *The Journal of biological chemistry*. 265:7248-7256.

Vance, J.E. 1991. Newly made phosphatidylserine and phosphatidylethanolamine are preferentially translocated between rat liver mitochondria and endoplasmic reticulum. *The Journal of biological chemistry*. 266:89-97.

Vance, J.E., S.J. Stone, and J.R. Faust. 1997. Abnormalities in mitochondria-associated membranes and phospholipid biosynthetic enzymes in the mnd/mnd mouse model of neuronal ceroid lipofuscinosis. *Biochimica et biophysica acta*. 1344:286-299.

Vetrivel, K.S., H. Cheng, W. Lin, T. Sakurai, T. Li, N. Nukina, P.C. Wong, H. Xu, and G. Thinakaran. 2004. Association of gamma-secretase with lipid rafts in post-Golgi and endosome membranes. *The Journal of biological chemistry*. 279:44945-44954.

Voelker, D.R. 1989. Phosphatidylserine translocation to the mitochondrion is an ATP-dependent process in permeabilized animal cells. *Proceedings of the National Academy of Sciences of the United States of America*. 86:9921-9925.

Voelker, D.R. 2003. New perspectives on the regulation of intermembrane glycerophospholipid traffic. *Journal of lipid research*. 44:441-449.

Voeltz, G.K., W.A. Prinz, Y. Shibata, J.M. Rist, and T.A. Rapoport. 2006. A class of membrane proteins shaping the tubular endoplasmic reticulum. *Cell*. 124:573-586.

Voss, C., S. Lahiri, B.P. Young, C.J. Loewen, and W.A. Prinz. 2012. ER-shaping proteins facilitate lipid exchange between the ER and mitochondria in S. cerevisiae. *Journal of cell science*. 125:4791-4799.

Wada, I., W.J. Ou, M.C. Liu, and G. Scheele. 1994. Chaperone function of calnexin for the folding intermediate of gp80, the major secretory protein in MDCK cells. Regulation by redox state and ATP. *The Journal of biological chemistry*. 269:7464-7472.

Walker, K.W., and H.F. Gilbert. 1995. Oxidation of kinetically trapped thiols by protein disulfide isomerase. *Biochemistry*. 34:13642-13650.

Walther, T.C., and R.V. Farese, Jr. 2009. The life of lipid droplets. *Biochimica et biophysica acta*. 1791:459-466.

Wanders, R.J., S. Ferdinandusse, P. Brites, and S. Kemp. 2010. Peroxisomes, lipid metabolism and lipotoxicity. *Biochimica et biophysica acta*. 1801:272-280.

Wang, S., and R.J. Kaufman. 2012. The impact of the unfolded protein response on human disease. *The Journal of cell biology*. 197:857-867.

Wang, X., B. Su, H.G. Lee, X. Li, G. Perry, M.A. Smith, and X. Zhu. 2009. Impaired balance of mitochondrial fission and fusion in Alzheimer's disease. *J Neurosci*. 29:9090-9103.

Wang, X., B. Su, S.L. Siedlak, P.I. Moreira, H. Fujioka, Y. Wang, G. Casadesus, and X. Zhu. 2008. Amyloid-beta overproduction causes abnormal mitochondrial dynamics via differential modulation of mitochondrial fission/fusion proteins. *Proceedings of the National Academy of Sciences of the United States of America*. 105:19318-19323.

Watson, P., A.K. Townley, P. Koka, K.J. Palmer, and D.J. Stephens. 2006. Sec16 defines endoplasmic reticulum exit sites and is required for secretory cargo export in mammalian cells. *Traffic (Copenhagen, Denmark)*. 7:1678-1687.

Wideman, J.G., N.E. Go, A. Klein, E. Redmond, S.W. Lackey, T. Tao, H. Kalbacher, D. Rapaport, W. Neupert, and F.E. Nargang. 2010. Roles of the Mdm10, Tom7, Mdm12, and Mmm1 proteins in the assembly of mitochondrial outer membrane proteins in Neurospora crassa. *Molecular biology of the cell*. 21:1725-1736.

Wieckowski, M.R., C. Giorgi, M. Lebiedzinska, J. Duszynski, and P. Pinton. 2009. Isolation of mitochondria-associated membranes and mitochondria from animal tissues and cells. *Nature protocols*. 4:1582-1590.

Wieckowski, M.R., G. Szabadkai, M. Wasilewski, P. Pinton, J. Duszynski, and R. Rizzuto. 2006. Overexpression of adenine nucleotide translocase reduces Ca2+ signal transmission between the ER and mitochondria. *Biochemical and biophysical research communications*. 348:393-399.

Williamson, C.D., and A.M. Colberg-Poley. 2009. Access of viral proteins to mitochondria via mitochondria-associated membranes. *Reviews in medical virology*. 19:147-164.

Williamson, C.D., A. Zhang, and A.M. Colberg-Poley. 2011. The human cytomegalovirus protein UL37 exon 1 associates with internal lipid rafts. *Journal of virology*. 85:2100-2111.

Wirtz, K.W. 2006. Phospholipid transfer proteins in perspective. *FEBS letters*. 580:5436-5441.

Wittgen, H.G., and L.C. van Kempen. 2007. Reactive oxygen species in melanoma and its therapeutic implications. *Melanoma research*. 17:400-409.

Yap, M.C., M.A. Kostiuk, D.D. Martin, M.A. Perinpanayagam, P.G. Hak, A. Siddam, J.R. Majjigapu, G. Rajaiah, B.O. Keller, J.A. Prescher, P. Wu, C.R. Bertozzi, J.R. Falck, and L.G. Berthiaume. 2010. Rapid and selective detection of fatty acylated proteins using omega-alkynyl-fatty acids and click chemistry. *Journal of lipid research*. 51:1566-1580.

Yi, M., D. Weaver, and G. Hajnoczky. 2004. Control of mitochondrial motility and distribution by the calcium signal: a homeostatic circuit. *The Journal of cell biology*. 167:661-672.

Young, F.B., S.L. Butland, S.S. Sanders, L.M. Sutton, and M.R. Hayden. 2012. Putting proteins in their place: palmitoylation in Huntington disease and other neuropsychiatric diseases. *Progress in neurobiology*. 97:220-238.

Yount, J.S., B. Moltedo, Y.Y. Yang, G. Charron, T.M. Moran, C.B. Lopez, and H.C. Hang. 2010. Palmitoylome profiling reveals S-palmitoylation-dependent antiviral activity of IFITM3. *Nature chemical biology*. 6:610-614.

Yuan, J.P., W. Zeng, G.N. Huang, P.F. Worley, and S. Muallem. 2007. STIM1 heteromultimerizes TRPC channels to determine their function as store-operated channels. *Nature cell biology*. 9:636-645.

Zampese, E., C. Fasolato, M.J. Kipanyula, M. Bortolozzi, T. Pozzan, and P. Pizzo. 2011. Presenilin 2 modulates endoplasmic reticulum (ER)-mitochondria interactions and Ca2+ cross-talk. *Proceedings of the National Academy of Sciences of the United States of America*. 108:2777-2782.

Zehmer, J.K., R. Bartz, B. Bisel, P. Liu, J. Seemann, and R.G. Anderson. 2009. Targeting sequences of UBXD8 and AAM-B reveal that the ER has a direct role in the emergence and regression of lipid droplets. *Journal of cell science*. 122:3694-3702.

Zhang, Q., J.N. Skepper, F. Yang, J.D. Davies, L. Hegyi, R.G. Roberts, P.L. Weissberg, J.A. Ellis, and C.M. Shanahan. 2001. Nesprins: a novel family of spectrin-repeat-containing proteins that localize to the nuclear membrane in multiple tissues. *Journal of cell science*. 114:4485-4498.

Zhang, S.L., Y. Yu, J. Roos, J.A. Kozak, T.J. Deerinck, M.H. Ellisman, K.A. Stauderman, and M.D. Cahalan. 2005. STIM1 is a Ca2+ sensor that activates CRAC channels and migrates from the Ca2+ store to the plasma membrane. *Nature*. 437:902-905.

Zhao, Y., S. Araki, J. Wu, T. Teramoto, Y.F. Chang, M. Nakano, A.S. Abdelfattah, M. Fujiwara, T. Ishihara, T. Nagai, and R.E. Campbell. 2011. An expanded palette of genetically encoded Ca(2)(+) indicators. *Science (New York, N.Y.* 333:1888-1891.

Zuppini, A., J. Groenendyk, L.A. Cormack, G. Shore, M. Opas, R.C. Bleackley, and M. Michalak. 2002. Calnexin deficiency and endoplasmic reticulum stress-induced apoptosis. *Biochemistry*. 41:2850-2858.